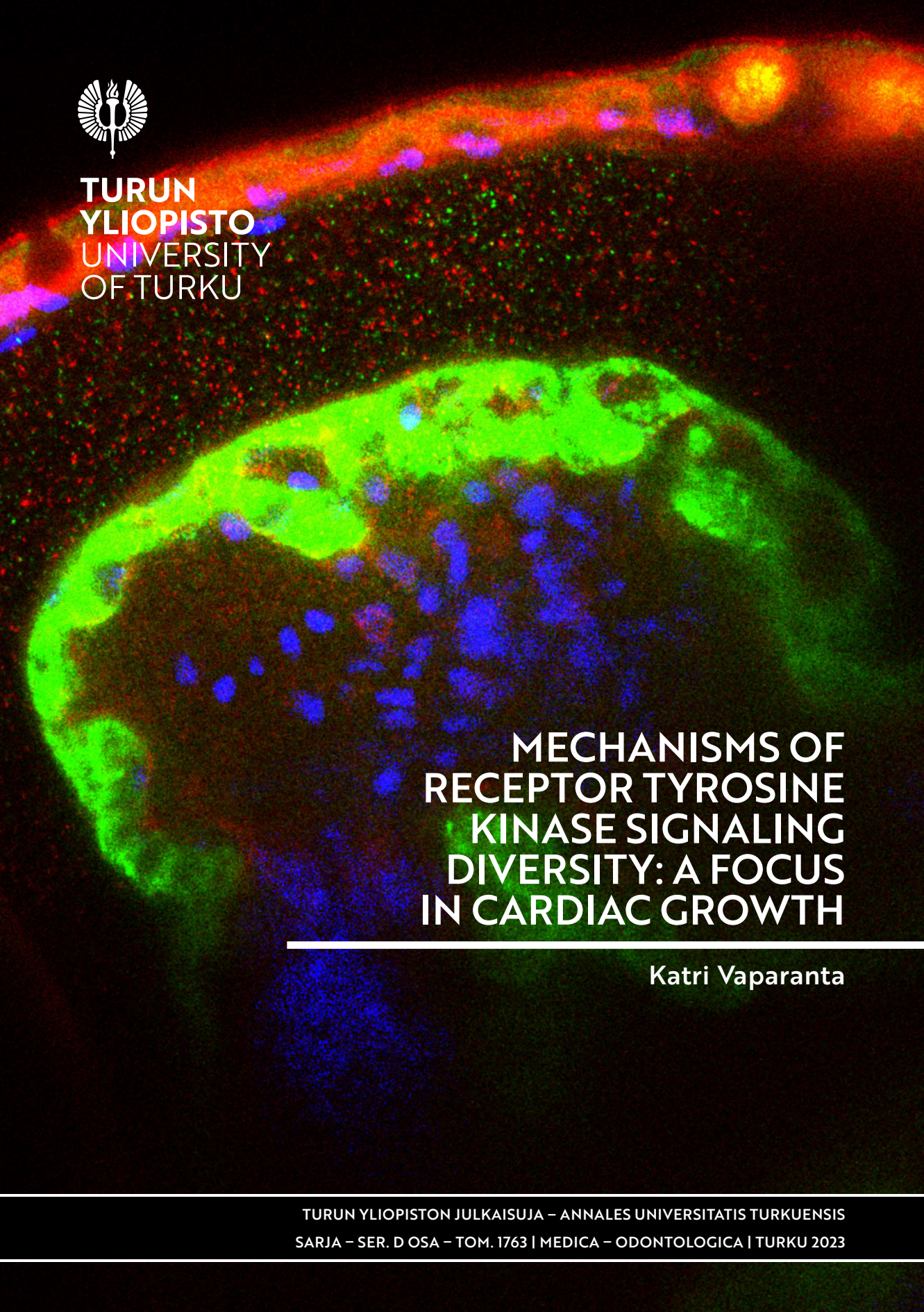

TURUN YLIOPISTO
UNIVERSITY OF TURKU

MECHANISMS OF RECEPTOR TYROSINE KINASE SIGNALING DIVERSITY: A FOCUS IN CARDIAC GROWTH

Katri Vaparanta

TURUN YLIOPISTON JULKAISUJA – ANNALES UNIVERSITATIS TURKUENSIS
SARJA – SER. D OSA – TOM. 1763 | MEDICA – ODONTOLOGICA | TURKU 2023

TURUN
YLIOPISTO
UNIVERSITY
OF TURKU

MECHANISMS OF RECEPTOR TYROSINE KINASE SIGNALING DIVERSITY: A FOCUS IN CARDIAC GROWTH

Katri Vaparanta

TURUN YLIOPISTON JULKAISUJA – ANNALES UNIVERSITATIS TURKUENSIS
SARJA – SER. D OSA – TOM. 1763 | MEDICA – ODONTOLOGICA | TURKU 2023

University of Turku

Faculty of Medicine
Institute of Biomedicine
Medical Biochemistry and Genetics
Turku Doctoral Programme of Molecular Medicine (TuDMM)

Supervised by

Professor Klaus Elenius, MD, PhD
Medicity Research Laboratories
Institute of Biomedicine
University of Turku
Turku Bioscience Center
University of Turku and Åbo Akademi
Turku, Finland

Reviewed by

Professor emeritus Heikki Ruskoaho, MD, PhD
Drug Research Program
Division of Pharmacology and
Pharmacotherapy
Faculty of Pharmacy
University of Helsinki
Helsinki, Finland

Professor Merja Heinäniemi, PhD
Faculty of Health Sciences
Institute of Biomedicine
University of Eastern Finland
Kuopio, Finland

Opponent

MD, PhD, Tuomas Tammela
Cancer Biology and Genetics Program
Sloan Kettering Institute
Memorial Sloan Kettering Cancer Center
Cell and Developmental Biology
Weill-Cornell Medical College
New York, USA

The originality of this publication has been checked in accordance with the University of Turku quality assurance system using the Turnitin OriginalityCheck service.

Cover Image: Katri Vaparanta

ISBN 978-951-29-9550-9 (PRINT)
ISBN 978-951-29-9551-6 (PDF)
ISSN 0355-9483 (Print)
ISSN 2343-3213 (Online)
Painosalama, Turku, Finland 2023

To the pursuit of knowledge

UNIVERSITY OF TURKU
Faculty of Medicine
Institute of Biomedicine
Medical Biochemistry and Genetics
KATRI VAPARANTA: Mechanisms of Receptor Tyrosine Kinase Signaling Diversity: A Focus in Cardiac Growth
Doctoral Dissertation, 341 pp.
Turku Doctoral Programme of Molecular Medicine (TuDMM)
November 2023

ABSTRACT

To understand organism function and disease and to target perturbed processes for therapy, comprehensive knowledge of the underlying cell signaling networks is required. However, mapping the interplay of the vast number of biomolecules involved in these networks remains challenging. As a result, efforts have focused on identifying the structural elements within biomolecules that facilitate signal transmission. Receptor tyrosine kinases (RTKs) regulate the function of several important organs and are most recognized as oncogenes in cancer. Research into the structural determinants of RTKs that govern their signaling has led to clinically approved therapies. However, some structural regions of these kinases remain poorly understood. In this thesis, the diversity of cell signaling arising from variation in an overlooked region in RTKs known as the extracellular juxtamembrane region was explored. A sequence motif that controls the cell surface location and the signaling of RTKs was identified, presenting a potential novel way to target RTKs for therapy.

The cell signaling pathways that regulate myocardial growth could be putatively re-activated to treat heart failure or inhibited to treat pathological hypertrophy. Additionally, these pathways may hold the key to regenerating the myocardium post-injury. A pathway promoting myocardial growth involving STAT5b and the RTK ErbB4 was uncovered in this thesis. VEGFB, traditionally associated with endothelial cells, was additionally observed to elicit myocardial growth through paracrine signaling involving ErbB RTKs. Activation of ErbB4 pathways in the heart with NRG-1 has improved the cardiac function of heart failure patients implying that the discoveries made in this thesis may aid in heart failure therapy development.

Finally, recent developments in omics technologies have facilitated the detection and quantification of the different layers of cell signaling networks. Consequently, a growing need for computational analyses capable of reverse-engineering cell signaling pathways from multi-omics data has emerged. In this thesis, a new computational approach specifically designed to discover cell signaling pathways from multi-omics data without the use of prior information was developed. These types of de novo methods remain essential for uncovering new cell signaling connections, which, in turn, can unveil potential new drug targets to treat disease.

KEYWORDS: cell signaling, extracellular juxtamembrane region, ErbB4, hypertrophy, motif, multi-omics, myocardial growth, receptor tyrosine kinase

TURUN YLIOPISTO
Lääketieteellinen tiedekunta
Biolääketieteen laitos
Lääketieteellinen biokemia ja genetiikka
KATRI VAPARANTA: Reseptorityrosiinikinaasien viestinnän monimuotoisuuden mekanismit: painotus sydänlihaksen kasvussa
Väitöskirja, 341 s.
Molekyylilääketieteen tohtoriohjelma
Marraskuu 2023

TIIVISTELMÄ

Elimistön toiminnan ja sairauksien ymmärtäminen sekä lääkekehitys edellyttää kattavaa tietoa solujen soluviestintäverkostoista. Koska soluviestintämolekyylejä on lukuisia, soluviestinnän tutkimus on keskittynyt löytämään toistuvia rakenteellisia soluviestintää välittäviä alueita soluviestintämolekyyleistä. Reseptorityrosiinikinaasit (RTK:t) ovat solun pinnan soluviestintämolekyylejä, jotka säätelevät useita elimistön tärkeitä toimintoja ja joiden rakenteen tutkimus on johtanut useisiin käytössä oleviin lääkkeisiin. RTK:iden rakenteessa sijaitsee alue solun ulkopuolella, jonka merkitystä ei ole aikaisemmin juurikaan selvitetty. Tämän alueen vaikutusta RTK:iden viestinnän monimuotoisuudelle tutkittiin tässä väitöskirjassa. Alueelta löydettiin sekvenssimotiivi, joka säätelee RTK:iden sijaintia solun pinnalla sekä niiden viestintää. Alueelle voidaan tulevaisuudessa mahdollisesti kohdentaa RTK:iden viestintää muuttavia lääkkeitä.

Soluviestintäreittejä, jotka säätelevät sydänlihaksen kasvua, voidaan mahdollisesti aktivoida sydämen vajaatoiminnan hoitamiseksi tai estää vahingollisen sydämen liikakasvun lieventämiseksi. Lisäksi näitä soluviestintäreittejä voidaan hyödyntää vaurion jälkeiseen sydänlihassolujen regeneraatioon. Sydänlihaksen kasvun soluviestintäreitteihin liittyviä havaintoja tehtiin tässä väitöskirjassa. RTK ErbB4:n todettiin aiheuttavan sydänlihaksen kasvua STAT5b viestinnän kautta. RTK ligandi VEGF-B:n puolestaan todettiin vaikuttavan sydänlihaksen kasvuun ErbB RTK:iden viestinnän avulla. Koska ErbB4 viestinnän aktivointi on parantanut sydämen vajaatoimintapotilaiden sydämen toimintaa, nämä havainnot saattavat edesauttaa sydämen vajaatoiminnan hoitojen kehitystä.

Omiikka-teknologioilla voidaan mitata soluviestintäverkostojen eri tasoja lähes kattavasti. Laskennallisia työkaluja kuitenkin tarvitaan, jotta omiikka-teknologioilla tuotettu tieto voidaan mallintaa soluviestintäreiteiksi. Uusi soluviestintäreittien mallinnusohjelma kehitettiin tässä väitöskirjassa. Mallinnusohjelma käyttää ainoastaan omiikka-teknologioilla saatua tietoa soluviestintäreittien mallinnukseen. Tämän kaltaisia vain mitattuun tietoon perustuvia menetelmiä tarvitaan uusien soluviestintäreittien löytämiseksi. Uudet soluviestintäreittien yhteydet puolestaan voivat paljastaa uusia tautimekanismeja ja toimia uusina lääkekohteina.

AVAINSANAT: ErbB4, multi-omiikka, reseptorityrosiinikinaasi, sekvenssimotiivi, soluviestintä, STAT, sydänlihaksen kasvu, sydänlihaksen liikakasvu

Table of Contents

Abbreviations **10**

List of Original Publications **14**

1 Introduction **15**

2 Review of the Literature **17**
2.1 Receptor tyrosine kinases 17
2.1.1 The ErbB receptor tyrosine kinases 17
2.1.1.1 Isoforms of ErbB4 19
2.1.2 The VEGF receptor tyrosine kinases 22
2.1.3 A detailed view of the structure of ErbB family receptor tyrosine kinases 23
2.1.3.1 Extracellular domain of ErbB receptors is essential for growth factor binding and receptor activation 24
2.1.3.2 The eJM region of ErbB receptors regulates receptor activation by restricted length, cleavage and glycolipid interactions .. 25
2.1.3.3 The transmembrane domain of ErbB receptors is involved in receptor dimerization 25
2.1.3.4 The iJM region of ErbB receptors controls receptor autophosphorylation by several mechanisms 26
2.1.3.5 The intracellular domain of ErbB receptors phosphorylates and interacts with downstream substrates, and is heavily regulated by post-translational modifications 27
2.1.4 The signaling of ErbB receptor tyrosine kinases 28
2.1.4.1 The STAT pathway 30
2.2 Myocardial growth 32
2.2.1 Myocardial growth during the life span 32
2.2.2 From pathological hypertrophy to heart failure 34
2.2.2.1 The difference between physiological and pathological hypertrophy 34
2.2.2.2 Maladaptation to decompensatory hypertrophy leads to heart failure 35
2.2.3 NRG-1/ErbB signaling in myocardial growth 35

2.2.3.1 NRG-1/ErbB signaling in cardiac injury models ... 37
2.2.4 STAT signaling in myocardial growth ... 40
2.2.5 VEGF signaling in myocardial growth ... 42
2.3 Module, network and pathway inference from omics data ... 42
2.3.1 Prior data-independent module, network and pathway inference methods for single omics data ... 44
2.3.1.1 Association measure-based methods ... 44
2.3.1.2 Non-association measure-based approaches ... 45
2.3.1.3 Community approaches outperform individual approaches ... 48
2.3.2 Efforts to develop prior data independent cell signaling pathway inference methods for multi-omics data are currently lacking ... 48

3 Aims ... 51

4 Materials and Methods ... 53
4.1 Experimental models ... 53
4.1.1 Cell culture (I, II, IV) ... 53
4.1.2 Primary cell isolation and culture (II) ... 53
4.1.3 Zebrafish embryos (II) ... 54
4.1.4 Adeno-associated virus-treated mice (II, III) ... 54
4.1.5 Patient samples (II) ... 54
4.2 Experimental procedures ... 55
4.2.1 Plasmid DNA cloning (I, IV) ... 55
4.2.2 Plasmid DNA and siRNA transfection (I, II, IV) ... 55
4.2.3 Retro- and lentivirus production and infection (I, II, IV) ... 55
4.2.4 CRISPR/Cas9 editing of zebrafish embryos (II) ... 56
4.2.5 Ligand stimulation and chemical and lectin inhibition (I, II) ... 56
4.2.6 Cell and tissue lysis (I, II, IV) ... 57
4.2.7 Affinity enrichment (I, II, IV) ... 57
4.2.8 Western analysis (I, II, III, IV) ... 57
4.2.9 Chemical cross-linking (I, II, IV) ... 58
4.2.10 Proximity ligation assay (I, II) ... 58
4.2.11 Immunofluorescence (I, II, IV) ... 58
4.2.12 Immunohistochemistry (II) ... 59
4.2.13 Live cell and organ imaging (I, II, IV) ... 60
4.2.14 Cell adhesion assay (IV) ... 60
4.2.15 Genomic DNA and RNA extraction (II, IV) ... 60
4.2.16 PCR and genomic sequencing (II) ... 60
4.2.17 Lipid and glycan overlay assay with synthetic peptides (I) ... 61
4.2.18 Mass spectrometry (I, II, IV) ... 61
4.2.19 RNA sequencing (IV) ... 62
4.3 Computational and statistical analyses ... 62
4.3.1 Data handling and analysis ... 62
4.3.1.1 Mass-spectrometry data (I, II, IV) ... 62

4.3.1.2 RNA sequencing data (IV) 63
4.3.1.3 Glycan array data (I) 63
4.3.1.4 Other data 63
4.3.2 Statistical analyses (I, II, III, IV) 64
4.3.3 Image analysis (I, II, IV) 64
4.3.4 Gene set enrichment and pathway analyses (I) 65
4.3.5 Custom approaches 65
4.3.5.1 Dimensionality reduction and clustering of published datasets (I, II) 65
4.3.5.2 JM-motif analysis (I) 66
4.3.5.3 Cleavage site prediction (IV) 66
4.3.5.4 De novo multi-omics pathway analysis (DMPA) (IV) 67
4.3.5.4.1 The DMPA algorithm 67
4.3.5.4.2 DMPA validation 68
4.3.5.4.3 Data simulation for parameter S sensitivity analysis 69
4.3.5.4.4 Benchmarking the DMPA 69
4.3.5.4.5 Prediction functions of DMPA 70

5 Results 71
5.1 A sequence motif in the eJM region determines the cell surface location and downstream signaling of receptor tyrosine kinases (I) 71
5.1.1 ErbB4 JM isoforms elicit differential signaling responses and localize to different plasma membrane microdomains 71
5.1.2 The difference in the subcellular location and STAT signaling responses of the ErbB4 JM-isoforms can be tracked back to key residues in the eJM region of ErbB4 JM-a 73
5.1.3 A sequence motif in the eJM region of receptor tyrosine kinases confers selective STAT activation and subcellular location of RTKs 74
5.1.4 The JM-a motif binds complex-type N-glycans in cell surface proteins such as β1-integrin 75
5.2 STAT5b mediates growth responses of the NRG-1/ErbB4 pathway in cardiomyocytes (II) 77
5.2.1 STAT5b signaling mediates NRG-1/ErbB4 induced hypertrophic growth *in vivo* and *in vitro* in murine cardiomyocytes 77
5.2.2 STAT5b controls hyperplastic growth of the myocardium of zebrafish embryos and the activation of STAT5 in embryonic zebrafish is controlled by the NRG-1/ErbB pathway 79
5.2.3 Dynamin-2 controls the subcellular location of ErbB4 and STAT5b signaling in cardiomyocytes 81
5.2.4 STAT5b signaling is perturbed in patients with pathological cardiac hypertrophy 82
5.3 VEGF-B activates ErbB growth signaling in the heart (III) 83

5.4 De novo multi-omics analysis (DMPA) models multi-omics data into regulatory modules and cell signaling pathways without the use of prior information (IV) 84
5.4.1 The association score of DMPA, the combined score, is conserved across datasets 84
5.4.2 DMPA uncovers known associations connected by a common upstream regulator 85
5.4.3 The ranking and adjustment of association scores and three feature clique discovery increase the accuracy of DMPA 86
5.4.4 The accuracy of DMPA is sensitive to the zero-inflation and S parameters 87
5.4.5 DMPA outperforms benchmark methods 88
5.4.6 DMPA of an in-house multi-omics dataset of the signaling of the cleaved intracellular domain of the receptor tyrosine kinase TYRO3 88
5.4.7 Prediction methods were designed to contextualize the results of DMPA 89
5.4.8 The function prediction approach of DMPA can predict cellular behavior 90

6 Discussion 91
6.1 The discovered sequence motif reveals a new functional region in receptor tyrosine kinases that could be putatively targeted for treatment 91
6.2 ErbB4 JM isoform-specific activation of a specific STAT5 subtype uncovers a putative candidate target for treatment of heart failure 92
6.3 Research into the cross-talk between angiogenic signals and myocardial growth signals reveal mechanisms of physiological myocardial growth 94
6.4 DMPA discovers multi-omics modules and pathways more consistently from more diverse datasets and with lower sample sizes than previous approaches 94
6.4.1 Limitations and future improvement strategies of DMPA 95

7 Summary/Conclusions 97

Acknowledgements 99

References 102

Original Publications 133

Abbreviations

AAV	adeno associated virus
ABL	Abelson murine leukemia viral oncogene homolog
ADAM	a disintegrin and metalloprotease
ADANET	adaptive structural learning of artificial neural networks
AKT	AKT serine/threonine kinase 1
ANOVA	analysis on variance
ARACNE	algorithm for the reconstruction of accurate cellular networks
AREG	amphiregulin
ATP	adenosine triphosphate
BCA	Bicinchoninic acid
BCL-2	B-cell lymphoma-2
BCL-XL	B-cell lymphoma-extra large
BS_3	bis(sulfosuccinimidyl)suberate
BSA	bovine serum albumin
BTC	betacellulin
C-terminal	carboxy-terminal
CLR	context likelihood of relatedness
CRISPR	clustered regularly interspaced short palindromic repeats
crRNA	crispr RNA
CV%	percent coefficient of variation
CYT	cytoplasmic
DAB	3,3′-Diaminobenzidine
DAG	diacyl glycerol
DAPI	4′,6-Diamidino-2-phenylindole dihydrochloride
DMEM	dulbecco's modified eagle medium
DMPA	de novo multi-omics pathway analysis
DNA	deoxyribonucleic acid
DREAM	dialogue on reverse engineering assessment and methods
DSP	dithiobis(succinimidyl propionate)
DTPB	Dimethyl dithiobispropionimidate
EDTA	Ethylenediaminetetraacetic acid

EGF	epidermal growth factor
EGFR	epidermal growth factor receptor
eJM	extracellular juxtamembrane region
EPGN	epigen
EREG	epiregulin
ERBB	erythroblastic leukemia viral oncogene
ERK	extracellular signal-regulated kinase
FDR	false discovery rate
FFPE	formalin-fixed paraffin embedded
FLT	fms related receptor tyrosine kinase
FLK1	fetal liver kinase-1
GENIE3	gene network inference with ensemble of trees 3
GGM	gaussian graphical model
GM3	monosialodihexosylganglioside 3
GRB2	growth factor receptor bound protein 2
GSEA	gene set enrichment analysis
GTP	guanosine triphosphate
HB-EGF	heparin-binding EGF-like growth factor
HBSS	Hank's balanced salt solution
HCL	hydrochloric acid
HFmrEF	heart failure with mid-range ejection fraction
HFpEF	heart failure with preserved ejection fraction
HFrEF	heart failure with reduced ejection fraction
HER	human epidermal growth factor receptor
HRP	horseradish peroxidase
ICD	intracellular domain
IGF-1	insulin-like growth factor 1
iJM	intracellular juxtamembrane region
IKK	IkappaB kinase
IL	interleukin
IP3	inositol 1,4,5-trisphosphate
JAK	Janus kinase
JM	juxtamembrane
JNK	c-Jun N-terminal protein kinase
JNKK	c-Jun N-terminal protein kinase kinase
KDR	kinase insert domain receptor
LFQ	label-free quantitation
LIF	leukemia inhibitory factor
MAPK	mitogen-activated protein kinase
MCODE	molecular complex detection

MEF	myocyte enhancer factor
MEK	mitogen-activated protein kinase kinase
MEKK	mitogen-activated protein kinase kinase kinase
MQ	milli-Q
mTOR	the mammalian target of rapamycin
Na3VO4	sodium orthovanadate
NaCl	sodium chloride
NaF	sodium fluoride
NCA	neighborhood component analysis
NCK	non-catalytic region of tyrosine kinase adaptor protein
NEDD4	neuronally expressed developmentally downregulated 4
NEMO	NF-kappa-B essential modulator
NF-κβ	nuclear factor kappa-light-chain-enhancer of activated B cells
Ni-NTA	nickel nitrilotriacetic acid
NP-hard	non-deterministic polynomial-time hard
NRG	neuregulin
NUMB	NUMB endocytic adaptor protein
NUMBL	NUMB like endocytic adaptor protein
OCT	optimal cutting temperature
ODE	ordinal differential equation
P-value	probability value
PAK	p21 (rac1) activated kinase 1
PBS	phosphate buffered saline
PCR	polymerase chain reaction
PDK1	phosphoinositide-dependent kinase-1
PFA	paraformaldehyde
PI3K	phosphoinositide 3-kinase
PIGF	placental growth factor
PIP2	phosphatidylinositol (4,5)-bisphosphate
PIP3	phosphatidylinositol (3,4,5)-trisphosphate
PLA	proximity ligation assay
PLC	phospholipase C
PMSF	phenylmethylsulfonyl fluoride
PRM	parallel reaction monitoring
PTB	phosphotyrosine-binding domain
PTM	post-translation modification
RAF	rapidly accelerated fibrosarcoma
RAS	rat sarcoma virus
RFU	relative fluorescence unit
RIPA	radioimmunoprecipitation assay

RNA	ribonucleic acid
RPMI	roswell park memorial institute
RT-PCR	real-time polymerase chain reaction
RTK	receptor tyrosine kinase
SDS-PAGE	sodium dodecyl sulfate polyacrylamide gel electrophoresis
SH2	src homology 2
SH3	src homology 3
SHC2	Src homology 2 domain containing transforming protein 2
shRNA	small hairpin RNA
siRNA	small interfering RNA
SOS	son of sevenless homolog
STAT	signal transducer and activator of transcription
STED	stimulated emission depletion
TBS	tris buffered saline
TBS-T	tris buffered saline with 0.1% Tween 20 detergent
TCEP	tris(2-carboxyethyl)phosphine
TGF-α	transforming growth factor α
TIGRESS	trustful inference of gene regulation using stability selection
TiO2	titaniumdioxide
TransNet	Transkingdom Network Analysis
tracRNA	trans-activating crispr RNA
Tris	tris(hydroxymethyl)aminomethane
TSAd	T cell specific adaptor protein
TYK2	tyrosine kinase 2
VEGF	vascular endothelial growth factor
VEGFR	vascular endothelial growth factor receptor
WGCNA	weighted correlation network analysis
WWP1	WW domain-containing E3 ubiquitin protein ligase 1
YAP1	yes-associated protein 1

List of Original Publications

This dissertation is based on the following original publications, which are referred to in the text by their Roman numerals:

I Vaparanta K, Jokilammi A, Tamirat M, Merilahti JAM, Salokas K, Varjosalo M, Ivaska J, Johnson MS, Elenius K. An extracellular receptor tyrosine kinase motif orchestrating intracellular STAT activation. *Nature Communications*, 2022 Nov 14;13(1):6953.

II Vaparanta K, Jokilammi A, Paatero I, Merilahti JAM, Heliste J, Hemanthakumar KA, Kivelä R, Alitalo K, Taimen P, Elenius K. STAT5b is a key effector of NRG-1/ERBB4-mediated myocardial growth. *EMBO Reports*, 2023; May 4;24(5):e56689.

III Kivelä R, Hemanthakumar KA, Vaparanta K, Izumiya Y, Kidoya H, Takakura N, Elenius K, Alitalo K. Endothelial cells regulate physiological cardiomyocyte growth via VEGFR2 -mediated paracrine signaling. *Circulation*, 2019;139:2570–2584.

IV Vaparanta K, Merilahti J, Ojala V, Elenius K. De Novo multi-omics pathway analysis (DMPA) designed for prior data independent inference of cell signaling pathways. *bioRxiv*, https://doi.org/10.1101/2022.02.05.479228.

1 Introduction

Cell signaling is the foundation for all cellular, tissue, and organ function and perturbation of cell signaling is the premise of disease. To comprehensively understand and model normal development and the initiation and progression of disease, a detailed understanding of the complex cell signaling networks inside and in between cells needs to be acquired. Majority of drug-based therapies function by altering cell signaling. Instead of individual research into distinct aspects of each signaling molecule a strategy to research the common structural determinants of cell signaling molecules that mediate signaling moieties have been applied (Mayer, 2015). This strategy has identified numerous functional domains and motifs in cell signaling molecules and has allowed accurate predictions of the function and role of unknown cell signaling molecules. This strategy has further guided drug development and has been instrumental in targeting the correct functional aspects of cell signaling molecules to efficiently treat disease.

Receptor tyrosine kinases (RTK) regulate several essential functions in the cell and are most well-recognized as oncogenes in cancer (Schlessinger, 2014). These revelations have focused research into understanding the structure-function relationship of RTKs. This thesis focuses on the diversity of signaling arising from the largely overlooked extracellular juxtamembrane region of RTKs. The RTK ErbB4 is utilized as a model receptor since natural variants that only differ in the extracellular juxtamembrane region are produced from this receptor (Elenius et al., 1997a). The wider perspective pursued by this thesis is to identify the mechanisms by which structural changes of RTK regions that reside outside the cell affect intracellular signaling. These mechanisms can then be further targeted by innovative therapeutic compounds since these mechanisms have the undeniable advantage of residing outside the cell. Extracellular regions in RTKs are more accessible to various therapeutic strategies than intracellular regions, which require therapeutic compounds to permeate the cell membrane.

In this thesis, a special emphasis on the effect of RTK signaling in myocardial growth was adopted. Cardiovascular diseases affect hundreds of thousands of people in Finland and hundreds of millions of people worldwide and remain the leading cause of death (Terveyden ja hyvinvoinnin laitos, 2023; World Health Organization,

2023). Increased myocardial growth is a compensatory response of the heart to combat stress such as the pressure overload caused by hypertension. Prolonged, however, the increased pathological myocardial growth can reduce left ventricular ejection fraction increasing the load of the heart. This overload can ultimately lead to heart failure, a condition where some of the growth signaling prevalent during the compensatory response is lost (Stansfield et al., 2014). Heart failure is one of the common causes of mortality from cardiovascular diseases (Emmons-Bell, Johnson and Roth, 2022). Myocardial growth pathways also have significance during heart regeneration after injury. Induction of cardiomyocyte renewal is one of the main goals for the future treatment of myocardial diseases (Eschenhagen et al., 2017a). Therefore, it is not surprising that an emphasis on uncovering the critical myocardial growth pathways has persisted. Theoretically both inhibition and stimulation of myocardial growth pathways may present a serviceable strategy to treat myocardial diseases depending on the condition of the disease. In this thesis, the role of the discovered interacting proteins of the well-established NRG-1/ErbB4 myocardial growth pathway was investigated. A focus to study the role of the interacting proteins that are selectively bound by the extracellular juxtamembrane domain variant of the receptor tyrosine kinase ErbB4 that is specifically expressed in cardiomyocytes was selected. NRG-1, the ligand for the ErbB4 receptor tyrosine kinase is expressed in the endothelial cells of the cardiac vasculature and is currently under clinical investigation as a therapy against heart failure (De Keulenaer et al., 2019). In addition to NRG-1, a receptor from a family of other receptor tyrosine kinases, the VEGFR1 is specifically expressed in the cardiac endothelial cells (Muhl et al., 2016). In this thesis, the effect of a ligand of this receptor, VEGFB, on the activation of the NRG-1/ErbB4 growth pathway in the myocardium was also researched. The cell signaling insights into the pathways of myocardial growth presented in this thesis may aid in future therapy development for myocardial diseases.

Recent advances have led to the ability to gather a wide array of high-throughput omics data on different stages of cell signaling (Karczewski and Snyder, 2018). This has presented a new challenge in the analysis of this multi-omics data to uncover the underlying cell signaling networks. Many approaches have been proposed with their apparent and non-apparent disadvantages. In this thesis, a new method to uncover cell signaling pathways from multi-omics data was developed that outperforms its closest predecessors. The proposed method is independent of previous knowledge making it non-susceptible to the limitations of our current knowledge. This capability makes the method especially beneficial in uncovering previously undetected cell signaling connections. These connections could reveal new disease mechanisms that could be the targets of future drug therapies.

2 Review of the Literature

2.1 Receptor tyrosine kinases

RTKs are cell surface proteins that mediate extracellular signals inside the cell by binding extracellular ligands and consequently transferring a phosphate group from adenosine-triphosphate (ATP) to the tyrosine residues of the C-terminal tails of their dimerization partners and intracellular substrates. In prototypical view RTKs form a dimer upon activation by growth factor binding and in an inactive state exist as monomers. Instead of dimers, however, some human RTKs such as the insulin receptor form other multimeric complexes. RTKs comprise of structural modules which ultimately determine their function. Due to higher structural similarity between a subset of the receptors, 19 sub-families of human receptor tyrosine kinases have been identified. (Robinson, Wu and Lin, 2000; Lemmon and Schlessinger, 2010; Wheeler and Yarden, 2015). The sub-family members have been considered to have co-evolved together with their perspective ligands and analogues of them can be found in most multi-cellular non-plant and non-fungi eukaryotes (Stein and Staros, 2006; Amit, Wides and Yarden, 2007; Wheeler and Yarden, 2015).

2.1.1 The ErbB receptor tyrosine kinases

The ErbB family of RTKs consist of four members, EGFR (ErbB1/HER1) (Ushiro and Cohens, 1980; Ullrich et al., 1984), ErbB2 (HER2) (Coussens et al., 1985), ErbB3 (HER3) (Kraus et al., 1989) and ErbB4 (HER4) (Plowman et al., 1993a) (Figure 1). ErbB2 and ErbB3 are unique among the receptor family, due to the inability of ErbB2 to bind ligands and ErbB3 to effectively phosphorylate substrates. ErbB2 is missing a ligand binding domain (Cho et al., 2003) and is constitutively erect in an active conformation (Garrett et al., 2003). The kinase domain of ErbB3 is missing key residues in the kinase domain that are considered important in the catalysis of phosphate transfer from ATP (Guy et al., 1994). Due to this lack ErbB3 is only able to autophosphorylate (Shi et al., 2010). Due to the mentioned inabilities, ErbB2 and ErbB3 preferably serve as heterodimerization partners for each other and the other ErbB receptors. ErbB receptors have 11 known ligands with differential binding specificities. Epidermal growth factor (EGF) (Cohen, 1962), transforming growth

factor alpha (TGF-α) (Riese et al., 1996b), amphiregulin (AREG) (Riese et al., 1996b), and epigen (EPGN) (Strachan et al., 2001) bind EGFR exclusively. Heparin binding EGF like growth factor (HB-EGF) (Elenius et al., 1997b), betacellulin (BTC) (Riese et al., 1996a; 1998) and epiregulin (EREG) bind both EGFR and ErbB4. Neuregulin-1 (NRG-1) (Plowman et al., 1993b; Carraway et al., 1994) and NRG-2 (Carraway et al., 1997; Chang et al., 1997) bind both ErbB3 and ErbB4. NRG-3 (Zhang et al., 1997) and NRG-4 (Harari et al., 1999), in turn, bind only ErbB4.

ErbB receptor knock-out studies have revealed the role of these essential cell surface receptors in the normal growth and development of several tissues and organs. ErbB receptor gene knockouts in mice are lethal at the embryonic stage with some variation between the genetic backgrounds. The development of bone, brain, heart and the epithelium of kidneys, lungs, skin, mammary glands and eyes is impaired by the genetic knock-outs (Gassmann et al., 1995; Lee et al., 1995; Sibilia and Wagner, 1995; Threadgill et al., 1995; Riethmacher et al., 1997; Kornblum et al., 1998; Sibilia et al., 1998; 2003; Lin et al., 2000; Tidcombe et al., 2003; Wang et al., 2004; Wagner et al., 2006). ErbB receptors, however, are best recognized for their oncogenic role in cancer. Several oncogenic mutations and genetic variations of the ErbB receptors have been identified and ErbB receptors are the targets of successful lung, breast, colorectal and head and neck cancer therapies (Yarden and Pines, 2012; Hynes and Author, 2016; Kiavue et al., 2019; Segers et al., 2020; Uribe, Marrocco and Yarden, 2021; Lucas et al., 2022).

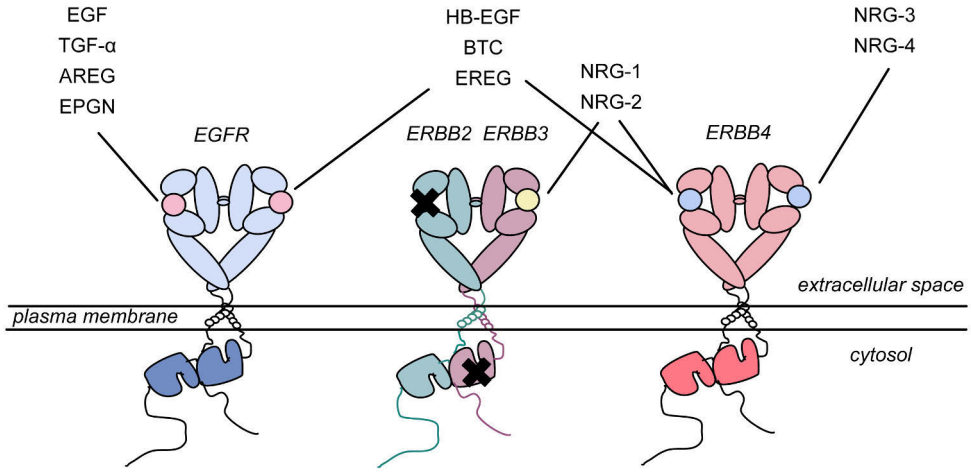

Figure 1. ErbB receptor tyrosine kinases and their ligands. The ligand binding domain of ErbB2 and the kinase domain of ErbB3 are defective (black cross), therefore ErbB2 and ErbB3 receptors preferably function as heterodimers. AREG: amphiregulin. BTC: betacellulin. EGF: epidermal growth factor. EGFR: epidermal growth factor receptor. EPGN: epigenin. ERBB: erythroblastic leukemia viral oncogene. EREG: epiregulin. HB-EGF: heparing binding EGF-like growth factor. NRG: neuregulin. TGF-α: transforming growth factor α. Modified from (Lemmon, Schlessinger and Ferguson, 2014).

2.1.1.1 Isoforms of ErbB4

ErbB4 is unique among the ErbB receptors since it is the only ErbB receptor from which four alternative isoforms are produced by alternative exon splicing (Figure 2). Inclusion of either exon 15 or 16 produces either the JM-a or the JM-b isoforms of ErbB4 that differ only in the extracellular juxtamembrane region (Elenius et al., 1997a). Inclusion or exclusion of the exon 26, in turn, produce the CYT-1 (cytoplasmic-1) and CYT-2 isoforms of ErbB4 (Elenius et al., 1999). This alternative splicing has been discovered to result in a significant difference in the function of the receptor. The JM-a exon encodes a 23 amino acid stretch that includes cleavage sites for the ADAM17 (a disintegrin and metalloprotease 17) protease that are lacking in the 13 amino acid long stretch in the JM-b isoforms (Rio et al., 2000). These cleavage sites allow only the JM-a isoforms to undergo regulated intramembrane proteolysis, where after cleavage by ADAM17, the intracellular domain (ICD) of the ErbB4 JM-a isoforms is released by the γ-secretase protease complex (Ni et al., 2001; Vidal et al., 2005). The released ICD acts as a soluble intracellullar signaling molecule and has been reported to localize to the nucleus to modify transcription by interacting with transcription factors and transcriptional repressors (Ni et al., 2001; Komuro et al., 2003; Williams et al., 2004; Linggi and Carpenter, 2006; Sardi et al., 2006; Zhu et al., 2006; Gilmore-Hebert, Ramabhadran and Stern, 2010; Sundvall et al., 2010; Paatero et al., 2012). The ErbB4 JM-a isoforms activate the transcription factor STAT5a (signal transducer and activator of transcription 5a) by phosphorylating STAT5a in the activating residue Y694. The released ICD of the ErbB4 JM-a isoforms couple with activated STAT5a in the nucleus to induce the transcription of lactation genes (Williams et al., 2004). Interestingly, the ErbB4 JM-b isoform has been reported to also localize in the nucleus in cardiomyocytes, but in contrast as a full-length receptor (Icli et al., 2012). The ErbB4 JM-a and JM-b isoforms induce opposing cellular outcomes in various cellular backgrounds. In mammary epithelial and breast cancer cell lines, expression of ErbB4 JM-a promotes uncontrolled growth and JM-b differentiation as estimated by the number of colonies and acini in 3D growth assays (Veikkolainen et al., 2011; Sundvall et al., 2012). In an embryonic fibroblast cell line, expression of ErbB4 JM-a induces cell survival and expression of JM-b cell death under serum starvation (Sundvall et al., 2010). In an epithelial kidney cell line, only the ErbB4 JM-a variant of the ErbB4 CYT-2 isoform induces cyst formation and tubulogenesis when grown in 3D in collagen (Zeng et al., 2007).

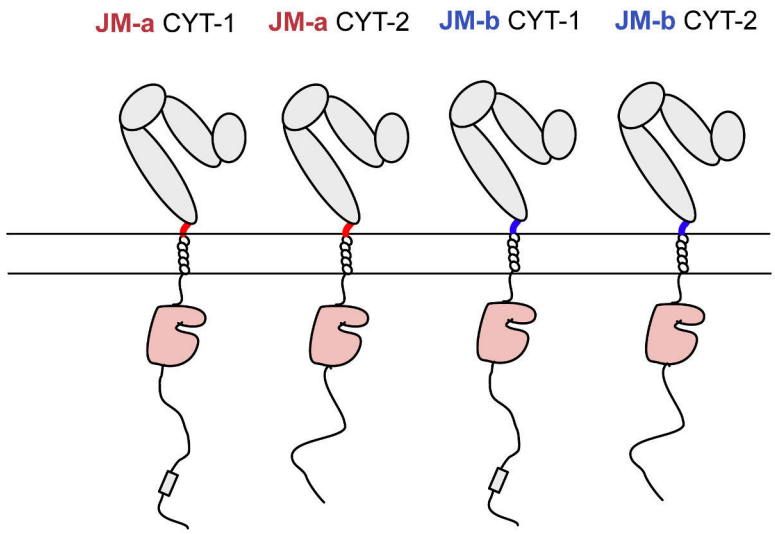

Figure 2. The isoforms of ErbB4. Alternative splicing produces the JM (juxtamembrane) and CYT (cytoplasmic) isoforms of ErbB4. Modified from (Veikkolainen et al., 2011).

The ErbB4 JM-a and JM-b isoforms are for the most part expressed in different tissues. The ErbB4 JM-a isoforms are predominantly expressed in the epithelial and the JM-b isoforms in the mesenchymal tissues. In the neural tissues both JM isoforms are expressed, but in different cell types (Elenius et al., 1997a; Veikkolainen et al., 2011). It is of note that to this day no cell type has been discovered that would naturally simultaneously express both JM-isoforms. The JM-isoform expression profile at single cell level, however, has not been sufficiently explored to attest the absence of such cell type.

Due to the tissue expression profile and cell-level isoform-specific investigations, different attributes of the physiological function of ErbB4 that have been discovered through genetic knock-out studies have been attributed to the different JM-isoforms. The mammary gland and kidney development have been attributed to the JM-a isoforms and the heart development to the JM-b isoforms (Gassmann et al., 1995; Elenius et al., 1997a; Jones et al., 1999; Long et al., 2003; Tidcombe et al., 2003; Muraoka-Cook et al., 2006; Veikkolainen et al., 2011; 2012; Skirzewski et al., 2020). Neural defects have been considered to be the result of the lack of both JM-isoforms (Elenius et al., 1997a; Tidcombe et al., 2003).

Isoform-specific knock-out of ErbB4 JM-a has further elucidated the role of the ErbB4 JM-isoforms in the development of different tissues. Genetic knock-out of ErbB4 JM-a isoforms had no adverse effects on the development of mammary glands, the heart, and the trigeminal ganglion, which are observed in the ErbB4 knock-out mice, where the genetic code for both JM-isoforms have been deleted. Cortical development, however, was significantly impaired. (Doherty et al., 2022).

Considering the previous research that has established ErbB4 JM-a as the activator of the central mammary gland factor STAT5a, the lack of effect on mammary gland development by the ErbB4 JM-a specific knock-out is surprising. However, the level of compensation that can be enacted by the ErbB4 JM-b isoform in the mammary gland has not been explored. Due to a lack of molecular mechanistic studies, it is unclear whether ErbB4 mediated STAT5a activation is still occurring in the JM-a isoform deficient mice or whether STAT5a signaling is also compensated by another factor such as STAT5b that has been previously discovered to be able to compensate for STAT5a in the mammary gland development (Liu et al., 1998).

The CYT-1 isoforms of ErbB4 contain an additional 16 amino acid long stretch in the C-terminal tail that is absent in the CYT-2 isoforms (Elenius et al., 1999). This stretch includes binding sites for PI3K (phosphoinositide 3-kinase), YAP1 (yes-associated protein) and the ubiquitin ligases Itch, Nedd4 (Neuronally expressed developmentally downregulated 4) and WWP1 (WW domain-containing E3 ubiquitin protein ligase 1). Due to these binding sites, the CYT-1 isoforms are more inclined to activate the PI3K-Akt pathway, induced YAP1 mediated transcription and to degrade than the CYT-2 isoforms (Elenius et al., 1999; Komuro et al., 2003; Sundvall et al., 2008; Feng et al., 2009; Zeng, Xu and Harris, 2009). All tissues that express ErbB4 seem to produce both CYT-1 and CYT-2 isoforms, except for placenta that only expresses the CYT-2 isoform (Elenius et al., 1999; Veikkolainen et al., 2011). Like the JM-isoforms, the CYT isoforms seem to affect differential cellular outcomes in different cell backgrounds. In an immortalized embryonic fibroblast cell line, expression of ErbB4 CYT-1, but not CYT-2, induced survival from starvation-induced cell death and chemotaxis (Kainulainen et al., 2000). In a kidney epithelial cell line, expression of ErbB4 CYT-1 promoted migration while expression of CYT-2 specifically suppressed it (Zeng et al., 2007). In adrenal gland pheochromocytoma cell line, only the expression of ErbB4 CYT-2 induced neurite outgrowth (Veikkolainen et al., 2011). In vivo the transgenic expression of the released ICD of ErbB4 CYT-1 induced early differentiation of mammary epithelia and the expression of the ICD of CYT-2 epithelial hyperplasia (Muraoka-Cook et al., 2009). When the full-length ErbB4 JM-a CYT-1 and CYT-2 isoforms were expressed in the mammary epithelia of transgenic mice, however, the CYT-1 isoform induced hyperplastic mammary lesions in 83% of mice and the CYT-2 isoform only in 17% of mice. The transgenic expression of full-length ErbB4 CYT-1 also decreased the proliferation of mammary epithelial cells during development. (Wali et al., 2014). These results indicate that the signaling of the ErbB4 JM-a CYT-isoforms involves more than the signaling of their released ICDs.

2.1.2 The VEGF receptor tyrosine kinases

The VEGF (vascular endothelial growth factor) family of RTKs consists of VEGFR1 (Flt1) (Shibuya et al., 1990; Matthews et al., 1991), VEGFR2 (Flk1, KDR) (Terman et al., 1991) and VEGFR3 (Flt4) (Alitalo et al., 1992) (Figure 3). The VEGF (vascular endothelial growth factor) receptors have five identified ligands that bind the receptors with different affinities. VEGF (VEGF-A) binds both VEGFR1 and 2 with a higher binding affinity for VEGFR1 (Ferrara and Henzel, 1989; De Vries et al., 1992; Terman et al., 1992). VEGF-B (Olofsson et al., 1996) and PIGF (placenta growth factor) (Maglione et al., 1991) bind only VEGFR1. VEGF-C and -D primarily bind VEGFR3 but after proteolytic processing can also bind VEGFR2 (Joukov et al., 1996; Lee et al., 1996; Orlandini et al., 1996). The VEGF receptors have two recognized co-receptors Neuropilin-1 and -2 that interact both with the receptors and the VEGF ligands (Chen et al., 1997; Kolodkin et al., 1997; Soker et al., 1998; Fuh, Garcia and de Vos, 2000; Karpanen et al., 2006; Xu et al., 2010).

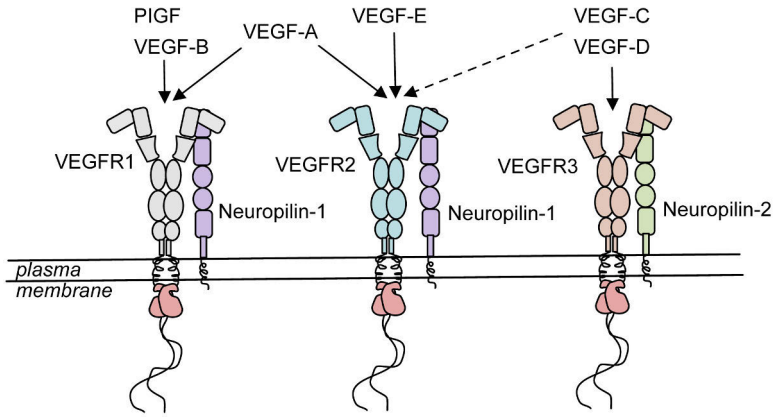

Figure 3. The VEGFR receptors, their ligands, and their co-receptors. VEGFR1 functions as a decoy receptor for VEGF-A. VEGF-C and VEGF-D mainly function as a ligand for VEGFR3, but proteolytic processing produces cleaved forms of these ligands that couple with VEGFR2 (dashed line). PIGF: placenta growth factor. VEGF: vascular endothelial growth factor. VEGFR: vascular endothelial growth factor receptor. Modified from (Olsson et al., 2006).

The function of both the VEGF ligands and receptors is heavily regulated by alternative splicing (Tischer et al., 1991; Kendall and Thomas, 1993; Maglione et al., 1993; Poltorak et al., 1997; Jingjing et al., 1999; Lange et al., 2003; Ebos et al., 2004; Woolard et al., 2004). Splicing produces short forms of both VEGFR1 and 2 that turn the receptors into extracellular ligand traps (Kendall and Thomas, 1993; Ebos et al., 2004; Albuquerque et al., 2009). Of the three receptors VEGFR1 has been discovered to function mainly as a decoy receptor that controls the availability

of VEGF for VEGFR2 (Hiratsuka et al., 1998; Rahimi, Dayanir and Lashkari, 2000). Genetic knock-out studies in mice have identified the essential role of the VEGF receptors and their ligands in vasculogenesis, angiogenesis and lymphangiogenesis. The genetic deletion of these receptors is lethal at embryonic stage due to defects in the development of the vasculature (Fong et al., 1995; 1999; Shalaby et al., 1995; Carmeliet et al., 1996; 2001; Dumont et al., 1998; Alitalo et al., 2004; Baldwin et al., 2005).

2.1.3 A detailed view of the structure of ErbB family receptor tyrosine kinases

RTKs comprise of extracellular, transmembrane and intracellular domains (Figure 4). These domains can further be divided into smaller functional domains such as kinase and ligand binding domains and even further into motifs such as binding motifs of various interacting proteins. The extracellular domain contains functional or non-functional ligand binding domains that vary in structure between RTK sub-families and to a lesser extent between sub-family members. The alpha-helical transmembrane domain consists of hydrophobic amino acid residues that anchor the receptor to the plasma membrane. The intracellular domain contains either a functional or non-functional kinase domain that oversees the phosphorylation of downstream substrates. The intracellular domain is enriched in motifs and domains that interact with intracellular signaling molecules (Lemmon and Schlessinger, 2010; Wheeler and Yarden, 2015).

EGFR was among the first discovered receptor tyrosine kinases. Ever since the discovery of EGFR and other family members of the ErbB family, ErbB receptors have been extensively studied and a vast amount of knowledge about the structure-function relationship of ErbB receptors has accumulated. ErbB receptors have been considered as the prototypical RTKs, although some previous reports have discovered unique structural features of ErbB receptors that are not shared by other RTKs (Ferguson, 2008; Lemmon, 2009; Lemmon and Schlessinger, 2010; Lemmon, Schlessinger and Ferguson, 2014).

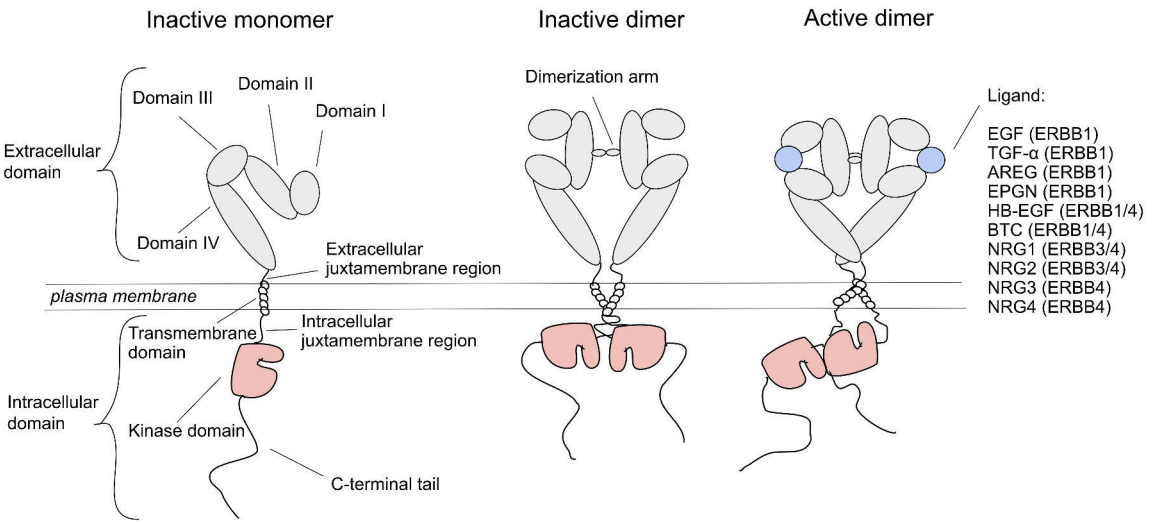

Figure 4. The structure of ErbB receptor tyrosine kinases and their inactive and active conformations. The receptors for the ligands are indicated in the parentheses. AREG: amphiregulin. BTC: betacellulin. EGF: epidermal growth factor. EPGN: epigenin. ERBB: erythroblastic leukemia viral oncogene. HB-EGF: heparin binding EGF-like growth factor. NRG: neuregulin. TGF-α: transforming growth factor α. Modified from (Ferguson, 2008; Arkhipov et al., 2013; Huang et al., 2021).

2.1.3.1 Extracellular domain of ErbB receptors is essential for growth factor binding and receptor activation

The extracellular domain of ErbB receptors contains four recognized domains (I–IV) and a short, 7–27 amino acids long, extracellular juxtamembrane region (eJM) (Figure 4). The domains I and III are enriched in β-helical leucine-rich repeat-like structures and directly bind to the receptor ligands. The domains II and IV in turn are cysteine rich. (Garrett et al., 2002; Ogiso et al., 2002). Crystal structures of the ErbB receptors have revealed that the ligand binding to the domains I and III results in a conformational shift that extends the receptor and reveals a dimerization arm in domain II (Figure 1) (Cho and Leahy, 2002; Ferguson et al., 2003; Bouyain et al., 2005). In the unbound tethered state, the dimerization arm is hidden by intramolecular interactions with key residues in domain IV (Cho and Leahy, 2002; Ferguson et al., 2003; Bouyain et al., 2005). Domain IV is also directly involved in dimerization by contacts in the dimerization interface that contribute to some extent to the stability of the dimer (Dawson et al., 2005; Lu et al., 2010). The extracellular EGFR domains I-IV host several N-glycosylation sites (Zhen, Caprioli and Staros, 2003). N-glycosylation of the domains I-IV has been discovered to have a critical role in the dimerization (Fernandes, Cohen and Bishayee, 2001; Takahashi et al., 2008), oligomerization (Tsuda, Ikeda and Taniguchi, 2000), ligand binding (Tsuda, Ikeda and Taniguchi, 2000; Yen et al., 2015), plasma membrane interactions

(Kaszuba et al., 2015) and autophosphorylation (Kawashima et al., 2009; Park et al., 2012; Yen et al., 2015) of the ErbB receptors, indicating that these post-translational modifications are essential for the function of these receptors. Different ligands induce either a juxtaposed or separate alignment of the C-terminal region of the Domain IV indicating that the extracellular domain also mediates the differential responses induced by different ligands (Huang et al., 2021).

2.1.3.2 The eJM region of ErbB receptors regulates receptor activation by restricted length, cleavage and glycolipid interactions

The eJM region is less researched than other domains and regions of ErbB RTKs and consequently, only a few known functions originating from this region have been reported (Figure 4). Extension of the eJM region has been reported to promote autoactivation of the receptor indicating that the restricted length of this region is crucial for controlled receptor activation (Sorokin, 1995). The eJM region of EGFR harbors a lysine residue, which was discovered to interact with the ganglioside GM3. This interaction was shown to lead to the inhibition of EGFR autophosphorylation indicating that interactions in this region may have a significant effect on receptor function (Coskun et al., 2011). Another mechanism arising from the eJM region that can significantly affect the function of ErbB receptors was discovered in the JM-a isoform of ErbB4. The eJM region of ErbB4 JM-a isoform was discovered to host cleavage sites for the ADAM17 protease. The cleavage by the ADAM17 protease releases the extracellular domain of the ErbB4 JM-a isoform thus compelling the receptor resistant to more ligand stimulation (Rio et al., 2000).

2.1.3.3 The transmembrane domain of ErbB receptors is involved in receptor dimerization

The transmembrane domain of the ErbB RTKs consists of an alpha helix of hydrophobic amino acid residues that span the plasma membrane (Figure 4). The transmembrane domain harbors GxxxG motifs that mediate the dimerization of the receptors (Lemmon et al., 1994). The transmembrane domains of ErbB receptors are known to self-associate (Mendrola et al., 2002), but autophosphorylation of the receptors has been resistant to the mutagenesis of the transmembrane region (Kashles et al., 1988; Carpenter et al., 1991; Lu et al., 2010), indicating more of a stabilizing role for the transmembrane domain in receptor dimerization. Mutagenesis of the more N-terminal GxxxG motif region of EGFR, however, reduced autophosphorylation of EGR by around 50% when stimulated with EGF indicating that this GxxxG motif region is more important for EGF induced receptor dimerization than the C-terminal GxxxG motif region (Endres et al., 2013). Cross-

linking and ToxR based transcriptional activation assay studies with transmembrane peptides have confirmed this observation by identifying the N-terminal GxxxG motif as the dimerization contact site between EGFR monomers and EGFR/ErbB2 dimers (Gerber, Sal-Man and Shai, 2004; Lu et al., 2010). Interestingly, not all ligands induce contact between the monomers in this motif region upon binding to the receptor, which would indicate that the transmembrane region is also involved in mediating the differential responses induced by differential ligand binding (Sinclair et al., 2018; Huang et al., 2021). More recent advances have indicated that the EGFR monomers dimerize in the more C-terminal GxxxG motifs when stimulated with the ligand TGFα (Sinclair et al., 2018; Huang et al., 2021) or when they form a dimer unstimulated (Landau and Ben-Tal, 2008; Arkhipov et al., 2013).

2.1.3.4 The iJM region of ErbB receptors controls receptor autophosphorylation by several mechanisms

Studies with structural variants of the EGFR receptor have identified the intracellular juxtamembrane (iJM) region in the intracellular domain of ErbB receptors as essential for autophosphorylation of the receptor (Zhang et al., 2006; Thiel and Carpenter, 2007; Red Brewer et al., 2009) (Figure 4). It has been discovered that one of the iJM regions interacts with one of the kinase domains in the receptor dimer, therefore stabilizing the dimerization of the kinase domains. This region in the iJM was termed the juxtamembrane latch. (Wood et al., 2008; Jura et al., 2009a; Red Brewer et al., 2009). Deletion of the regions outside of the juxtamembrane latch still abolishes EGFR autophosphorylation indicating that the latch is not the only essential subregion in the iJM region (Thiel and Carpenter, 2007; Jura et al., 2009a). The region outside the juxtamembrane latch includes an alpha helix that interacts with its counterpart during dimerization (Red Brewer et al., 2009; Endres et al., 2013). Interaction between phosphatidylinositol 4,5-bisphosphate in the inner leaflet of the plasma membrane and the alpha helix is needed to stabilize the iJM alpha helix dimer (Halim, Koldsø and Sansom, 2015; Maeda et al., 2018). The interaction in between the iJM alpha helices varies depending on the bound ligand indicating that this region is also important for mediating the responses of differential ligand binding (Scheck et al., 2012; Doerner, Scheck and Schepartz, 2015). The basic residues of the region outside the juxtamembrane latch were additionally discovered to interact with anionic plasma membrane lipids and this interaction was shown to be involved in the clusterization of the receptor in the plasma membrane. Disruption of the receptor clusterization negatively affected autophosphorylation indicating that interaction with the anionic plasma membrane lipids is yet another mechanism by which the iJM region controls ErbB receptor autophosphorylation. (Wang et al., 2014). The mutation of these basic residues conferred ligand-independent activation

of EGFR indicating that these residues also serve in an auto-inhibitory role (Bryant et al., 2013; Mohr et al., 2020).

In the JM-a variant of ErbB4 receptor, the intracellular domain is cleaved off from the receptor by γ-secretase after the extracellular domain is shed by the ADAM17 protease. The site for this cleavage resides in the iJM region of ErbB4. (Elenius et al., 1997a; Ni et al., 2001; Vidal et al., 2005). Downstream of the γ-secretase cleavage site a nuclear localisation signal is located in the receptor that allows the released ICD of ErbB4 to enter the nucleus (Williams et al., 2004).

2.1.3.5 The intracellular domain of ErbB receptors phosphorylates and interacts with downstream substrates, and is heavily regulated by post-translational modifications

In addition to the iJM the ICD of ErbB receptors consists of a kinase domain and the C-terminal tail (Figure 4). The kinase domain as per its name is responsible for the phosphorylation of substrates and consists of a N-terminal and C-terminal lobe. The ATP binding pocket resides between the lobes. Activation of the receptors by ligand binding induces the kinase domains of the monomers to form an asymmetric dimer so that the C-lobe of the 'activator' kinase domain interacts with the N-lobe of the 'receiver' kinase domain. Only the C-terminal tail of the 'activator' is consequently phosphorylated by the 'receiver' kinase domain of EGFR homodimers and ErbB2/ErbB4 heterodimers. (Zhang et al., 2006; Qiu et al., 2008; Ward and Leahy, 2015). In the EGFR/ErbB2 and EGFR/ErbB4 heterodimers and ErbB4 homodimer both the C-terminal tails following the receiver and activator kinase domains are phosphorylated (Ward and Leahy, 2015). The kinase domains form a symmetric dimer in the inactive receptor dimers (Jura et al., 2009a; Arkhipov et al., 2013).

The C-terminal tail is a labile intrinsically disordered region full of ErbB autophosphorylation dependent substrate binding motifs (Schulze, Deng and Mann, 2005; Feracci et al., 2011; Keppel et al., 2017; Wang et al., 2018). These motifs are mainly bound by the phosphotyrosine-binding (PTB), Src homology 2 (SH2), Src homology 3 (SH3) and WW domains of the downstream substrates of ErbB receptors (Komuro et al., 2003; Schulze, Deng and Mann, 2005). The function of the intracellular domain of ErbB receptors is heavily regulated by various post-translational modifications (PTMs). On top of the phosphorylation of the autophosphorylation sites that allows for the binding of substrates, the ICDs of ErbB receptors are regulated by tyrosine phosphorylation by intracellular tyrosine kinases (Stover et al., 1995; Yamauchi et al., 1997; Tanos and Pendergast, 2006), serine/threonine phosphorylation (Hunter, Lingt and Cooper, 1980; Davis, 1988; Takishima et al., 1991; Theroux et al., 1992; Barbier et al., 1999), ubiquitiniation (Levkowitz et al., 1998), sumoylation (Sundvall et al., 2012; Packham et al., 2015),

acetylation (Song et al., 2011), palmitoylation (Runkle et al., 2016) and neddylation (Oved et al., 2006). These PTMs have a diverse effect on the function of the receptor and serve as more than just the mediators of intracellular receptor interactions (Stover et al., 1995). Changes in receptor sorting and receptor degradation (Levkowitz et al., 1998; Oved et al., 2006), in the intracellular localization of the receptor (Tanos and Pendergast, 2006; Knittle et al., 2017) and receptor activity (Hunter, Lingt and Cooper, 1980; Davis, 1988; Theroux et al., 1992; Barbier et al., 1999; Runkle et al., 2016) have at least been observed as a consequence of these PTMs.

There are some indications that the C-terminal tail regulates receptor function by mechanisms that do not involve interplay with other intracellular molecules. Deletion studies of the C-terminal tails of ErbB receptors have indicated that the more N-terminal part of the C-terminal tail has an autoinhibitory role and the more C-terminal part would promote receptor activation (Walton et al., 1990; Alvarez et al., 1995; Kovacs et al., 2015). The autoinhibitory role for the N-terminal part is supported by crystal structures of the inactive kinase domain that revealed packing of this region against the N-lobe of the kinase domain (Zhang et al., 2006; Wood et al., 2008; Jura et al., 2009b). Another finding that supports the suggested additional roles for the C-terminal tail is the observed conformational changes in the C-terminal tail after autophosphorylation (Lee and Koland, 2005; Lee, Hazlett and Koland, 2006; Okamoto and Sako, 2018; Regmi et al., 2020). These hypothetical mechanisms of the C-terminal tail, however, remain to be confirmed.

2.1.4 The signaling of ErbB receptor tyrosine kinases

RTKs acts as amplifiers that multiply the signal mediated by ligand binding by activating several intracellular signaling cascades that canonically lead to changes in gene expression. Most of these cascades are shared among human receptor tyrosine kinase families, but receptor and receptor family specific signaling cascades may also exist. It is of note that the signaling of RTKs is not mechanistically uniform or independent of the cellular environment. While RTKs transmit their signals through roughly the same downstream effectors, the determinants that allow only some activated RTKs to activate certain downstream effectors in specific contexts, remain poorly defined due to lack of comparative studies. Here the main cascades activated by the prototypical ErbB family RTKs are shortly reviewed (Figure 5).

The signaling cascades of ErbB receptors primarily start with the binding of adaptor proteins to the autophosphorylated residues. The binding of Src homology 2 domain containing transforming protein 2 (SHC2) or growth factor receptor-bound protein 2 (GRB2) starts a cascade involving Sons of sevenless (SOS), rat sarcoma virus (RAS) proteins, rapidly accelerated fibrosarcoma (RAF) kinases,

mitogen-activated protein kinase kinase (MEK) and extracellular signal-regulated kinases (ERK) that leads to changes in gene transcription that most often translate to cell proliferation and growth (McKay and Morrison, 2007). Other mitogen-activated protein kinases (MAPKs) like those involved in the apoptotic c-Jun N-terminal kinase (JNK) cascade (including p21-activated kinases (PAKs), c-Jun N-terminal kinase kinase (JNKK), JNK, c-Jun and c-Fos) (Bost et al., 1997), p38 MAPK cascade or ERK5 cascade (including Mitogen-activated protein kinase kinase kinase 2/3 (MEKK2/3), MEK5, ERK5 and myocyte enhancer factor 2 (MEF)) are also activated by ErbB receptors through the adaptors non-catalytic region of tyrosine kinase adaptor proteins (NCKs) and T cell specific adaptor protein (TSAd) (Bost et al., 1997; Poitras et al., 2003; Sun et al., 2003; Huang, Jacobson and Schaller, 2004). The JNK cascade can also be activated by the guanine nucleotide exchange factors VAVs that activate small GTP proteins Rhos or RACs (Olson et al., 1996; Kaminuma et al., 2001) and are bound by ErbB receptors (Pandey et al., 2000; Ojala et al., 2020). Activation of the JNK cascade by the VAVs usually leads to cytoskeletetal rearrangement or changes in cell migration (Huang, Jacobson and Schaller, 2004). The binding of the adaptor protein CRK to EGFR has been discovered to induce the activation of the Abelson murine leukemia viral oncogene homolog (ABL) kinase (Birges et al., 1992; Sriram et al., 2014).

The binding of phosphatidylinositol 3-kinases (PI3Ks) to the autophosphorylated sites of ErbB receptors induces the PI3Ks to convert phosphatidylinositol (4,5)-bisphosphate (PIP2) to phosphatidylinositol (3,4,5)-trisphosphate (PIP3), which consequently activates the Protein kinase B (Akt) pathway through pyruvate dehydrogenase kinase 1 (PDK1). The PI3K/Akt pathway is often associated with cell anabolism by inhibition of the natural inhibitors of mammalian target of rapamycin (mTOR), cell growth and survival. (Carter and Downes, 1992; Soltoff et al., 1994; Sepp-Lorenzino et al., 1996). Calcium signaling is controlled by the ErbB receptors through the activation of phospholipase C γ (PLCγ) that converts phosphatidylinositol 4,5 bisphosphate (PtdIns(4,5)P2) into inositol 1,4,5-trisphosphate (IP3) and diacylglycerol (DAG). DAG in turn activates the protein kinase Cs (PKCs) and increased concentration of IP3 in the cytosol results in the release of calcium to the cytosol. (Margolis et al., 1989; Peles et al., 1991; Vecchi, Baulida and Carpenter, 1996; Yang et al., 2013; Obeng et al., 2020). ErbB receptors also induce nuclear factor kappa-light-chain-enhancer of activated B cells (NF-κβ) signaling by the IkappaB kinases (IKKs) and NF-kappa-B essential modulator (NEMO) (Merkhofer, Cogswell and Baldwin, 2010; Shostak and Chariot, 2015).

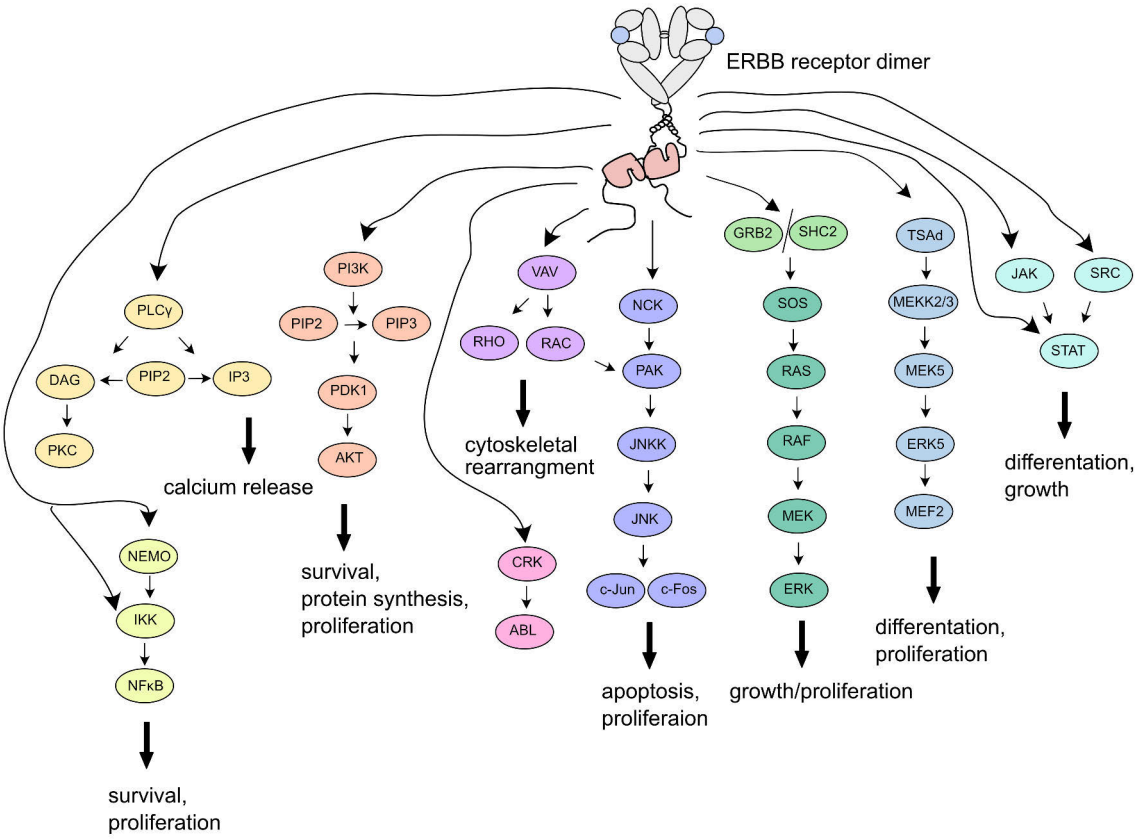

Figure 5. The common signaling pathways activated by ErbB receptors. The cellular outcomes most often associated with the signaling pathways when activated by ErbB receptors are indicated. ABL: Abelson murine leukemia viral oncogene homolog. AKT: AKT serine/threonine kinase. DAG: diacylglycerol. ERK: extracellular signal-regulated kinase. GRB2: growth factor receptor bound protein 2. IKK: IkappaB kinase. IP3: inositol trisphosphate. JAK: Janus kinase. JNK: c-Jun N-terminal protein kinase. JNKK: c-Jun N-terminal protein kinase kinase. NCK: non-catalytic region of tyrosine kinase adaptor protein. NEMO: NF-kappa-B essential modulator. NFκB: nuclear factor kappa-light-chain-enhancer of activated B cells. MEF2: myocyte enhancer factor 2. MEK: mitogen-activated protein kinase kinase. MEKK2/3: mitogen-activated protein kinase kinase kinase 2/3. PAK: p21 (rac1) activated kinase 1. PDK1: phosphoinositide-dependent kinase-1. PI3K: phosphoinositide 3-kinase. PIP2: phosphatidylinositol (4,5)-bisphosphate. PIP3: phosphatidylinositol (3,4,5)-trisphosphate. PKC: protein kinase C. PLCγ: phospholipase C γ. RAF: rapidly accelerated fibrosarcoma. RAS: rat sarcoma virus. SHC2: Src homology 2 domain containing transforming protein 2. SOS: son of sevenless homolog. STAT: signal transducer and activator of transcription. TSAd: T cell specific adaptor protein. Modified from (Yarden and Sliwkowski, 2001).

2.1.4.1 The STAT pathway

Signal transducer and activators of transcription (STAT) proteins can be activated by the ErbB receptors via Src family or Janus family kinases (JAK1, JAK2, JAK3

and TYK2) and presumably also directly (David et al., 1996; Leaman et al., 1996; Olayioye et al., 1999; Muraoka-Cook et al., 2008). The human genome encodes seven different STAT proteins, STAT1, STAT2, STAT3, STAT4, STAT5a, STAT5b and STAT6 (Schindler et al., 1992; Shuai et al., 1992; Copeland et al., 1995; Wakao, Gouilleux and Groner, 1995). The two STAT5s are considered to be the result of an evolutionary gene duplication event and share high, over 96%, amino acid sequence homology (Copeland et al., 1995; Mui et al., 1995). Despite the high sequence homology, the two STAT5s have both redundant and specific functions (Grimley, Dong and Rui, 1999). STATs function as transcription factors that induce the transcription of their target genes (Schindler et al., 1992; Shuai et al., 1992). The cellular outcome upon STAT activation depends on which STAT is activated and on the cellular context. Generally, STAT1 induces the transcription of pro-apoptotic factors, STAT3 and STAT5s induce survival and growth and all STATs have prominent but differential roles in immune cell functions. STAT5a is additionally a key factor in the differentiation of mammary glands and lactation (Levy and Darnell, 2002; Villarino, Kanno and O'Shea, 2017; Philips et al., 2022).

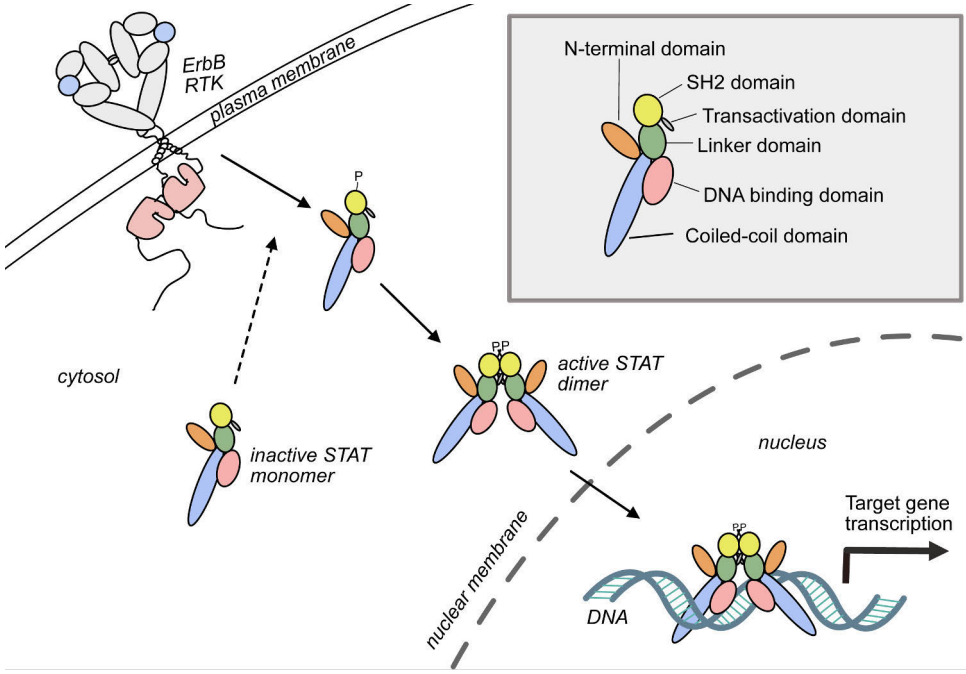

Figure 6. The structure and function of STATs as downstream effectors of ErbB RTKs. ErbB receptors phosphorylate STATs in the activating tyrosine residue in the SH2 domain. This phosphorylation leads to the dimerization of STATs and accumulation of the STAT dimers into the nucleus or mitochondria. In the nucleus or mitochondria, the activated STAT dimers induce the transcription of their target genes. P: phosphorylated residue. SH2: SRC homology domain 2. STAT: signal transducer and activator of transcription. RTK: receptor tyrosine kinase. Modified from (Levy and Darnell, 2002; Li et al., 2023).

Upon activation by phosphorylation of the activating tyrosine residue, the STATs dimerize and accumulate into the nucleus to the promoter sites of their target genes (Shuai et al., 1992; 1994) (Figure 6). In inactivated monomer state, the STATs are diffusely located both in the cytosol and nucleus (Zeng et al., 2002; Liu, McBride and Reich, 2005). STATs consist of an N-terminal domain that is involved in STAT oligomerization (Vinkemeier et al., 1998; John et al., 1999), a coiled-coiled domain, a DNA binding domain that binds to DNA target sequences in the promoter sites (Horvath, Wen and Darnell, 1995), a SH2 domain that binds to phosphorylated tyrosine residues and acts as the dimerization interface for the activated dimer (Shuai et al., 1994), a linker domain and, a C-terminal transactivation domain (Figure 6). The activating tyrosine residue resides in the SH2 domain (Shuai et al., 1993). The STATs bind to other transcription factors, co-activators and co-repressors through the coiled-coil, DNA-binding, linker and transactivation domains (Bhattacharya et al., 1996; Horvath et al., 1996; Yang et al., 1999; Zhu et al., 1999; Nakajima et al., 2001). The nuclear localization signal for the inactive monomer resides in the coiled-coil domain and the nuclear localization for the active dimer in the DNA-binding domain (Strehlow and Schindler, 1998; McBride et al., 2002; Zeng et al., 2002; Liu, McBride and Reich, 2005).

RTKs have the tendency to activate some but not all STATs in the same cellular context (Korpelainen et al., 1999; Olayioye et al., 1999; Yang et al., 2009). The mechanisms of selective STAT activation by RTKs remain unknown.

2.2 Myocardial growth

2.2.1 Myocardial growth during the life span

During embryogenesis the cardiac progenitor cells originate from the mesoderm (Garcia-Martinez and Schoenwolf, 1993; Tam et al., 1997). Two different sources called heart fields of progenitor cells from the mesoderm that finally constitute the myocardium have been identified (Buckingham, Meilhac and Zaffran, 2005). These pools of progenitor cells are highly proliferative, and the initial heart tube is mainly developed by the proliferation of these progenitor cells (van den Berg et al., 2009; de Boer et al., 2012). The already formed cardiomyocytes contribute to the myocardial growth later by re-entering the cell cycle in a process called dedifferentiation when the heart tube loops to form the four distinct chambers (Christoffels et al., 2000; Soufan et al., 2006). Further myocardial growth and trabecular formation during the embryonic and fetal stage is achieved by locally varying rates of cardiomyocyte proliferation (Li et al., 1996; de Boer et al., 2012). The signal for the formation of the trabeculae comes from the endocardial lining (Meyer and Birchmeier, 1995; Meyer et al., 1997; Luxán et al., 2016). After trabecular formation the cardiomyocyte division is mainly controlled

by the epicardium (Sucov et al., 2009). At the perinatal period the proliferation rate of cardiomyocytes drastically declines. One week after birth, the proliferation of most cardiomyocytes has seized in mice (Li et al., 1996). In humans, cardiomyocyte proliferation contributes significantly to myocardial growth still within the first 20 years, but postnatal, childhood, adolescent and adult myocardium growth is mainly accomplished by cardiomyocyte hypertrophy (Li et al., 1996; Mollova et al., 2013; Alkass et al., 2015; Bergmann et al., 2015). The annual renewal rate of cardiomyocytes at the adult stage is very low, less than 1% (Bergmann et al., 2015). The different stages of myocardium development during the lifespan are visualized in Figure 7.

During the peri- and postnatal period, a proportion of the cardiomyocytes become binucleated or polyploid (Soonpaa et al., 1996; Walsh et al., 2010; Mollova et al., 2013; Alkass et al., 2015; Bergmann et al., 2015). In human the polyploidization occurs over the first two decades (Bergmann et al., 2015). These polyploid and binucleated cardiomyocytes are considered to be terminally differentiated and unable to divide. Regeneration of cardiomyocytes after injury is accomplished by proliferation of the remaining mononuclear and diploid cardiomyocytes, suggesting that the size of the pool of mononuclear and diploid cardiomyocytes in the myocardium contributes to the extent of its regenerative capability. (Bersell et al., 2009; Senyo et al., 2013; Patterson et al., 2017). The current consensus in the field is that cardiac stem cells and progenitors contribute minimally to the regeneration of cardiomyocytes in adults, less than 0.01% per year (Van Berlo et al., 2014; Sultana et al., 2015; Eschenhagen et al., 2017b). In the adult zebrafish, the cardiomyocytes retain their ability to proliferate. The adult zebrafish cardiomyocytes remain diploid and mononuclear suggesting that these, indeed, are the key characteristics of cardiomyocytes that maintain regenerative capability. (Poss, Wilson and Keating, 2002; Belmonte et al., 2010) Consistently, introduction of polyploidization to adult zebrafish cardiomyocytes limits their regenerative capability (González-Rosa et al., 2018).

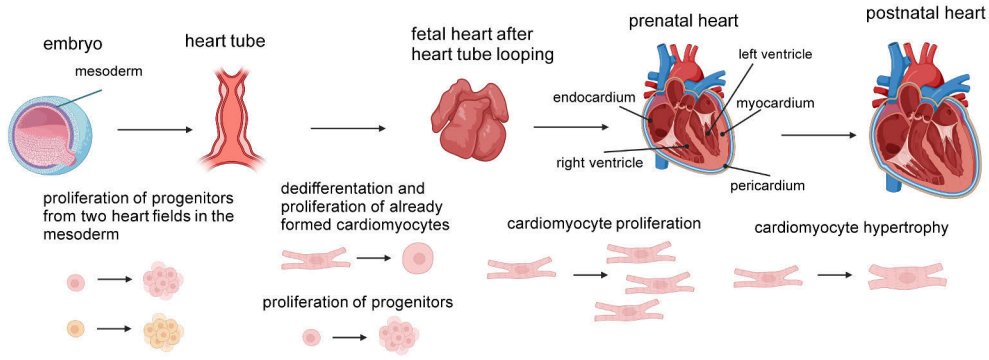

Figure 7. Myocardial growth at different stages of life.

2.2.2 From pathological hypertrophy to heart failure

2.2.2.1 The difference between physiological and pathological hypertrophy

The postnatal myocardium compensates against sustained increased workload and ventricular wall stress by inducing hypertrophic growth. Based on the type of stimulus and the phenotype of the cardiac enlargement, two different types of cardiac hypertrophy have been identified: physiological and pathological (Figure 8). While physiological hypertrophy has a beneficial effect on the cardiac function, pathological hypertrophy leads to impaired cardiac function. Physiological hypertrophy is characterized by a milder proportional and mainly eccentric enlargement of the myocardium and increased cardiomyocyte diameter both in width and length. Pathological hypertrophy in turn is concentric where the dimensions of the chamber are reduced in relation to the increase in ventricular wall mass. The cardiomyocytes in pathological hypertrophy are enlarged more in width than in length. The stimuli that lead to physiological hypertrophy are mainly normal postnatal growth, pregnancy, and exercise. Pathological hypertrophy in turn is triggered by increased pressure overload caused by hypertension, aortic stenosis, volume overload caused by valve or kidney diseases, myocardial hypoxia or other myocardial diseases. While association of certain signaling pathways to certain type of hypertrophy have been discovered, it is of note that several myocardial growth pathways can play a role in both types of hypertrophy. The current consensus in the field suggests that the outcome of each myocardial growth signal is context-dependent (Nakamura and Sadoshima, 2018).

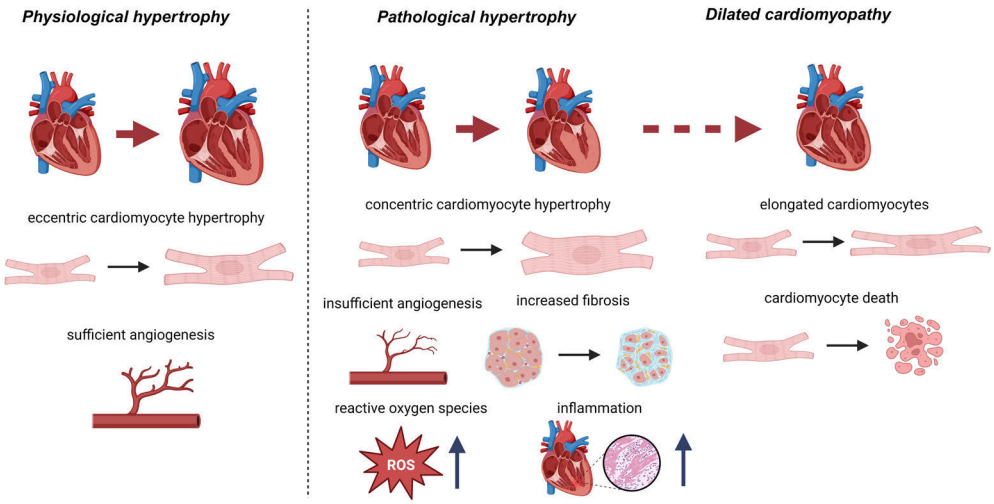

Figure 8. The hallmarks of physiological and pathological hypertrophy. Pathological hypertrophy can lead to dilated cardiomyopathy and heart failure.

2.2.2.2 Maladaptation to decompensatory hypertrophy leads to heart failure

While physiological hypertrophy induced by exercise or pregnancy is reversible, pathological hypertrophy will persist without therapeutic intervention. Pathological hypertrophy will often lead to a condition called dilated cardiomyopathy marked by ventricular chamber dilation and cardiomyocyte elongation. This progression from the initial short-term adaptive concentric response of pathological hypertrophy to the maladaptive remodeling leads to contractile dysfunction and finally to heart failure. The hallmarks of pathological hypertrophy that do not occur in physiological hypertrophy, exacerbate the condition by reducing the contractility of the ventricular myocardium. These hallmarks include increased fibrosis, cardiomyocyte death, dysregulated calcium signaling, insufficient angiogenesis, inflammation and altered cardiomyocyte metabolism favouring the production of reactive oxygen species. (Nakamura and Sadoshima, 2018). Heart failure is categorized into three groups based on preserved, mid-range or reduced ejection fraction (HFpEF, HFmrEF, HFrEF), a measure that represents the fraction of blood volume ejected from the left ventricle in one heartbeat (Borlaug, 2020; Murphy, Ibrahim and Januzzi, 2020; Savarese et al., 2022).

2.2.3 NRG-1/ErbB signaling in myocardial growth

Early knock-out studies in mice identified the essential role of NRG-1, ErbB2 and ErbB4 in ventricular trabeculation (Gassmann et al., 1995; Lee et al., 1995; Meyer and Birchmeier, 1995). During trabeculation NRG-1 is secreted by the endothelial cells from the endocardial lining (Meyer and Birchmeier, 1995). The secreted NRG-1 activates the ErbB2/ErbB4 heterodimer in the cardiomyocytes, which induces the cardiomyocytes to proliferate and form the trabeculae (Lee et al., 1995; Meyer and Birchmeier, 1995). The Nrg-1, Erbb2 and Erbb4 knock-outs in mice are embryonically lethal due to defects in heart function due to insufficient trabeculation and growth of the ventricular wall (Gassmann et al., 1995; Lee et al., 1995; Meyer and Birchmeier, 1995). To circumvent this, conditional knock-out studies have been performed in adult mice. Conditional knock-out of genes along the NRG-1/ErbB2/ErbB4 signaling axis in the myocardium results in dilated cardiomyopathy in adult mice suggesting that the signaling pathway is not only crucial during development but also needed to maintain the adult myocardium (Crone et al., 2002; Özcelik et al., 2002; García-Rivello et al., 2005). This observation was further confirmed by experiments demonstrating that the administration of the anti-ErbB2 antibody trastuzumab caused cardiomyopathies in some breast cancer patients especially when coupled with the administration of anthracyclines such as doxorubicin (Ennis S Lamon et al., 2001; Wadhwa et al., 2009; Bowles et al., 2012). In concordance, doxorubicin-mediated cardiomyopathy has been discovered to be associated with microRNA 146a mediated degradation of ErbB4

mRNA in cardiomyocytes (Horie et al., 2010). The NRG-1/ErbB2/ErbB4 signaling axis is also involved in the physiological hypertrophy induced by pregnancy (Lemmens, Doggen and De Keulenaer, 2011). Genetic deletion of another ligand of the ErbB2/ErbB4 heterodimer, HB-EGF, leads to a similar myocardial growth defect in embryonic and adult mice than the deletion and the conditional deletion of the genes along the NRG-1/ErbB2/ErbB4 signaling axis (Iwamoto et al., 2003; Yamazaki et al., 2003). The phenotype reminiscent of dilated cardiomyopathy of the adult HB-EGF null mice was exacerbated by the genetic deletion of another ligand for ErbB2/ErbB4 heterodimer betacellulin (Jackson et al., 2003).

NRG-1 is expressed by endothelial cells in the endocardium and capillaries of the adult heart (Cote et al., 2005; Lemmens et al., 2006; Iivanainen et al., 2007) and released mainly by the ADAM17 protease (Montero et al., 2000). In the adult heart ErbB2 and ErbB4 are mainly expressed in the cardiomyocytes (Özcelik et al., 2002). It is of note, that only the JM-b isoforms of ErbB4 are expressed in the post-natal heart (Elenius et al., 1997a; Veikkolainen et al., 2011; Wang et al., 2021).

NRG-1 induces proliferation of isolated cardiomyocytes at embryonic stage and hypertrophy at post-natal stage indicating that the NRG-1/ErbB2/ErbB4 signaling axis is involved in both phases of cardiomyocyte growth (Zhao et al., 1998; Baliga et al., 1999). Transgenic overexpression of ERBB2 leads to a type of cardiomegaly in neonatal and adult mice where both proliferative and hypertrophic cardiomyocyte growth occurs along with cardiomyocyte dedifferentiation (D'uva et al., 2015). Studies in zebrafish have indicated that the role of the NRG-1/ErbB signaling pathway in myocardial growth is conserved in different species. Defects in trabeculation and ventricular wall growth are observed in transgene zebrafish embryos expressing a mutated version of Erbb2 or a ligand-trap for the Erbb4 ligand Nrg2a or in larvae treated with a small molecule inhibitor of ErbB receptors (Fleming et al., n.d.; Liu et al., 2010; Rasouli and Stainier, 2017). Overexpression of transgene Nrg1 in adult zebrafish leads to cardiomegaly similarly to the transgenic overexpression of ERBB2 in adult mice with the exception of only inducing cardiomyocyte proliferation and dedifferentiation and no cardiomyocyte hypertrophy (D'uva et al., 2015; Gemberling et al., 2015).

The trabeculation and ventricle wall growth effect of NRG-1/ErbB2/ErbB4 signaling axis during cardiogenesis has been attributed to Erk signaling due to a correlation of the change in phosphorylated Erk levels in the myocardium of the left ventricle with NRG-1 null or wild-type phenotype in mice (Lai et al., 2010). NRG-1 has been discovered to stimulate the phosphorylation of Erk in cardiomyocytes in several in vivo and in vitro models (Baliga et al., 1999; Sawyer et al., 2002; Kuramochi, Guo and Sawyer, 2006; Liu et al., 2006; Lemmens, Doggen and De Keulenaer, 2011). In isolated adult cardiomyocytes, the expression of hypertrophic genes induced by NRG-1 treatment was downregulated with an inhibitor targeting the upstream regulator of Erk,

MEK (Baliga et al., 1999). However, treatment with ErbB2 siRNA, ErbB4 siRNA or with an anti-ErbB2 antibody has had only a slight or no effect on the phosphorylation levels of Erk in NRG-1 stimulated cardiomyocytes (Sawyer et al., 2002; Kuramochi, Guo and Sawyer, 2006; Wang et al., 2021). Due to a discrepancy in the effect magnitude of ErbB2 and ErbB4 siRNA treatment on NRG-1 induced phosphorylation of Erk and cardiomyocyte hypertrophy, a recent report concluded that the activation of Erk alone is not sufficient to induce the level of cardiomyocyte hypertrophy that is induced by NRG-1 treatment (Wang et al., 2021). Chemical inhibition of ErbB1 and ErbB2 with lapatinib, however, has been shown to downregulate the NRG-1 induced phosphorylation of Erk in the left ventricle, which raises the question of the role of ErbB1 in the process. Indeed, the phosphorylation of ErbB1 in the left ventricle increases by NRG-1 treatment and is downregulated by lapatinib (Lemmens, Doggen and De Keulenaer, 2011). While the signals for phosphorylated ErbB1 and Erk after NRG-1 administration may arise from non-myocytes in the left-ventricle, administration of the ErbB1 ligand EGF is sufficient to phosphorylate Erk in isolated cardiomyocytes and in the left ventricle (Rebsamen et al., 2000; Lemmens, Doggen and De Keulenaer, 2011). A significant downregulation of basal Erk phosphorylation in response to anti-ErbB2 treatment has, however, been observed in non-stimulated cardiomyocytes (Pentassuglia et al., 2007). Similarly, the hypertrophic cardiomyocyte response to the transgenic expression of constitutively active ErbB2 is attenuated by the chemical inhibition of both Erk and Akt pathways (D'uva et al., 2015). Inhibition of Erk also reduced cardiomyocyte proliferation and dedifferentiation, while inhibition of Akt additionally reduced only cardiomyocyte proliferation, in the transgenic ErbB2 mice model (D'uva et al., 2015). Inhibition of the PI3K/Akt pathway, however, has been reported to be unable to attenuate NRG-1 induced protein synthesis and expression of hypertrophy genes in isolated cardiomyocytes, but still to be sufficient to disrupt the sarcomeric structure (Baliga et al., 1999). Due to the partly conflicting results in isolated cardiomyocytes and *in vivo* in the myocardium, it remains unclear which aspects of the myocardial growth response of NRG-1 are mediated by Erk and Akt signaling and to what extent.

2.2.3.1 NRG-1/ErbB signaling in cardiac injury models

Administration of recombinant NRG-1 induces proliferation of cardiomyocytes after myocardial infarction induced injury in mice (Bersell et al., 2009). Administration of recombinant NRG-1 also has improved survival of the treated animals and the structure and function of the left ventricle in several *in vivo* models of cardiac injury induced by myocardial infarction (Liu et al., 2006; Bersell et al., 2009; Fang et al., 2010; Gu et al., 2010; Guo et al., 2012; Hill et al., 2013; Galindo et al., 2014), doxorubicin (Liu et al., 2006; Bian et al., 2009), myocarditis (Liu et al., 2006), diabetes (Li et al., 2011) and pacing (Liu et al., 2006) (Table 1). In addition to improved left ventricle function and

cardiomyocyte proliferation, administration of recombinant NRG-1 reduced cardiomyocyte apoptosis in doxorubicin induced (Bian et al., 2009), myocardial infarction induced (Fang et al., 2010; Guo et al., 2012) and diabetes induced (Li et al., 2011) cardiomyopathy. The reduced apoptosis was attributed to the activation of the PI3K/Akt pathway since chemical inhibition of the PI3K/Akt pathway increased cardiomyocyte apoptosis in NRG-1 treated animals (Bian et al., 2009; Fang et al., 2010). The NRG-1 induced cardiomyocyte proliferation after injury was additionally attributed to the activation of PI3K/Akt pathway. This conclusion was reached due to reduction of DNA-synthesis by the ectopic expression of the natural inhibitor of the PI3K/Akt pathway, PTEN, in NRG-1 treated adult rat ventricular cardiomyocytes (Bersell et al., 2009). In infarcted hearts NRG-1 administration also reduced the scar size. The reduction in scar size was similarly attributed to the PI3K/Akt pathway since treatment with a PI3K/Akt inhibitor increased the size of the myocardial scar of NRG-1 treated mice. (Fang et al., 2010).

NRG-1 has been investigated as a treatment for heart failure in phase I, II and III clinical trials (Table 2). A decrease in mortality and a moderate improvement in the ejection fraction of the left ventricle has been observed in patients treated with recombinant NRG-1 in these trials. (Gao et al., 2010; 2018; Jabbour et al., 2011; Lenihan et al., 2016). However, more comprehensive clinical studies are ongoing and are needed to determine the viability of recombinant NRG-1 as a treatment for heart failure (trials NCT01251406, NCT01944683, NCT01258387, NCT04468529 and NCT03388593 in clinicaltrials.gov). The efficacy of NRG-1 as a heart failure therapy has also been disputed. In an in vivo study of the efficacy of NRG-1 in post myocardial infarction injury the investigators came into a conclusion that the benefits of the NRG-1 treatment in improving the ejection fraction of the heart are outweighed by the increase in left ventricular hypertrophy, which in the study resulted in reduced cardiac output. (Zurek et al., 2020). The investigators in the study were unable to discover an increase in cardiomyocyte proliferation in NRG-1 treated rats in contrast to the earlier in vivo study in mice (Bersell et al., 2009; Zurek et al., 2020). Earlier studies have also discovered a role for the NRG-1/ErbB2/ErbB4 signaling axis in pathological hypertrophy since it has been previously reported that NRG-1 is upregulated during the first adaptive concentric phase of pathological hypertrophy (Lemmens et al., 2006). Similarly, cardiomyocyte-specific transgenic overexpression of ErbB2 has led to concentric hypertrophy (Sysa-Shah et al., 2012). ErbB2 and ErbB4 mRNA and protein levels are, however, severely down-regulated when pathological hypertrophy has advanced to heart failure (Rohrbach et al., 1999; 2005), indicating that the loss of the NRG-1/ErbB2/ErbB4 signaling axis might be one of the reasons why the shift from pathological hypertrophy to heart failure occurs. In concordance, polymorphisms in the ErbB4 gene are associated with the risk of heart failure and overall death (Wang et al., 2016).

Table 1. Effects of recombinant human NRG-1 administration in cardiac injury models.

Injury model	Effects of NRG-1 administration	Reference
Myocardial infarction induced by ligation of the left anterior descending coronary artery of 2-month-old mice	Improved ejection fraction, reduced compensatory hypertrophy and ventricular dilatation, smaller infarct scar size, and increased cardiomyocyte proliferation compared to control treated mice	(Bersell et al., 2009)
Myocardial infarction induced by intracoronary balloon occlusion of adult swine	Improved ejection fraction and smaller left ventricular inner diameter compared to untreated swine	(Galindo et al., 2014)
Ischemia/reperfusion injury induced by ligation of the left anterior descending coronary artery of male adult rats	Reduced infarct size and reduced cardiomyocyte apoptosis compared to sham treated rats	(Fang et al., 2010)
Myocardial infarction induced by ligation of the left anterior descending coronary artery of adult rats	Improved ejection fraction and reduced left ventricular diameter compared to control treated rats	(Gu et al., 2010)
Myocardial infarction and heart failure induced by coronary ligation of adult rats	Improved ejection fraction, reduced left ventricular diameter, decreased cardiomyocyte apoptosis, and decreased production of reactive oxygen species compared to control treated rats	(Guo et al., 2012)
Myocardial infarction induced by ligation of the left coronary artery of adult male rats	Improved fractional shortening compared to control treated rats	(Hill et al., 2013)
Myocardial infarction induced by ligation of the left anterior descending coronary artery of adult rats	Improved ejection fraction, reduced left ventricular diameter, improved left ventricle contractility and reduced renin angiotensin system activation compared to control treated rats	(Liu et al., 2006)
Doxorubicin cardiomyopathy induced by doxorubicin administration to adult rats	Improved left ventricle contractility, less cardiac damage and improved overall survival compared to control treated rats	(Liu et al., 2006)
Injury induced by single-dose doxorubicin administration to adult mice	Improved left ventricle contractility, less cardiac damage and improved overall survival compared to control treated mice	(Bian et al., 2009)
Myocarditis induced by infection of adult mice with CV-B3 enteroviruses	Improved ejection fraction, less cardiac damage and improved overall survival compared to control treated mice	(Liu et al., 2006)
Chronic rapid pacing induced by insertion of a pacing lead into the right ventricle of adult dogs	Improved ejection fraction, and improved left ventricular contractility compared to control treated dogs	(Liu et al., 2006)
Diabetic cardiomyopathy induced by injection of streptozotocin into postnatal rats	Improved left ventricle contractility, reduced cardiomyocyte apoptosis and reduced ventricular fibrosis compared to control treated rats	(Li et al., 2011)

Table 2. Effects of recombinant human NRG-1 administration in clinical trials.

Clinical trial	Effects of NRG-1 administration	Reference
Phase I trial to assess the efficacy of NRG-1 administration along with standard therapy for the treatment of chronic heart failure patients with left ventricle ejection fraction <40%	Improved left ventricle ejection fraction compared to baseline	(Jabbour et al., 2011)
Phase I trial to assess the efficacy and tolerability of a single dose of NRG-1 along with standard therapy for the treatment of ventricular dysfunction and heart failure patients with left ventricle ejection fraction <40%	Improved left ventricle ejection fraction compared to baseline and placebo treated subjects	(Lenihan et al., 2016)
Phase II trial to assess the safety and efficacy of NRG-1 administration along with standard therapy for the treatment of chronic heart failure patients with left ventricle ejection fraction ≤40%	Improved left ventricular ejection fraction compared to baseline but not to placebo treated subjects	(Gao et al., 2010)
Phase III trial to assess the efficacy and safety of a weekly bolus of EGF-like domain of human NRG-1 along with standard therapy for the treatment of chronic heart failure	Decrease in mortality especially within a patient subgroup with <1600 fmol/mL NT-proBNP serum levels compared to placebo treated subjects	(Gao et al., 2018)

2.2.4 STAT signaling in myocardial growth

A role for STAT proteins in myocardial growth was first indicated with the discovery that the hypertrophic agonist leukemia inhibitory factor (LIF) activates STAT3 in isolated rat cardiomyocytes (Kodama et al., 1997). The role for STAT3 in LIF mediated cardiomyocyte hypertrophy was confirmed with infection of murine cardiomyocytes with adeno viruses carrying either wild-type or mutated STAT3 (Kunisada et al., 1998). Little later another hypertrophic agonist, angiotensin II, was discovered to activate STAT5 in neonatal rat ventricular cardiomyocytes (McWhinney, Dostal and Baker, 1998). Since then, the activation of both STAT3 and STAT5 has been detected in cardiomyocytes after stimuli with several hypertrophic factors in addition to LIF and angiotensin II including cardiotrophin-1 (Fukuzawa et al., 2000), interleukin-9 (Yang et al., 2020) and EGF (Rebsamen et al., 2000). The role of STAT3 and STAT5 in angiotensin II-induced cardiomyocyte hypertrophy has been confirmed in in vitro cardiomyocyte cell lines and *in vivo* with siRNA-mediated knock-down and chemical inhibitors, respectively (Han et al., 2018; Jin, Wang and Ma, 2022). The activation of both STAT3 and STAT5 is detected in pressure overload induced hypertrophy (Pan et al., 1997; 1999; Kimura et al., 2018) and some of the hypertrophic factors that are known to activate either

STAT3 or STAT5 or both are expressed in response to pressure overload (Schunkert et al., 1990; Pan et al., 1998; 1999).

Cardiomyocyte-specific transgenic overexpression of STAT3 in mice induces myocardial hypertrophy and protects against doxorubicin induced myocardial injury (Kunisada et al., 2000). Mice with cardiomyocyte specific deletion of STAT3 in turn have dilated left ventricles and develop heart failure spontaneously with age. The detected myocardial dysfunction is partly the result of increased fibrosis, but there are indications that cardiomyocyte apoptosis was also increased in the myocardium of STAT3 cardiac-null mice (Jacoby et al., 2003). A polymorphism in the STAT5b gene, in turn, is associated with the risk of dilated cardiomyopathy (Peng et al., 2012).

Both STAT3 and STAT5 have been discovered to mediate the cardioprotective effect of various stimuli. STAT3 mediates the cardioprotective effect of postconditioning, insulin and IL-11 against ischemia-reperfusion injury (Fuglesteg et al., 2008; Tian et al., 2011; You et al., 2011; Obana et al., 2012) and controls the transcription of cardioprotective and anti-apoptotic genes in the injured cardiomyocytes (Bolli et al., 2011). STAT5 in turn is essential for the cardioprotective effect of remote ischemic preconditioning (Heusch et al., 2012; Wu et al., 2017; Chen et al., 2018). It is of note that both STAT3 and STAT5 seem to elicit the cardioprotective effect by inducing the transcription of the anti-apoptotic genes BCL-2 and BCL-XL and by controlling the activation of the PI3K/Akt pathway (Fuglesteg et al., 2008; Bolli et al., 2011; Tian et al., 2011; You et al., 2011; Chen et al., 2018). Indeed, it has been suggested that STAT3 compensates for STAT5 in electroacupuncture-mediated cardioprotection against ischemia-reperfusion injury (Guo et al., 2021) and STAT3 is activated in the heart of STAT5 conditional knock-out mice (Chen et al., 2018). The activation of the PI3K/Akt pathway is also downregulated by a STAT5 inhibitor in stretched isolated rat cardiomyocytes indicating that the hypertrophic effect of the STAT5 signaling during pressure overload in cardiomyocytes might also be due to regulation of the activation of the PI3K/Akt pathway (Kimura et al., 2018).

Cardiomyocyte specific knock-out of NUMB (NUMB endocytic adaptor protein) and NUMB-L (NUMB like endocytic adaptor protein) in embryonic mice has been discovered to lead to increased ErbB2 mediated activation of STAT5 in the myocardium. The increased STAT5 activation increased nuclear localization of YAP1 and consequent cell cycle re-entry and proliferation of cardiomyocytes, suggesting that regulation of YAP1 might be one of the mechanism by which STAT5 controls hyperplastic cardiomyocyte growth (Hirai et al., 2017). Another mechanism by which STAT5b specifically can elicit cardiomyocyte proliferation has been suggested by the investigations on the effect of growth hormone on the human myocardium. Growth hormone deficient subjects suffer from a severe myocardial

growth defect that impairs the function of the heart (Amato et al., 1993; Merola et al., 1993; Sartorio et al., 1997). Growth hormone elicits it responses via the activation of STAT5b which in turn induces the transcription of IGF-1 (Udy et al., 1997; Woelfle, Billiard and Rotwein, 2003; Woelfle, Chia and Rotwein, 2003). The administration or transgenic expression of growth hormone or IGF-1 induces cardiomyocyte proliferation even in adult cardiomyocytes (Kajstura et al., 1994; Reiss et al., 1996; Brüel, Christoffersen and Nyengaard, 2007). This suggests that STAT5b could putatively induce hyperplastic cardiomyocyte growth by inducing the transcription of IGF-1. In addition, persistent transgenic expression of IGF-1 has also been connected to cardiomyocyte hypertrophy (Delaughter et al., 1999). IGF-1 activates the PI3K/Akt pathway in cardiomyocytes implying that the regulation of the activation of the PI3K/Akt pathway by STAT5b could also be the consequence of increased transcription of IGF-1 (Matsui et al., 1999; Fujio et al., 2000).

2.2.5 VEGF signaling in myocardial growth

Along with angiogenesis, angiogenic factors such as VEGFs can induce myocardial growth. Administration of adeno-associated viruses encoding or transgenic expression of VEGF-B or PIGF has induced hypertrophic growth of the myocardium in several *in vivo* models (Tirziu et al., 2007a; Karpanen et al., 2008; Jaba et al., 2013). The induced hypertrophy has been considered as physiological since no reduction in the heart function has been detected in these models. The myocardial growth induced by angiogenic factors has mainly been thought to occur through secretion of myocardial growth signals from the endothelial cells, but there are reports that indicate that the receptors for the angiogenic factors are also expressed in the myocardium. VEGFR1 and VEGFR2 have been detected in cardiomyocytes and injection of adeno-associated viruses encoding VEGF-A or VEGF-B had an anti-apoptotic effect on cardiomyocytes under ischemia-reperfusion injury. No additional growth, however, has been detected in isolated rat cardiomyocytes treated with VEGF-A or VEGF-B indicating that the growth phenotype of transgenic or adeno-associated virus mediated VEGF-B expression is originating from endothelial cells (Zentilin et al., 2010). Adeno-associated virus-based gene delivery of VEGF-B also induces proliferation of cardiomyocytes in the failing myocardium in mice (Huusko et al., 2012).

2.3 Module, network and pathway inference from omics data

Ever since the advent of high-throughput technologies, cell signal pathway inference has been a constant aim in systems biology. The inception of the concept can be

mapped back to the development of microarray technologies that allowed the instantaneous measurement of the expression level of multiple and later all transcripts of an organism (Schena et al., 1995; DeRisi, Iyer and Brown, 1997; Wodicka et al., 1997). Quickly after, different strategies to identify regulatory modules in the microarray data were developed and gene regulatory module and network inference became a long-standing goal in the field (Tamayo et al., 1999; Barkai et al., 2002). On top of these methods, analysis methods that allowed the investigator to test the enrichment of already discovered cell signaling pathways in high-throughput data were envisioned (Dennis et al., 2003; Hosack et al., 2003; Subramanian et al., 2005). One of these methods called the gene set enrichment analysis (GSEA) instantaneously became popular to an extent that it is still one of the most widely used pathway discovery methods to this day (Subramanian et al., 2005).

Over the years more high-throughput technologies were developed that allowed the more comprehensive measurement of the expression of almost all proteins, transcripts, post-translational modifications, metabolites, epigenetic modifications, gene modifications, molecular interactions, lipids, or miRNAs. These approaches were named omics approaches and the suffix omics was added to the end of the name of the biological entity that was being measured to indicate the study of the entirety of the specific biomolecule (Dai and Shen, 2022). Nowadays, it is common to measure more than one omics layer from the same samples, giving rise to a field called multi-omics (Karczewski and Snyder, 2018).

The current single-omics and multi-omics pathway and module discovery methods can be roughly divided into two categories: the methods that utilize prior data in the inference and the ones that are independent of prior knowledge. The approaches that utilize prior information have been discovered more accurate when relevant prior information is available but tend to be prone to overfitting and biases due to the incompleteness, skewness and context-dependency of prior information (Maetschke et al., 2014; Garrido-Rodriguez et al., 2022). The skewness of the prior information stems from the unequal level of information available per feature leading to models where in the worst case the features without any prior information available are ignored and the ones with high level information are endorsed in the inference. If the context-dependency of prior information is ignored, the resulting inference might predict connections that do not occur in the studied context. The benefit of prior information-independent approaches is in the discovery of previously unreported cell signaling connections that are easily missed by prior information-dependent approaches that can weigh the known connections over new ones. (Garrido-Rodriguez et al., 2022). Here a focus on only the prior data-independent inference methods was selected.

2.3.1 Prior data-independent module, network and pathway inference methods for single omics data

2.3.1.1 Association measure-based methods

The initial and most widely used signaling module (cluster) and network methods for single-omics data rely on association (co-expression) measures like the correlation coefficients. In network representations (Figure 9), the association measures define the strength of the edges between the nodes that represent the features such as genes, proteins or transcripts in the omics dataset. Correlation-based signaling module and network methods such as the weighted correlation network analysis, WGCNA, have been considered the benchmark for other signaling module and network inference methods (Langfelder and Horvath, 2008). Mutual information has been proposed as an alternative association measure for the correlation coefficients especially to improve the inference of non-linear associations in single omics data (Steuer et al., 2002; Margolin et al., 2006). Correlation-based measures, however, outperform mutual information in discovering linear relationships (Song, Langfelder and Horvath, 2012). In most cases the performance of correlation coefficients and mutual information has been discovered to be comparable (Steuer et al., 2002; Song, Langfelder and Horvath, 2012). Since it has been discovered that the pairwise gene relationships are mostly linear and calculation of correlation coeffecients is more straight-forward, less computationally demanding, and unconstrained by sample size, correlation-based methods are preferred over the mutual information-based methods in gene regulatory network discovery (Song, Langfelder and Horvath, 2012). An analysis of variance-based association score η^2 has outperformed the Pearson's correlation coefficient in finding true gene regulatory relationships (Küffner et al., 2012).

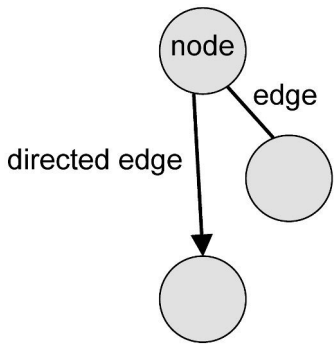

Figure 9. Network representation. Association measures define the edges of the network and nodes represent the features (e.g., proteins, transcripts, genes, post-translational modifications sites) of omics datasets.

Topological overlap measures have been used to weigh the initial correlation coefficient-based networks with increased inference accuracy as a result (Yip and Horvath, 2007). Topological overlap measures represent the number of shared neighbours for a pair of feature nodes in a network presentation and consider the feature pairs with higher amount of common neighbours as more highly associated. Gaussian graphical models (GGM) and other partial correlation-based methods have been also proposed to consider the effect of the other features in the dataset to the pairwise association between two features (Rice, Tu and Stolovitzky, 2005). Gaussian graphical models, however, cannot handle high-dimensional omics datasets, i.e. datasets where the number of features is significantly higher than the number of samples, requiring shrinkage approaches such as the graphical lasso and and the Ledoit-Wolf shrinkage to overcome the high dimensionality problem (Ledoit and Wolf, 2004; Friedman, Hastie and Tibshirani, 2008). The high dimensionality problem (also known as the $n << p$ problem) arises from the need for the sample covariance matrix to be invertible to infer the GGM (Ledoit and Wolf, 2004). The shrinkage approaches have been discovered to cause bias to the final network, reducing the applicability of GGMs (Bernal et al., 2021). Partial correlation-based signaling network and module methods, however, excel in differentiating between causal correlations and spurious correlations (Werhli, Grzegorczyk and Husmeier, 2006; Zuo et al., 2014). Spurious correlations are considered as correlations that arise from the influence of a confounding factor instead of a causal link. Directed networks can also be learned with partial correlation-based methods, but their performance have been only proven with simulated data (Zuo et al., 2014). Different approaches such as the background elimination step in the CLR algorithm and the technique in the ARACNE algorithm that removes edges based on the data processing inequality principle, have been also developed to eliminate indirect associations in mutual information networks (Margolin et al., 2006; Faith et al., 2007).

2.3.1.2 Non-association measure-based approaches

Several non-association measure-based approaches have also been developed to infer cell signaling module and networks from single omics data. The Dialogue on Reverse Engineering Assessment and Methods (DREAM) challenges are crowd-sourced calls for computational methods to solve biological and medical data analysis problems and provide an unbiased benchmark for the assessment of the submitted methods. One of the objectives in the DREAM3, DREAM4 and DREAM5 challenges have been to infer gene regulatory networks either from simulated or real omics data (Prill et al., 2010; Marbach et al., 2012). The best performing algorithms in these DREAM challenges were all based on other principles than association measures. The most consistent performer in the in-silico network DREAM3

challenge combined both noise models and ordinal differential equations (ODE) (Yip et al., 2010). After the DREAM3 challenge, other ODE based methods have also been proposed but mostly only for time-series data (Oates et al., 2014; Mao et al., 2022). The winner of the DREAM4 In Silico Multifactorial challenge and the DREAM5 network inference challenge in turn was a regression-tree based ensemble machine learning method called GENIE3 (Huynh-Thu et al., 2010). It is of note that the association measure η^2-based algorithm ANOVA η^2 outperformed GENIE3 in the DREAM5 network inference challenge with real omics datasets. The ANOVA η^2 algorithm, however, did include prior information on to the inference, which makes it unclear if the better performance was only due to the utilization of additional information. (Küffner et al., 2012). A linear regression-based approach TIGRESS ranked third in the DREAM5 network inference challenge. Enhanced performance over GENIE3 in the DREAM5 challenge datasets was, however, reported by the developers of TIGRESS after parameter optimization (Haury et al., 2012). TIGRESS was also discovered to outperform the other methods in the DREAM5 network inference challenge in discovering directed network connections (Xiao et al., 2022).

After the DREAM5 challenge, other machine learning ensemble methods that reportedly outperform GENIE3 in gene regulatory network inference with the DREAM datasets have been developed such as ADANET (Sławek and Arodź, 2012) and ENNET (Slawek and Arodz, 2013). Both ADANET and ENNET use boosting to train either regression tree or stump-based weak learners (Sławek and Arodź, 2012; Slawek and Arodz, 2013).

Several approaches have been suggested as direct alternatives for the association measure-based methods. Regression methods have been proposed as an alternative to mutual information in discovering non-linear relationships. Spline and polynomial regression have been discovered to function similarly to mutual information networks (Song, Langfelder and Horvath, 2012), but other regression approaches such as sparse regression with Lasso have also been proposed (Friedman, Hastie and Tibshirani, 2008). To solve the directionality and the conditional dependency of the molecular associations in omics data, Boolean and Bayesian networks have been proposed as an alternative to partial correlation-based methods (Friedman et al., 2000; Shmulevich et al., 2002). The Boolean logic, however, has been considered too simplistic to describe the complex regulatory relationships of biomolecules and Bayesian networks reportedly outperform Boolean networks in gene regulatory network discovery (Li et al., 2007). Both Bayesian and Boolean networks, however, suffer from computational complexity. The computational complexity expands with larger networks making it exceedingly computer resource consuming to solve regulatory networks from genome-wide expression data with Boolean or Bayesian networks. Indeed, solving the exact structure of a Bayesian network has been classified as a non-deterministic polynomial-time hard (NP-hard) problem (Koivisto and Sood, 2004). Efforts, however, have been

made to reduce the computational complexity of Bayesian networks by for instance implementing a mutual information-based candidate auto selection or node ordering by pair-wise causal inference testing to reduce the combination of neighbours that need to be considered (Xing et al., 2017; Wang, Audenaert and Michoel, 2019). The advantages and limitations of both association score-based and non-association score-based methods are summarized in Table 3.

Table 3. Summary of the reported advantages and limitations of previously proposed prior data independent module, network and pathway inference methods.

Method	Reported advantages	Reported limitations
Correlation based-methods	Robust, fast and easy to compute, excels in discovering linear relationships	Can't discover non-linear relationships, can't differentiate between spurious and direct associations, can't solve directionality
Mutual-information-based-methods	Excels in discovering non-linear relationships, performance similar to correlation-based methods	Less straight-forward to compute than correlation, can't differentiate between spurious and direct associations, can't solve directionality
Partial-correlation-based-methods	Excels in discovering the directions of the associations, excludes spurious associations	Requires shrinkage approaches to function with high-dimensional datasets
ODE models	Describes the quantitative relationships between features	Requires extensive parameter estimation, mostly suited for time-series data
Regression tree-based ensemble methods	Reportedly outperform other methods, can capture both linear and non-linear relationships and can be used to solve directionality	Performs better with simulated datasets than real omics datasets, performs worse with real omics datasets than best performing association measure-based methods
Boolean networks	Excels in discovering the directions of the associations, excludes spurious associations	Considered too simplistic, outperformed by Bayesian networks, computational complexity reduces utility with high dimensional datasets
Bayesian networks	Excels in discovering the directions of the associations, excludes spurious associations	Computational complexity reduces utility with high dimensional datasets
Other regression-based methods	Excels in discovering non-linear relationships, can be used to solve directionality	No reported advantages over mutual-information based-methods

2.3.1.3 Community approaches outperform individual approaches

The organizers of both the DREAM3 and DREAM5 challenges concluded that combining more than one approach produces a more accurate inference of gene regulatory networks than applying the best performing method alone due to more consistent performance across datasets. The organizers discovered systematic errors in the inference methods that were compensated by the other approaches in the community inference. The final edges in the combined approach were selected by the combined average rank from the individual approaches. (Marbach et al., 2010; 2012). Including the 5 best performing approaches in the community inference had an additive effect, which was not observed with the inclusion of the 5 worst performers (Marbach et al., 2012). This indicates that the accuracy of the individual approach is also important for successful community inference. The performance of an individual approach was not tied to its core principles. Correlation, mutual information, ensemble, regression, Bayesian network and meta (approaches combining more than one principle) based approaches were all both among the best and worst performers indicating that a successful implementation is more important than the choice of the core principle. (Marbach et al., 2010; 2012). Similarly, a combination approach EnsInfer was discovered to increase the accuracy of the inference of gene regulatory networks over individual gene regulatory inference methods (Shen, Coruzzi and Shasha, 2023). These observations underline the importance of developing a variety of accurate inference methods for single omics regulatory module and network inference that are based on different core principles. The aim should not be to only create a method that outperforms other individual inference approaches, but a complementary method that also adds additive value to a community approach.

2.3.2 Efforts to develop prior data independent cell signaling pathway inference methods for multi-omics data are currently lacking

A recent review listed the current proposed unsupervised computational multi-omics integration methods (Vahabi and Michailidis, 2022). Astonishingly, none of the approaches mentioned in the review were designed to uncover cell signaling pathways from multi-omics data without the use of prior information. Instead, several pathway discovery methods that utilize prior information in different stages of the inference have been developed (Vaske et al., 2010; Paull et al., 2013; Koh et al., 2019; Liu et al., 2019; Dugourd et al., 2021; Garrido-Rodriguez et al., 2022; Palshikar et al., 2023). Recent research emphasis in multi-omics data analysis has been mainly in developing clusterization, feature extraction and dimensionality reduction approaches (Cantini et al., 2021; Vahabi and Michailidis, 2022). While

clusterization approaches can find modules from multi-omics data and have been proven effective in stratifying samples and in predicting clinical outcome and biomarkers, there is little evidence that the high-weight features connected by the latent factors would represent cell signaling pathways (Cantini et al., 2021; Vahabi and Michailidis, 2022).

While prior information independent cell signaling and module inference approaches specifically for multi-omics data have not been yet developed, the approaches originally applied to single omics data module and network discovery have been applied to multi-omics data. WGCNA and other correlation network-based methods have been applied to analyze and combine multi-omics data (Acharjee et al., 2016; Zoppi et al., 2021). Since a formal analysis on their applicability to multi-omics data has not been conducted it is unclear what the modules and networks inferred and integrated by these methods truly represent. An inference method designed for certain single omics modality might have limited function in a multi-omics context for several reasons. One, it has been well established that data produced by different omics technologies follow different probability distributions, can be bounded or unbounded, discrete or continuous and therefore are governed by different key parameters (Mirza et al., 2019; Tarazona, Arzalluz-Luque and Conesa, 2021). A cell signaling module and network method designed to infer cell signaling connections from single omics data will have limited performance with heterogenic multi-omics data if the inference method is dependent on the parametric assumptions of the input data. Second, data sparsity is highly variable between the data produced by different omics technologies and cell signaling module and network inference methods for single omics vary in how well they can handle missing values in the data (Mirza et al., 2019; Song et al., 2020; Tarazona, Arzalluz-Luque and Conesa, 2021). While data imputation approaches have been developed, it is generally accepted that these can cause bias to downstream analyses especially if the number of missing values is significant in the dataset (Song et al., 2020). Third, the number of features identified by different omics approaches is variable and not all single omics module and network approaches can be scaled to perform with a significantly higher number of features (Mirza et al., 2019). Since the original validation of these methodologies have usually been performed only with certain single omics data, a coordinated effort should be made to validate their accuracy also with the diverse multi-omics data. The integration of the different modalities of the heterogenous multi-omics data is another non-trivial challenge that has not been addressed by the approaches that have been only designed for single-omics data (Mirza et al., 2019; Tarazona, Arzalluz-Luque and Conesa, 2021).

Some prior data independent multi-omics analysis approaches have been developed with the intention of uncovering causal relationships between multi-omics modules. An approach called Transkingdom Network Analysis (TransNet) has been

developed to discover causal links between different omics modules (Rodrigues, Shulzhenko and Morgun, 2018). TransNet first identifies modules from a correlation network by the cluster identification method MCODE (Bader and Hogue, 2003) and then uses correlation to discover the features that link these two modules (Rodrigues, Shulzhenko and Morgun, 2018). An approach called LemonTree first discovers consensus multi-omics modules from Gibbs sampled modules inferred from expression data and then computes a regulator-to-module score for each separately listed regulator (Bonnet, Calzone and Michoel, 2015). LemonTree is not a completely prior information independent approach since the suggested regulators are supplied based on prior knowledge (Bonnet, Calzone and Michoel, 2015). Due to a lack of formal analysis it is unclear how successful TransNet and LemonTree is in discovering causal multi-omics relationships. Based on the limited amount of available approaches and lack of rigorous validation, it is clear that more effort into developing prior information independent methods that can discover causal relationships between multi-omics modalities needs to be exerted.

3 Aims

By understanding the modular nature of cell signaling pathways, researchers have been able to identify and target the specific structural determinants in cell signaling molecules that regulate the aberrant signaling involved in disease processes. The modular research approach has identified several functional regions in the cell signaling molecules that are the targets of clinically approved drug-based therapies. The structure-function relationship of receptor tyrosine kinases was selected as a focus in this thesis, since receptor tyrosine kinases are the key regulators of several important organ functions and they have been successfully targeted as a therapy for cancer. As one of the primary objectives, the effect of structural variation in the extracellular juxtamembrane region of receptor tyrosine kinases on the diversity of the downstream signaling of receptor tyrosine kinases was researched. The extracellular juxtamembrane region is one of the least researched structural regions in receptor tyrosine kinases but has the benefit of residing outside the cell membrane. This advantageous location allows for more variable therapy development due to higher accessibility compared to intracellular regions such as the kinase domain that require the therapeutic compound to pass the cell membrane.

To investigate the diversity of signaling originating from the extracellular juxtamembrane region the natural JM isoforms of the receptor tyrosine kinase ErbB4 was utilized. This allowed for the identification of a signaling pathway that was specific for the ErbB4 JM-b isoform specifically expressed in cardiomyocytes. The ligand for the ErbB4 receptor tyrosine kinase NRG-1 has been identified as a critical regulator of cardiomyocyte growth and is currently investigated in clinical trials as a therapy for heart failure. Due to the therapeutic potential of NRG-1, the identification of the downstream pathways of NRG-1 and ErbB4 that induce the survival and growth of cardiomyocytes was considered a serviceable strategy to uncover new molecular targets for heart failure treatment. Therefore, investigation on the role of the discovered ErbB4/STAT5b pathway in myocardial growth was selected as one of the primary aims in this thesis. The role of the NRG-1/ErbB signaling in VEGFB mediated cardiomyocyte growth was additionally investigated as a secondary aim to understand the cardiomyocyte-based mechanisms that allow an endothelial derived signal to induce cardiomyocyte growth.

Recent developments in omics technologies have allowed the collection of more comprehensive measurements on the state of cell signaling. The accumulation of vast cell signaling molecule information has created the undeniable need for computational methods that can reverse-engineer cell signaling pathways from multi-level molecular information. To create a tool that can discover new cell signaling pathways from multi-omics derived information, the design of a de novo multi-omics pathway inference method was selected as one of the primary aims in this thesis. A de novo approach is especially suited in uncovering new signaling connections compared to prior information dependent approaches that are prone to inherit the bias from the incompleteness, skewness and context-dependency of prior information.

The specific objectives of this thesis were as follows:

1. To research the mechanisms of cell signaling diversity arising from the extracellular juxtamembrane region of receptor tyrosine kinases.
2. To uncover the role of the discovered cardiomyocyte specific ErbB4/STAT5b pathway in myocardial growth to aid in heart failure therapy development.
3. To investigate the role of NRG-1/ErbB signaling in endothelium derived VEGFB signaling induced physiological myocardial growth.
4. To develop the first prior-information independent approach designed to infer cell signaling pathways from multi-omics data.

4 Materials and Methods

4.1 Experimental models

The reagents, antibodies, constructs, cell lines and DNA and RNA sequences utilized in this thesis are listed in the Resources Table in I and Reagents and Tools table in II, and in the Supplementary Materials and Methods of III and in IV. The details of ligand, siRNA, antibody and chemical inhibitor concentrations and incubation times, mass spectrometry gradients, and mass spectrometry instrument and analysis settings can be found in the Materials and Methods section of articles I–IV.

4.1.1 Cell culture (I, II, IV)

MDA-MB-468, COS-7, WM-266-4, Phoenix Ampho HEK293 and HEK293T cells were cultured in DMEM and MCF-7 and HC11 cells in RPMI 1640 supplemented with 10% fetal bovine serum, 2 mM Ultra-Glutamine and 50 U/ml penicillin-streptomycin. The culture medium of MCF-7 cells was additionally supplemented with 10 nM estrogen and 1:2000 insulin solution and the culture medium of HC11 cells with 10 ng/ml EGF and 1:2000 insulin solution. The culture medium of stably transduced MDA-MB-468, HC11 and WM-266-4 cells was supplemented with 3 µg/ml puromycin. All cell lines were incubated at 37°C in the presence of 5% CO_2.

4.1.2 Primary cell isolation and culture (II)

The heart of male NMRI neonatal mice (not more than 3 days old) were excised, minced, washed twice with ice-cold HBSS (Hank's balanced salt solution) and enzymatically digested with an enzyme mix from the Cardiomyocyte Isolation kit consisting of papain and thermolysin for 30 minutes at 37°C under gentle agitation. The samples were centrifuged at 900 g for 5 minutes and the supernatant was washed twice with ice-cold ADS buffer (Louch, Sheehan and Wolska, 2011). A percoll gradient was used twice to isolate the cardiomyocytes from other cell types as previously described (Louch, Sheehan and Wolska, 2011). TC20 automated counter was used to determine the concentration and viability of trypan blue stained cardiomyocytes. The isolated cardiomyocytes were plated on culture plates coated

with 1% gelatin or in coverslips coated with 2% growth factor reduced matrigel in plating medium consisting of 68% DMEM, 17% 199, 10% horse serum and 5% fetal bovine serum. The plating medium was changed into maintenance medium consisting of 80% DMEM, 20% 199, 5 mM Creatine, 2 mM Carnitine and 5 mM Taurine after 2 days.

4.1.3 Zebrafish embryos (II)

Zebrafish embryos of casper strain were obtained from the Zebrafish Core of Turku Bioscience Center (University of Turku and Åbo Akademi). The embryos were produced by natural breeding in allocated breeding tanks, collected, washed and incubated in E3-medium in a humified incubator. For anesthesia, tricaine at the end concentration of 200 mg/ml was used. The embryos were euthanized under anesthesia in 4% paraformaldehyde or in 2x Laemmli buffer followed by mechanical dissociation. For live imaging studies, the embryos were anesthetized and embedded into low melting point agarose.

4.1.4 Adeno-associated virus-treated mice (II, III)

Weight matched adult male wild type C57BL/6JOlaHsd mice obtained from Envigo Harlan were injected with a total of 5×10^{11} AAV9 particles encoding the indicated constructs intraperitoneally. A total of 4×10^{11} AAV9 particles encoding the scrambled control construct or a construct of murine extracellular domain of ErbB4 fused to the Fc region of IgG (mErbB4-Fc) were injected in combination of either 1×10^{11} of particles encoding murine VEGFB186 (mVEGFB186) or control constructs. Two weeks after the injections, the animals were terminally anesthetized with intraperitoneal injection of ketamine and xylazine and euthanized by cervical dislocation. The heart was excised, and the serum collected. The heart weight was measured and normalized to the pre-euthanasia body weight. For the preparation of cryosections, a transverse mid-section of the heart was embedded in OCT and snapfrozen in liquid nitrogen-cooled 2-methylbutane containing 2% pentane. The apex of the heart was either snapfrozen in liquid nitrogen or freshly lysed for biochemical analyses.

4.1.5 Patient samples (II)

Formalin-fixed paraffin-embedded myocardial tissue sections from 19 patients who underwent medical autopsy at Turku University Hospital between 2008 and 2017 were acquired from Auria Biobank. The patient samples were divided into hypertrophy and control cohorts based on the histopathological analysis of

cardiomyocyte hypertrophy. The hypertrophy cohort (6 cases of aortic valve stenosis, 4 cases of alcoholic cardiomyopathy, 3 cases of idiopathic cardiomyopathy) included patients with the median age of 67 of which 77% were males. The control cohort (2 cases of liver cirrhosis, 1 case of metastatic pancreatic carcinoid, 1 case of pulmonary embolism, 1 case of sepsis due to Streptococcus pneumoniae, and 1 case of cholangiocarcinoma) included patients with the median age of 48 of which 50% were males.

4.2 Experimental procedures

4.2.1 Plasmid DNA cloning (I, IV)

Four different strategies of plasmid DNA cloning were utilized. One, point mutations were introduced to the plasmids with site directed primers and PCR using Phusion High-Fidelity DNA polymerase or KAPA HiFi DNA polymerase. Two, receptor variants were produced with Gibson Assembly with synthetic gene blocks and NEBuilder HiFi DNA Assembly Master Mix. Three, constructs were transferred to pDest-eGFP-N1 vector backbone from the corresponding pDONR223 vectors with Gateway cloning with Gateway LR Clonase II Enzyme mix. Four, a pX330 neo backbone and constructs were assembled from a neomycin cassette sequence extracted by PCR or synthetic gene fragments and restriction enzyme cleaved pX330-U6-Chimeric_BB-CBh-hSpCas9 backbone with BbsI or EcoRV restriction enzymes and T4 DNA ligase. All cloning reagents were used according to the manufacturer's recommendations.

4.2.2 Plasmid DNA and siRNA transfection (I, II, IV)

For plasmid DNA transfection of COS-7 and MCF-7 cells, Fugene 6 and Hilymax were used. For plasmid DNA transfection of WM-266-4 cells, jetPRIME was utilized. For siRNA transfection of MDA-MB-468 and HC11 cells, Lipofectamine 2000 was used and for siRNA transfection of MCF-7 cells, siLentFect was used. All transfection reagents were used according to the manufacturer's recommendations. For silencing studies, the siRNAs were used at a 25–50 nM concentration for 24–48 hours before analysis.

4.2.3 Retro- and lentivirus production and infection (I, II, IV)

For lentivirus production, a third-generation lentiviral packaging system was utilized (Dull et al., 1998). Lentiviral packaging vectors and the shRNA carrying vectors were co-transfected into HEK293T cells. The media containing the viruses was

collected from the transfected HEK293T cultures after 48 and 72 hours and sterile filtered. Primary cultures and cell line cultures were infected with the collected media with 8 µg/ml polybrene at a multiplicity of infection corresponding to 1 or 2. To produce retroviral media for the transduction of stably expressing cell lines, the indicated pBABE Puro plasmids were transfected to Phoenix Ampho packaging cell line with Fugene 6. The media were collected at 24 hours and 48 hours after transfection, sterile-filtered, and supplied to the target cells with 3 µg/ml polybrene. The transduced cells were selected with 3 µg/ml puromycin.

4.2.4 CRISPR/Cas9 editing of zebrafish embryos (II)

For the generation of guide RNAs, 5 µl of 100 µM crispr RNAs (crRNA) and 100 µM trans-activating crispr RNA (tracRNA) were combined. Duplexes were annealed in a thermal cycle in 95°C for 5 minutes followed by incremental cooling down at 0.1°C/s to 25°C and 5-minute incubation at 25°C. Nuclease-free duplex reaction buffer was added to adjust the final concentration to 25 µM. A microliter of the duplex mixture was incubated with 1.25 µl of EnGen Cas9 NLS solution, 1.75 µl H_2O, and 1 µl of phenol red solution for 5 min at 37°C to create the crRNA:tracRNA:Cas9 complexes. Nanoject II microinjector was used to inject 2.3 nl of the crRNA:tracRNA:Cas9 complex solution into 1–4 cell stage zebrafish embryos.

4.2.5 Ligand stimulation and chemical and lectin inhibition (I, II)

Recombinant RTK ligands were utilized to analyze the effect of ligand stimulation on downstream signaling with western analysis and immunofluorescence, and on cell survival and growth with live cell imaging. Recombinant NRG-1 was utilized to study ErbB4-dependent cardiomyocyte and cardiac morphology and function with imaging. AG1478, lapatinib, gefitinib or dynasore was utilized to analyze the effect of ErbB RTK or dynamin-2 inhibition to cardiomyocyte signaling and cardiomyocyte and cardiac morphology and function with real-time PCR, western analysis, and imaging. TAPI-0 and GSI-IX were used to inhibit the proteolytic cleavage of ErbB4. Lectins were used to block protein-glycan interactions to study receptor downstream RTK signaling, location and cell survival with western analysis and imaging.

4.2.6 Cell and tissue lysis (I, II, IV)

Serum starved cells were treated with the indicated reagents and lysed in 0.1% Triton X-100, 1 mM EDTA, 5 mM NaF, 10 mM Tris-HCl, pH 7.4, and dissolved Pierce Protease Inhibitor Mini Tablet. Affinity enrichment samples enriched with Ni-NTA were lysed with 70 mM octyl-β-D-glucopyranoside, 25 mM Tris-HCl pH 7.5, 150 mM NaCl, Pierce protease and phosphatase inhibitor mini tablet. Cells intended for proteomic or phosphoproteomic analysis with mass spectrometry were lysed with 6 M guanidine hydrochloride, 100 mM Tris-HCl pH 8.5, 5 mM Tris(2-carboxyethyl)phosphine (TCEP), and 10 mM chloroacetamide. A middle portion of the excised hearts of AAV injected mice were homogenized with bead beating in RIPA buffer (1 mg/ml aprotinin, 1 mg/ml leupeptin, 1 M PMSF, 1 M NaF, 0.1 M Na_3VO_4, 0.5% Triton X-100, and 0.5% NP-40 in PBS, pH 7.4). Zebrafish embryos were homogenized with an electronic pestle either to the lysis buffer of NucleoSpin TriPrep kit or to 6x Laemmli buffer and incubated for 10 min in 100°C for western analysis. Bradford and bicinchoninic acid (BCA) assays were used to measure protein concentration.

4.2.7 Affinity enrichment (I, II, IV)

Cell lysate was precleared with G-sepharose, streptavidin-sepharose or G-magnetic beads that were cross-linked to normal IgG for 1 hour at +4°C under agitation. The precleared cell lysate was incubated with the indicated primary antibodies and G-sepharose, PHA-L lectin and streptavidin-sepharose, streptavidin-sepharose alone, HisPur Ni-NTA magnetic beads, Pierce anti-c-Myc magnetic beads, or G-magnetic beads cross-linked to the indicated primary antibodies for 3–24 hours at 4°C under agitation. The precipitate was washed 7 times with 0.2% Tween 20 in PBS or 5 times with TBS-T buffer (125 mM Tris, 750 mM NaCl, 0.25% Tween-20, pH 7.4). The precipitates intended for mass spectrometry analysis were additionally washed twice with PBS and once with MilliQ water or only once with MilliQ water. The proteins were eluted from the beads either with 2x Laemmli buffer in 100°C for 5 minutes, with 0.2 M glycine or with 6 M guanidine hydrochloride, 5 mM tris(2-carboxyethyl)phosphine, 10 mM chloroacetamide, and 100 mM Tris, pH 8.5 at 95°C for 10 min. Pierce high-select TiO_2 phosphopeptide enrichment kit was utilized to enrich desalted phosphopeptides.

4.2.8 Western analysis (I, II, III, IV)

Denatured protein samples were run on SDS-PAGE, transferred to nitrocellulose membranes, and probed with the indicated antibodies. Two different strategies for band detection were used. The membranes were either probed with infrared dye (IR)-

conjugated or horse radish peroxidase (HRP)-conjugated secondary antibodies. The membranes probed with IR-conjugated secondary antibodies were imaged with the Odyssey CLx Imager. The membranes probed with HRP-conjugated secondary antibodies were incubated for 5 minutes with Super-Signal West Pico Chemiluminescent substrate or Femto Maximum Sensitivity Substrate and the signal was captured with an X-ray film. The signal density was quantified with ImageStudio Lite.

4.2.9 Chemical cross-linking (I, II, IV)

For interaction studies, 2 mM DSP or DTPB in 1xPBS was used for 2 or 10 minutes to chemically cross-link proximal proteins in cells in culture plates. For interaction studies analyzed with mass spectrometry, normal IgG and primary antibodies were cross-linked to G-magnetic beads with 3 mM BS_3 for 30 minutes under agitation. The cross-linking reactions were quenched with 50 mM Tris-HCl pH 7.4 and incubated in room temperature for 15 min.

4.2.10 Proximity ligation assay (I, II)

The proximity ligation assays (PLA) of protein-protein associations were performed with the Duolink or the Navinci system according to manufacturers' recommendations. The primary antibodies were used at a 1:100 dilution. The PLA signals were imaged with Zeiss LSM 780 or Zeiss LSM 880 confocal microscopes with 40× Zeiss C-Apochromat or 40x Zeiss LD LCI Plan-Apochromat objectives.

4.2.11 Immunofluorescence (I, II, IV)

Cells grown on coverslips were fixed and permeabilized with methanol at -20°C for 10–15 minutes or in 4% paraformaldehyde for 20 minutes following a 10-minute incubation in 0.1% TritonX-100 in PBS. To block non-specific antibody binding, the coverslips were incubated in 3% BSA in PBS for 30 minutes. The coverslips were incubated with the indicated primary antibodies for 1.5–24 hours. Zebrafish embryos were fixed and permeabilized with 4% PFA and 0.2% Triton X-100 in PBS for 30 minutes. To block non-specific antibody binding, the embryos were blocked with 3% BSA and 0.2% Tween 20 in PBS for 1 hour under gentle agitation. The embryos were incubated with the indicated primary antibodies for 24 hours in 4°C under gentle agitation. Ten µm thick cryosections were cut from the cryoblocks, fixed with acetone, and stored in -80°C. The sections were rehydrated in room temperature in PBS for 30 minutes and the non-specific antibody binding was blocked with 3% BSA

in PBS for 30 minutes. The sections were incubated with the indicated primary antibodies for 3 hours.

Alexa-conjugated secondary antibodies were used to detect the primary antibodies and DAPI (4′,6-diamidino-2-phenylindole) and Alexa-555-conjugated phalloidin to detect the nucleus and actin, respectively. Abberior STAR conjugated secondary antibodies were additionally used to detect the primary antibodies in super-resolution microscopy samples. Coverslips were incubated with secondary antibodies, phalloidin and DAPI for 1 hour at room temperature and zebrafish embryos 18 hours at 4°C under gentle agitation. Coverslips were washed four times for 5 minutes with PBS and zebrafish embryos four times for 30 minutes with 0.2% Triton-X in PBS under gentle agitation after primary and secondary antibody incubation. Mowiol was used for the mounting of coverslips imaged with confocal microscopy and ProLong Diamond Antifade Mountant for the mounting of super-resolution microscopy samples.

The immunofluorescence samples were imaged with Zeiss LSM 780 or 880 confocal microscopes with the 40× Zeiss C-Apochromat and 63× Zeiss C-Apochromat or the 40× Zeiss LD LCI Plan-Apochromat objectives. The super-resolution microscopy samples were imaged with Abberior STED (stimulated emission depletion) microscope with 100× Olympus UPLSAPO objective or Deltavision OMX microscope with 60× SIM Olympus Plan Apo N objective.

4.2.12 Immunohistochemistry (II)

Formalin-fixed paraffin embedded (FFPE) blocks were prepared from adherent cells. The adherent cells were detached with trypsin-EDTA, washed twice with ice-cold PBS and fixed with 10% neutral-buffered formalin in PBS for 20 minutes. The cells were washed twice with PBS and moulded into 1.5% agarose in PBS. The agarose pellets were transferred to 70% ethanol and embedded into paraffin blocks according to the standard protocol of the Histology Core Facility of the Institute of Biomedicine, University of Turku. The FFPE tissue blocks were sectioned with a microtome to 5 µm sections onto microscope slides. The sections were deparaffinized, rehydrated, and the antigen retrieval was performed in Tris-EDTA pH 9.0 in a microwave oven for 7 minutes in 600 W and 7 minutes in 450 W. Incubation with hydrogen peroxide and normal antibody diluent was used to inhibit non-specific enzyme function and antibody binding. The sections were stained with automated Labvision autostainer with 1:500 dilution of anti-pSTAT5 antibody for 60 minutes. The anti-pSTAT5 signal was detected with BrightVision Goat Anti-Mouse/Rabbit IgG HRP two step detection system with a horseradish peroxidase (HRP)-conjugated secondary antibody. Mayer's hematoxylin was used for counter-staining for 1 minute in room temperature and the coverslips were mounted on top

of the sections with Pertex. Panoramic P1000 slide scanner was used to image the sections.

4.2.13 Live cell and organ imaging (I, II, IV)

Cell death and survival of ligand stimulated, lectin treated, and siRNA treated and transfected adherent cells was examined by live cell imaging with the IncuCyte ZOOM system. The IncuCyte ZOOM software was utilized to determine the confluence and the morphology of the cells in the acquired phase-contrast images. The number of dying cells was determined by the distinct rounded morphology and higher intensity of dead cells in phase-contrast images. Zeiss AxioZOOM.V16 microscope with 1.0× PlanApo Z objective with 80× magnification was used to capture fast time lap videos of the hearts of anesthetized zebrafish embryos embedded into low melting point agarose.

4.2.14 Cell adhesion assay (IV)

The cells were detached with 5 mM EDTA and plated onto fibronectin-coated xCELLigence E-plates. The xCELLigence RTCA analyzer (Agilent) was utilized to measure the cell impedance for 24 hours.

4.2.15 Genomic DNA and RNA extraction (II, IV)

For the extraction of RNA from primary cultures or tissue samples, TRIsure RNA Isolation agent was used according to the manufacturer's protocol. The tissue samples were homogenized before RNA extraction. For the extraction of RNA from cell line cultures, NucleoSpin RNA Plus kit was utilized. Genomic DNA and RNA was extracted from zebrafish embryos with the NucleoSpin TriPrep kit according to the manufacturer's instructions.

4.2.16 PCR and genomic sequencing (II)

Extracted total RNA was reverse transcribed to cDNA with Sensifast cDNA Synthesis Kit according to the manufacturer's protocol. Real-time RT-PCR reactions were prepared by mixing primers, 5′ 6-FAM-labeled probes and TaqMan universal Master Mix II and run with QuantStudio 12K Flex Real-Time PCR System. The genomic DNA isolated from zebrafish embryos was amplified with nested PCR with sequential PCR reactions utilizing outer and inner primers and the Taq polymerase in a thermal cycler. The amplified genomic DNA regions were Sanger sequenced.

4.2.17 Lipid and glycan overlay assay with synthetic peptides (I)

Biotin-conjugated cyclic peptides corresponding to the eJM region of ErbB4 JM-a and JM-b isoform were commercially synthesized. The peptides were desalted, and the buffer exchanged to 0.1% formic acid with Empore Extraction disc C18 membrane (3 M) according to the manufacturer's protocol. The peptides were incubated with Membrane lipid assay membranes (Echelon Bioscience) in 3% BSA in PBST and detected with IR-800 conjugated streptavidin and Odyssey CLx Imager. The mammalian glycan array analysis was performed by the Consortium for Functional Glycomics' (CFG) Protein-Glycan Interaction Core (Boston, USA), where the peptides were incubated with the glycan arrays reconstituted in 150 mM NaCl and 1 mM $CaCl_2$ in 20 mM Tris-HCl (pH 7.4).

4.2.18 Mass spectrometry (I, II, IV)

Affinity enrichment samples analysed with mass spectrometry where either run on SDS-PAGE or directly processed. The SDS PAGE gels containing the affinity enrichment samples were fixed in 25% isopropanol and 10% acetic acid mixture for 18 hours and stained with Coomassie or PageBlue stain. Each sample lane was excised from the gel into 5 or 11 fractions. Each fraction was separately destained, dried, alkylated and trypsin-digested at 37°C for 18 hours. The directly processed affinity enrichment samples diluted with 0.2 M glycine were trypsin-digested at 37°C for 18 hours and methanol-chloroform precipitated. The guanidine hydrochloride in the other directly processed affinity enrichment samples was diluted to 2 M and the samples were trypsin digested in 37°C for 18 hours or Lys-C digested for 1 hour at 37°C and trypsin digested for 18 hours in 37°C. The digestion reaction was quenched with trifluoroacetic acid and the samples were desalted with a tC18 SepPak 96-well plate. The digested peptides were dried with a vacuum centrifuge. The dried samples were resuspended into 0.1% formic acid for mass spectrometry analysis. The peptide samples were analysed either in Proteomics Core Laboratory in the University of Tartu or in the Turku Proteomics Facility at Turku Bioscience (University of Turku and Åbo Akademi University). The peptide samples were analysed with Easy-nLC 1200 liquid chromatography system, Easy-nLC 1200 liquid chromatography system or Easy-nLC 1000 system coupled to Thermo Fisher Scientific LTQ Orbitrap XL, Orbitrap Q-Exactive HF instrument, Orbitrap Lumos Fusion instrument or LTQ Orbitrap Velos Pro mass-spectrometer. Parallel reaction monitoring (PRM) mass spectrometry samples were run on Easy-nLC 1200 liquid chromatography system coupled to an Orbitrap Lumos Fusion instrument (Thermo Fisher Scientific). Online PRM method designer Picky was used to select the cleaved

peptides of β1-integrin and a scheduled PRM method was used to simultaneously target the peptides selected by Picky during the mass spectrometry run.

4.2.19 RNA sequencing (IV)

The quality check for the RNA was performed with Advanced Analytical Fragment Analyzer. TruSeq Stranded mRNA HT Kit and 300 ng of RNA was used for library preparation. Illumina TruSeq RNA UD Indices were used for indexing. Illumina HiSeq3000 was utilized for paired-end (75 base pairs) sequencing. The quality-check, library preparation and sequencing steps were carried out in the Turku Bioscience Centre sequencing core (University of Turku and Åbo Akademi).

4.3 Computational and statistical analyses

4.3.1 Data handling and analysis

4.3.1.1 Mass-spectrometry data (I, II, IV)

The mass spectrometry spectra were searched against the proteome of the organism of cell line origin with Metamorpheus (Solntsev et al., 2018) or MaxQuant (Cox and Mann, 2008) for peptide and protein identification. The reference proteomes were downloaded from Uniprot (Bateman et al., 2021). The peptide and protein abundances were quantified with FlashLFQ (Millikin et al., 2018) or MaxQuant. Skyline (MacLean et al., 2010) was used to analyze the data from the PRM-mass spectrometry. Prosit (Gessulat et al., 2019) was utilized to predict the spectral library for the PRM data analysis.

The LFQ intensities of the affinity enriched proteins were normalized to the sum of the total LFQ intensity in one sample or sample fraction. To derive the sample-wise total protein intensities, the protein-wise sample fraction protein LFQ intensities were added. Additional median normalization was used to correct for experiment-wise variation in individual protein abundance for statistical testing. The statistical significance of protein enrichment in the affinity enriched samples was estimated by fitting a probability distribution function with an Epanechnikov kernel to the corresponding protein intensities in a control sample and drawing the P-value for the intensities of the tested sample from the fitted cumulative density function. The averaged P-values were FDR-corrected. The threshold for significant enrichment was determined as pseudolog2 fold change above 0.585 against the control and FDR-corrected P-value below or equal to 0.05. Experimentally derived interactome data from PSICQUIC (del-Toro et al., 2013) and STRING (Szklarczyk

et al., 2019) and subcellular location data from Compartments (Binder et al., 2014) database were used to visualize the affinity enriched proteins into network modules. The proteins identified in the PHA-L lectin pull-down that were not identified in the control streptavidin beads only condition were considered significantly enriched.

4.3.1.2 RNA sequencing data (IV)

For the quality-check of the RNA sequencing reads, FastQC (Babraham Bioinformatics) was utilized. For the quality and index trimming, PRINSEQ (Schmieder and Edwards, 2011) and Trimmomatic (Bolger, Lohse and Usadel, 2014) were utilized. For the pseudoalignment of the reads to human transcriptome Ensembl v96 (Yates et al., 2020), kallisto (Bray et al., 2016) was utilized. For the removal of the experiment-wise batch effect, batchelor (Haghverdi et al., 2018) was utilized. The transcripts per million (TPM) values were library size normalized. For differential expression analysis, DeSeq2 (Love, Huber and Anders, 2014) was utilized. Fold change above 1.5 and the FDR adjusted P-value equal or higher to 0.05 were used as a cut-off for significantly differentially expressed transcripts.

4.3.1.3 Glycan array data (I)

The glycan array data was provided as relative fluorescence units (RFUs). Sample-wise total RFU values were used to normalize the glycan array data. The threshold for background signal was set on 50% for the percent coefficient of variation (CV%) value and 50 for normalized RFU. Glycans with RFU values below and CV% values above the threshold were excluded from the final dataset. The statistical significance of the enrichment of a monosaccharide and its linkage in the glycans that associated primarily with the JM-a peptide was calculated with two-tailed Mann-Whitney U-test and the resulting P-value was Benjamini-Hochberg corrected. To calculate the enrichment RFU values of monosaccharides and their linkages in the glycans that associated primarily with the JM-a peptide were compared to the normalized values of monosaccharides and their linkages in glycans that associated equally or primarily with the JM-b peptide.

4.3.1.4 Other data

Densitometric western analysis data, real-time RT-PCR data, colocalization data and signal intensity data was either median normalized or normalized to the range to account for experiment-wise variation in total values. The cell impedance index values were normalized to the cell index values of the remaining cells after 24 hours measurement. The published dataset on RTK interactomes (Salokas et al., 2022) was

transformed into binary data due to the significant number of missing values. The enrichment in JM-a-like or JM-b-like RTK group was determined by at least 5-fold representation in the group and FDR-corrected P-value cut-off of 0.05. The P-values were determined through the binomial cumulative distribution function.

4.3.2 Statistical analyses (I, II, III, IV)

Statistical testing was performed with Matlab R2016a, R and GraphPad Prism. The normality and equality of variance assumptions of the datasets were tested with Shapiro–Wilkis, Kolmogorov–Smirnov, Bartlett's and Brown–Forsythe tests. For datasets for which the normality and equality of variance assumptions were true, one- or two-tailed T-test or one-way or two-way analysis of variance (ANOVA) tests were utilized for comparisons between groups. Dunnet's multicomparison test or two-tailed T-test was utilized for post hoc ANOVA analyses. For datasets for which the normality assumption, but not the equality of variance assumption was true, two-tailed T-test with Welch's correction or Brown-Forsythe one-way ANOVA was utilized. Dunnet's multicomparison test was utilized for post hoc ANOVA analyses. For datasets for which the normality assumption was false, two-tailed Mann-Whitney U-test, Kruskal-Wallis one-way ANOVA or Mackskill two-way ANOVA was utilized. Mann-Whitney U-test and Dunnet's multicomparison test were used for post hoc analyses. The multiple testing error was accounted with either Benjamini, Krieger and Yekutieli, Benjamini-Hochberg or false discovery rate (FDR) correction.

4.3.3 Image analysis (I, II, IV)

The cololocalization of two fluorescent signals in images was quantified with the algorithm of Villalta et al. (Villalta et al., 2011). As the output of the algorithm, 4 different measures of colocalization are reported: Pearson correlation, Manders overlap, m1/m2, and k1/k2. Only one measure was visualized and the degree of colocalization was confirmed with the other measures. The fluorescent signal intensity in PLA images was quantified with Fiji (Schindelin et al., 2012) and normalized to the number of nuclei. The amount of fluorescent PLA signals and the number of nuclei were counted with the particle analyzer function of Fiji. The location of the PLA signals relative to the cell edges was determined with SpatTrack (Lund et al., 2014). The fluorescent signal intensity and the DAB signal intensity in deconvoluted images were determined with Fiji. The 2-dimensional morphology of imaged cells was determined with the MorphoLibJ (Legland, Arganda-Carreras and Andrey, 2016) library in Fiji.

4.3.4 Gene set enrichment and pathway analyses (I)

The gene set enrichment analysis on subcellular location of the interactome of ErbB4 JM-a and JM-b and JM-a-like and JM-b-like RTKs was performed with the Panther overrepresentation test with Fisher's Exact test. The annotations from the GO cellular compartment v 10.5281 (Ashburner et al., 2000) were utilized. The statistical significance of the overlap of the subcellular location annotations of ErbB4 JM-a and JM-a-like RTKs and ErbB4 JM-b and JM-b-like RTKs was determined with the χ^2 test. The statistical significance of the lack overlap between the enriched subcellular location annotations of JM-a-like and JM-b-like RTKs was estimated with an empirically determined probability distribution. The RTKs were repeatedly randomized into two groups of the same size as the JM-a-like and JM-b-like RTK groups and the subcellular location enrichment of the interactome partners of the randomized groups were determined. The overlap of the enriched subcellular locations of the randomized groups was calculated and a normal distribution was fitted to the overlap values. The P-value was estimated from the cumulative normal probability distribution.

Stochastic neighbourhood embedding (Hinton and Roweis, 2003) was utilized to derive a one-dimensional representative value for each sample (n=8) and for each pathway annotation (number of features included ranging from 5 to 207) from the ErbB JM-isoform interactomes. Molecular Signatures Database v7.5.1 (Liberzon et al., 2011) was used as the source for the pathway annotations and pathway annotations that had less than 5 common genes with the interactome datasets were excluded. The statistical significance of differential pathway representation in the interactomes of ErbB4 JM-a and JM-b was determined with the Mann-Whitney U-test.

4.3.5 Custom approaches

4.3.5.1 Dimensionality reduction and clustering of published datasets (I, II)

The published transcriptome and interactome and proximity labelling datasets were acquired from Gene Expression Omnibus (Edgar, Domrachev and Lash, 2002) (identifiers: GSE36961, GSE1145, GSE14190, GSE12337, GSE56348, GSE5500) or from the publication of Salokas et al. (Salokas et al., 2022), respectively. The expression values of the genes involved in the NRG-1/ErbB4/STAT5b pathway in the transcriptome datasets were subjected to principal component analysis with R in Rstudio. The interactome and proximity labelling datasets were subjected to the neighbourhood components analysis (NCA) with the dimensionality reduction

toolbox of Matlab 2016a (Goldberger et al., 2005). The 2-dimensional clustering of the samples from normal control and hypertrophic cardiomyopathy groups and JM-a and JM-b like RTKs was examined. The relative sum of the Euclidian distances within groups against the sum of Euclidian distances between groups was used as the measure for the clustering. An empirical probability distribution was estimated by repeated rounds of randomization to estimate the statistical significance of the clustering. The JM-a and JM-b like RTKs were used as classification labels for the NCA. To define the empirical probability distribution the classification labels were randomized. Several initializations for the NCA were performed and the average case was reported.

4.3.5.2 JM-motif analysis (I)

To derive the JM sequence motifs, several sequence models weighing the different residues between residues 627–632 in ErbB4 JM-a and in ErbB4 JM-b sequences were iterated on the eJM sequences of experimentally tested RTKs. A sliding window analysis was developed to calculate the similarity score for each sequence window in the eJM regions. The similarity scoring was based on the similarity of the sequence window to the 627–632 residues in ErbB4 JM-a and JM-b isoform sequence. The PAM250 matrix was used a source for the similarity scores. The accuracy of the derived motif sequences was tested on their ability to accurately categorize experimental data. The statistical significance of the categorization was determined with the cumulative probability density function of a binomial distribution. To assume equal probability for incorrect and correct categorization, the parameter p of the binomial probability density function was set to 0.5.

4.3.5.3 Cleavage site prediction (IV)

To predict the cleavage sites for ADAM12 and ADAM17 in the extracellular juxtamembrane region of TYRO3, a 0^{th} order Markov chain was used to determine the probability of a cleavage site in a 10-residue long sequence window based on the positional amino acid frequencies determined by two peptide screens (Caescu, Jeschke and Turk, 2009; Tucher et al., 2014). The probability of no cleavage site was determined from the same sequence windows with a 0^{th} order Markov chain and the relative frequencies of amino acid residues in proteins. At least a twofold increase in the probability of a cleavage site over no cleavage site was considered to indicate the presence of a cleavage site. Residues 1–35 upstream the transmembrane domain were considered in the analysis.

4.3.5.4 De novo multi-omics pathway analysis (DMPA) (IV)

4.3.5.4.1 The DMPA algorithm

The DMPA models single-omics data into network modules and combines the modules into multi-omics pathways. The DMPA is based on two key principles: the combination of two association measures, the correlation and stoichiometry scores and neighbourhood maximization (Figure 1 in IV). The correlation score in DMPA between the expression values of two features is calculated by the Spearman rank correlation:

$$\rho = 1 - \frac{6 \sum d^2}{n(n^2 - 1)}$$

where d is the difference between ranks of the expression values of two features in each sample in n number of samples. The stoichiometry score, in turn, is determined by the interquartile range of sample-wise variation in the relative expression values of two features F in samples n:

$$if\ median(F1_{1,\dots,n}) > median(F2_{1,\dots,n})$$

$$stoichiometry\ score = \frac{Q_3}{Q_1}\ in\ \frac{F1_1}{F2_1}, \frac{F1_2}{F2_2}, \dots, \frac{F1_n}{F2_n}$$

$$if\ median(F2_{1,\dots,n}) > median(F1_{1,\dots,n})$$

$$stoichiometry\ score = \frac{Q_3}{Q_1}\ in\ \frac{F2_1}{F1_1}, \frac{F2_2}{F1_2}, \dots, \frac{F2_n}{F1_n}$$

Q_1 and Q_3 denote the first and third quartile value in the sorted set of the relative expression values. For sparse datasets a version of the stoichiometry score that adjusts the stoichiometry score based on the pattern of missing values was created. In the zero-inflated version of the DMPA the stoichiometry score is inflated when the expression value from only one of the features is missing and deflated when the expression values are missing for both features in the same sample. The correlation and stoichiometry scores for all feature pairs are ranked by each feature and adjusted to a linear scale between 1 and 0. The feature pair with the highest correlation score and lowest stoichiometry score is assigned 1 as the correlation and stoichiometry score. The ranked and adjusted correlation and stoichiometry scores are combined with non-weighted multiplication to derive the combined score.

Two cut-off parameters C and S were designed to exclude feature pairs with low combined scores from the analysis to reduce computational run time. The parameter C defines how many feature pairs per feature should in minimum be considered for each feature. The parameter S defines for how many features in the dataset feature

pairs should be considered. A script that visualizes the distribution of the maximum raw stoichiometry and correlation scores for each feature was created to guide in the parameter S choice. The parameter C choice is only dependent on the size of the dataset and should be adjusted from the default value 1 only if the examined dataset has low dimensionality. After cut-off highest scoring three feature cliques are searched for each feature in the dataset from the remaining combined scores of the feature pairs. For all features i=1,…,n the sum of the combined scores C between feature i and features j=1,…,n excluding i and features k=1,…,n excluding i and j is maximized:

$$argmax\ C_{ij} + C_{jk} + C_{ik}$$

The three feature cliques are combined and trimmed into larger and smaller modules based on common features in three steps that can be partially controlled by parameter choices. First all three feature cliques that share two common features are combined. This step is reiterated until no modules with two common features remain. Second, small modules with one common feature can be combined based on the user defined setting for the parameter 7, that determines the combined size of the modules that can be combined. Lastly, small modules created by the previous step can be combined into larger modules based on the user defined setting for parameter 8, that determines the combined size of the modules that can be combined based on only one common feature. The last combination step is redundant if the second combination step is not allowed. After each combination step the features that have been combined into larger modules are removed from the remaining three feature cliques. The DMPA allows for one feature to be included in more than one module.

The combination of the network modules into multi-omics pathways follows the same pipeline than the initial network module inference from single omics data. Instead of the expression values for each feature a median expression value of all features in a module is used in the inference.

4.3.5.4.2 DMPA validation

The conservation of the stoichiometry, correlation and combined scores and the ability for DMPA to discover previously reported associations was examined to validate the DMPA. The conservation of the scores was determined by using DMPA to create modules and multi-omics pathways from the first dataset and then examining the median score for the feature pairs and the module pairs in the modules and pathways in a second dataset. The previously reported associations were acquired from STRING (Szklarczyk et al., 2019), PhosphoSitePlus (Hornbeck et al., 2019), ChEA3 (Keenan et al., 2019), ENCODE (Abascal et al., 2020), ReMap (Hammal et al., 2022), EWAS Atlas (Xiong et al., 2022), Rhea (Bansal et al., 2022)

and PathwayCommons (Cerami et al., 2011) databases. The number of known associations in all inferred network modules and multi-omics pathways was quantified. Modules and multi-omics pathways of the same size were repeatedly simulated by randomization to define an empirical probability distribution. The number of known associations was quantified from the randomized modules and pathways and a probability distribution function was fitted with an Epanechnikov kernel to the values. A P-value for the DMPA derived modules and pathways and the relative distance from the median of the probability distribution was determined from the probability distribution. The published single- and multi-omics data used in the validation were acquired from the publications of Batth et al. (Batth et al., 2018) and Karayel et al. (Karayel et al., 2020), and from ArchS4 (Lachmann et al., 2018), LinkedOmics (Vasaikar et al., 2018) and MetaboLights (Haug et al., 2020) databases.

4.3.5.4.3 Data simulation for parameter S sensitivity analysis

To examine the sensitivity of DMPA to parameter S choice, normally distributed, beta-distributed, and negative binomially distributed feature expression values were simulated into modules as detailed in the Supplementary Materials and Methods in IV. The true positive and false positive rate was quantified with different parameter S values, different feature set sizes and with different number of features with no module associations.

4.3.5.4.4 Benchmarking the DMPA

To benchmark DMPA, WGCNA (Langfelder and Horvath, 2008), the partial correlation method LOPC (Zuo et al., 2014), GENIE3 (Huynh-Thu et al., 2010) and the multi-omics integration method TransNet (Rodrigues, Shulzhenko and Morgun, 2018) were used to infer modules, networks, and connections between multi-omics modules according to the developer's instructions. Transcriptome data from ArchS4 and multi-omics data from LinkedOmics (Vasaikar et al., 2018) was utilized. To compare DMPA against the network inference method LOPC, network edges were assigned between the features in the modules by the remaining connections of the original three feature cliques. The number of known associations in the modules, networks and connected multi-omics modules were quantified and its statistical significance estimated as described in the DMPA validation section 4.3.5.4.2. Instead of number of known associations inside modules, number of known associations connected by a network edge was quantified from the networks inferred with LOPC and DMPA. The statistical significance of the multi-omics module connections inferred with DMPA and TransNet was additionally estimated similarly

to the statistical significance of multi-omics pathways, but instead of randomizing the modules only the connections between the modules were repeatedly randomized for the estimation of the empirical probability distribution. The runtime and the fraction of the features included in the modules was also measured.

4.3.5.4.5 Prediction functions of DMPA

Upstream transcription factor and kinase prediction, subcellular location prediction and function prediction modalities were developed for the transcriptome, phosphoproteome and interactome modules and multi-omics pathways inferred with the DMPA, respectively. The details of the created prediction methods are presented in the Supplementary Materials and Methods section in IV.

5 Results

5.1 A sequence motif in the eJM region determines the cell surface location and downstream signaling of receptor tyrosine kinases (I)

5.1.1 ErbB4 JM isoforms elicit differential signaling responses and localize to different plasma membrane microdomains

The differences between the ErbB4 JM-isoforms were investigated to study the structure function relationship of the eJM region of receptor tyrosine kinases. The ErbB4 JM-isoforms were discovered to differentially activate and associate with STAT5a, STAT5b and STAT3 in several cell lines when assessed with immunofluorescence, proximity ligation assay and western analysis (I, Fig. 2 and Supplementary Fig. 5a–d; Figure 10a–b). Phosphorylation in the activating Y694 (in STAT5a)/ Y699 (in STAT5b) residue or Y705 (in STAT3) and nuclear localization were used as a measure for STAT activation. ErbB4 JM-a was observed to primarily associate with STAT5a and ErbB4 JM-b with STAT5b and STAT3 (I, Fig. 2 and Supplementary Fig. 5a–d; Figure 10a–b). Since the JM-a isoform has been discovered to be prone to the regulated intramembrane proteolysis by ADAM17 and γ-secretase (Rio et al., 2000; Ni et al., 2001; Vidal et al., 2005), the activation of STAT5s was examined with a cleavage resistant mutant V675A of ErbB4 JM-a and with ADAM17 and γ-secretase inhibitor treatments and western analysis (I, Supplementary Fig. 6c–l). Blocking the cleavage of ErbB4 JM-a resulted in increased ErbB4 mediated STAT5a activation and decreased STAT5b activation, indicating that an unknown mechanism in the eJM region is controlling the STAT subtype activation preference of ErbB4 JM-isoforms.

To examine the difference in the signaling of ErbB4 isoforms more comprehensively, the interactome of ErbB4 JM-a and JM-b was analyzed with affinity enrichment mass spectrometry. ErbB4 JM-a and JM-b were discovered to interact with vastly different signaling proteins that were associated with distinct cell signaling pathways (I, Supplementary Fig. 2–3). The Janus-kinase TYK2 was discovered to primarily associate with the JM-b isoform both in the affinity enrichment samples analyzed with mass spectrometry and with western analysis (I, Fig. 1c-d and Supplementary Fig. 2). Treatments with siRNAs confirmed that the

activation of STAT5b by the JM-b isoform was dependent on TYK2, while no Janus kinase was discovered to regulate the activation of STAT5a by ErbB4 JM-a in western analyses (I, Fig. 1e–f; Figure 10c).

The subcellular location of ErbB4 JM-a and JM-b was additionally examined with super resolution immunofluorescence microscopy (I, Fig. 1a–b and Supplementary Fig. 1; Figure 10d–e). ErbB4 JM-a and JM-b were discovered to partially localize into different microdomains in the cell surface. The difference in the cell surface localization of ErbB4 JM-isoforms remained even when the cleavage resistant mutant of ErbB4 JM-a was examined.

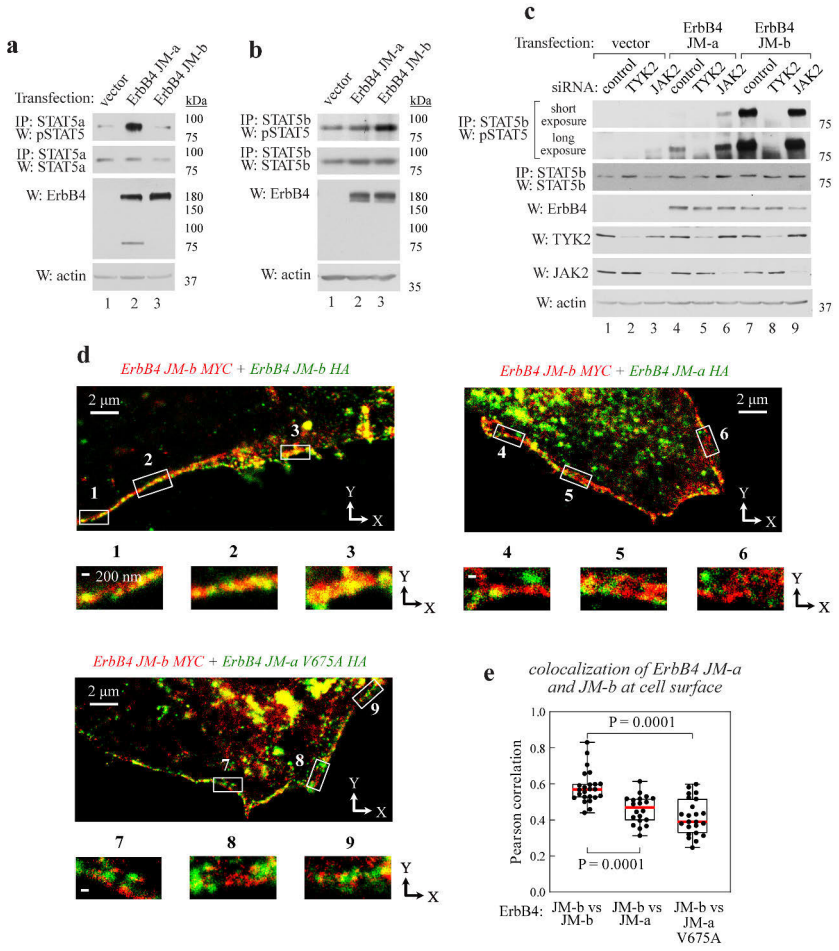

Figure 10. ErbB4 JM-a and JM-b activate different STAT5s and localize to different regions in the plasma membrane. **a**–**b**: Western analysis on the activation of STAT5s in cells expressing ErbB4 JM-isoforms. **c**: Western analysis on the effect of siRNA mediated TYK2 knock-down on activation of STAT5b. **d**: Superresolution stimulated emission depletion microscopy images on the localization of different tagged ErbB4 variants in the plasma membrane. V675A: cleavage resistant variant of ErbB4 JM-a.

5.1.2 The difference in the subcellular location and STAT signaling responses of the ErbB4 JM-isoforms can be tracked back to key residues in the eJM region of ErbB4 JM-a

A structural analysis was conducted to identify the putative key residues 630 and 631 in the eJM region of ErbB4 JM-a and JM-b that could be the origin for the observed differences of the JM-isoforms (I, Fig. 3a). Molecular dynamics simulations revealed no significant conformational changes generated by the structural differences in the JM-isoforms (I, Fig. 3b–c and Supplementary Fig. 8e). The residues identified by the structural analysis in the JM-a isoforms were mutated into the corresponding ones in the JM-b isoform and the ability for the mutant to activate STAT5s and localize with ErbB4 JM-isoforms was examined (I, Fig. 3d–g; Figure 11). The ErbB4 JM-a S630I/H631E variant was discovered to activate STAT5b over STAT5a and colocalize more with the JM-b isoform in the cell surface compared to the JM-a isoform in western and super resolution microscopy analyses (I, Fig. 3d–g; Figure 11). The H631E mutation alone was discovered to be sufficient to disrupt the ability of ErbB4 JM-a to activate STAT5a (I, Fig. 4i) while mutation of the S630 along with other serines, threonines and asparagines in the JM-a region had no effect on the activation of STAT5a in western analyses (Supplementary Fig. 7a–b). The D632 residue was additionally discovered as relevant for STAT5a activation although it is shared among the JM-isoforms (I, Fig. 4i).

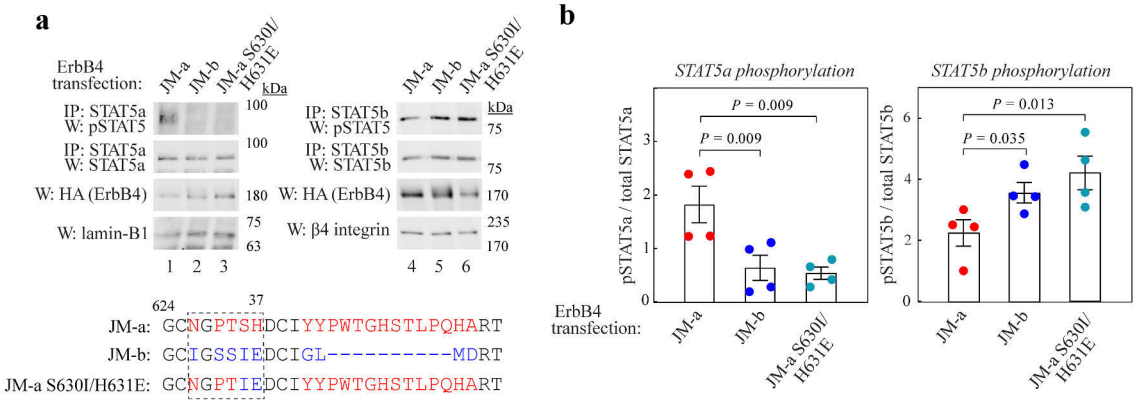

Figure 11. Mutational analysis on the key residues in ErbB JM-a that confer selective STAT5 activation. **a**–**b**: Western analysis on the activation of STAT5s by the JM-a S630/H631 variant.

5.1.3 A sequence motif in the eJM region of receptor tyrosine kinases confers selective STAT activation and subcellular location of RTKs

The STAT5 subtype activation preference of other ectopically expressed and endogenous RTKs was examined to explore the frequency of selective STAT5 activation among the RTKs. A clear preference for the activation of a specific STAT5 subtype was discovered for almost all tested receptor tyrosine kinases (I, Fig. 4a–f, 5a–b). In the ErbB family of RTKs, the ErbB receptors that activated STAT5b, activated also STAT3 and colocalized more with ErbB4 JM-b than JM-a (I, Fig. 4c–d and Supplementary Fig. 9a–b). The ErbB receptors that activated STAT5a in turn colocalized more with ErbB4 JM-a than JM-b in the cell surface (I, Fig. 4a-b and Supplementary Fig. 9a–b).

To discover sequence motifs in the eJM regions of RTKs, different motif models based on the critical residues in ErbB4 JM-a and JM-b were fitted to the eJM sequences of RTKs. The capacity of the motif models to correctly categorize RTKs based on the STAT5 subtype activation preference was examined (I, Supplementary Dataset 5). The best scoring JM-a and JM-b motif models correctly categorized all RTKs experimentally verified to selectively activate STAT5 subtypes (I, Fig. 4g–h; Figure 12). The validity of the derived JM sequence motifs was examined by substituting the critical residues in ErbB4 JM-a and JM-b with the alternative residues suggested by the motifs. Point mutations designed to disrupt the motifs were also tested. Substitution of the JM-a residue H631 into lysine, arginine, glutamine, or asparagine or the D632 residue into glutamic acid, asparagine, glutamine, or histidine retained the ability of ErbB4 JM-a to activate STAT5a at least to some extent (I, Fig. 4i). Only the substitutions H631E and D632L designed to break the JM-a motif were able to disrupt the ability of ErbB4 JM-a to activate STAT5a (I, Fig. 4i). None of the tested substitutions influenced the ability of ErbB4 JM-b to activate STAT5b (I, Fig. 4j). These results indicate that the JM-a motif has an active role in conferring the selective STAT5 subtype activation of RTKs and that the JM-b motif is passive. This was further confirmed by statistical analysis that discovered that only the JM-a motif is enriched in the eJM regions of RTKs ($P = 0.017$).

The statistical significance of JM motif-based clustering of RTKs was examined in published interactome datasets. The RTKs were observed to statistically significantly cluster into groups based on the JM motif. This indicates that the interactomes of RTKs are partially dependent on the JM motif in the eJM region (I, Fig. 5d). JM motif-based interactomes of RTKs were defined and a significant overlap was discovered on the enriched subcellular locations of the interactomes of ErbB4 JM-a and other RTKs containing a JM-a motif and ErbB4 JM-b and other RTKs containing a JM-b motif (I, Supplementary Fig. 11). This further suggests that the subcellular location of RTKs is partially determined by the JM motif.

a *JM-a sequence motif*

G-X(2,3)-[HRKQN]-[DEQNH]
G-X(2,3)-[DEQNH]-[HRKQN]

RTK	motif	amino acids
JM-a	GPTSHD	627-632
EPHA10	GSRDQS	558-563
EPHA2	GSKVHE	518-523
EPHA6	GYSQKF	525-530
EPHB3	GSGAQQ	547-552
EPHB4	GQEHHS	519-524
ERBB2	GCPAEQ	641-646
ERBB3	GPELQD	623-628
FGFR1	GLSHHS	348-353
FGFR2	GREKEI	364-369
FGFR3	GFSHHS	346-351
KIT	GNNKEQ	510-515
PDGFRA	GAENRE	508-513
PDGFRB	GQDTQE	515-520
ROS	GISENI	1843-1848
TIE1	GPVQES	745-750
TRKA	GDPVEK	405-410
VEGFR1	GTSDKS	750-755
VEGFR2	GAQEKT	756-761

b *JM-b sequence motif*

G-X(1,2)-{HRKQN}-[EDQ](1,2)-{HRKQN}

RTK	motif	amino acids
JM-b	GSSIED	627-632
AXL	GQAQPV	429-434
EGFR	GPGLEG	630-635
EPHA4	GDFSEP	522-527
EPHA7	GKMFEA	540-545
EPHA8	GRFSQA	521-526
FGFR4	GLSYQS	340-345
FLT3	GTSCET	521-526
IGF1R	GSWTDP	914-919
INSR	GSWTEP	934-939
IRR	GPEEED	911-916
MERTK	GWVDYA	484-489
RON	GAPLQV	928-933
TYRO3	GPWSQP	403-408

Figure 12. The eJM sequence motifs identified by selective STAT5 activation by RTKs. In color the RTKs that were experimentally verified to preferentially activate STAT5a (red) or STAT5b (blue) are indicated.

5.1.4 The JM-a motif binds complex-type N-glycans in cell surface proteins such as β1-integrin

To screen for a mechanism for the selective STAT activation conferred by the JM-a motif in RTKs, the interaction of the eJM region of ErbB4 JM-a and JM-b with lipids and glycans was examined. Synthetic peptides corresponding to the residues 621–633 in ErbB4 JM-a and JM-b were incubated with a lipid overlay assay and the mammalian glycan array (I, Supplementary Fig. 12a). The JM-a peptide was discovered to bind glycans with a greater affinity than the JM-b peptide (I, Fig. 6a and Supplementary Fig. 13). Complex-type N-glycans with a β1,6-branch were especially enriched among the glycans that bound the JM-a peptide with greater affinity ($P = 0.023$). No differential binding to lipids was discovered for the JM-a and JM-b peptide (I, Supplementary Fig. 12b–c). A lectin screen was conducted to identify the glycan structures involved in ErbB4 JM-a mediated STAT5a activation. The DSL, STL and PHA-L lectins were discovered to significantly affect the ErbB4 JM-a mediated STAT5a activation (I, Fig. 6c; Figure 13a), but not the ErbB4 JM-b mediated STAT5b activation (I, Fig. 6d). DSL and STL bind the β1,4-branch and

PHA-L the β1,6-branch of complex-type N-glycans (I, Fig. 6b; Figure 13b). DSL and STL also reduced the RTK-mediated activation of STAT5 subtypes by the ErbB receptors containing the JM-a motif but not by those containing the JM-b motif (I, Supplementary Fig. 14a–c). Since the survival of cells stimulated with the ligands of RTKs with a JM-a motif was discovered to be STAT5a dependent (I, Fig. 5c), the effect of the DSL, STL and PHA-L lectin treatment on the survival of cells stimulated with ligands of RTKs containing a JM-a or JM-b motif was examined. DSL, STL and PHA-L lectin treatment significantly reduced the survival of the cells stimulated with the ligands binding RTKs containing a JM-a motif, but not the cells stimulated with ligands binding RTKs containing a JM-b motif (I, Fig. 6e–f and Supplementary Fig. 14d–f).

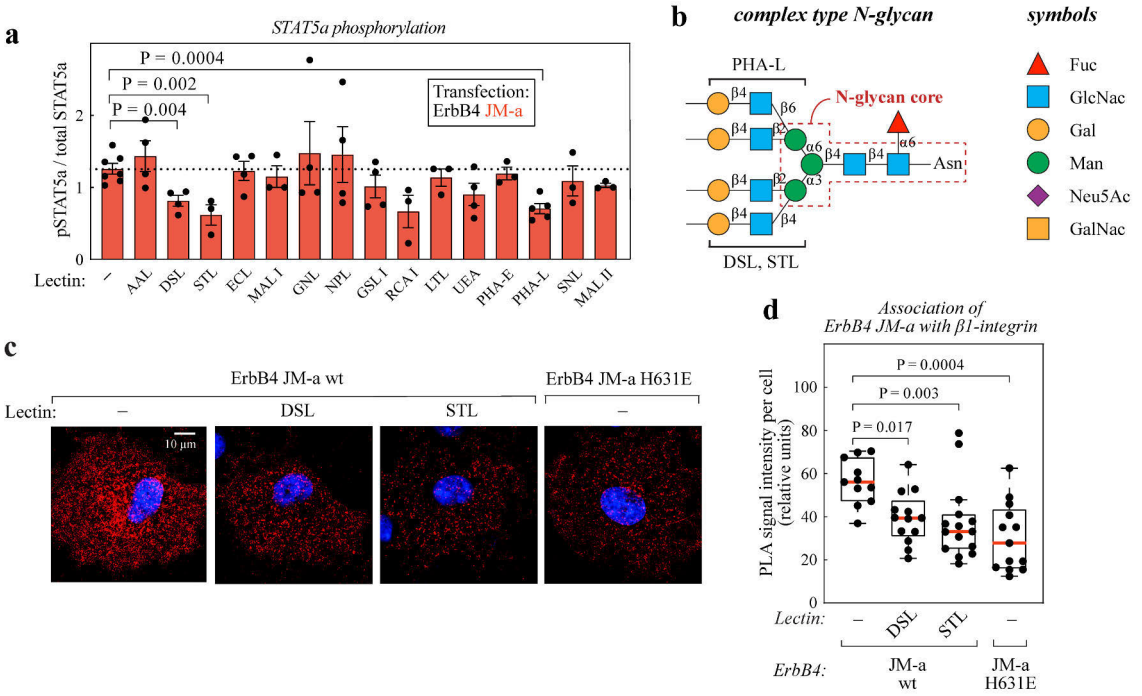

Figure 13. The association between complex-type N-glycans and ErbB4 JM-a region is required for STAT5a activation and association with β1-integrin. **a**: A lectin screen to identify the glycan structures that are involved in the activation of STAT5a by ErbB4 JM-a. The level of STAT5a activation was measured with western analysis. **b**: A schematic depicting the binding sites of the indicated lectins in the complex-type N-glycans. **c**–**d**: Proximity ligation assay of ErbB4 JM-a variants and β1-integrin in lectin treated or untreated cells. H631E: mutation that disrupted ErbB4 JM-a mediated activation of STAT5a.

To identify the cell surface proteins that carry the type of complex-type N-glycans the JM-a motif region associates with, an affinity enrichment with the PHA-

L lectin was carried out in three separate cell lines and analyzed with mass spectrometry. Beta1-integrin was identified as one of the N-glycosylated cell surface proteins in all three cell lines where selective STAT5 activation by ErbB4 JM-isoforms occurs (I, Fig. 2c–d, 6g). In concordance, ErbB4 JM-a was discovered to interact with and colocalize more with β1-integrin than ErbB4 JM-b in affinity enrichment and immunofluorescence samples analyzed with PRM mass spectrometry and super resolution microscopy (I, Supplementary Fig. 15). The effect of DSL, STL and PHA-L lectin treatment and the H631E point mutation in ErbB4 JM-a on the association and colocalization between ErbB4 JM-a and β1-integrin was examined with proximity ligation assay and immunofluorescence (I, Fig. 6h–k; Figure 13c-d). The DSL, STL and PHA-L lectin treatments and the H631E point mutation disrupted the association and colocalization of ErbB4 JM-a with β1-integrin (I, Fig. 6h–k; Figure 13c–d). This indicates that the association between ErbB4 JM-a and β1-integrin is both dependent on the N-glycosylation of β1-integrin and on the JM-a motif.

5.2 STAT5b mediates growth responses of the NRG-1/ErbB4 pathway in cardiomyocytes (II)

5.2.1 STAT5b signaling mediates NRG-1/ErbB4 induced hypertrophic growth *in vivo* and *in vitro* in murine cardiomyocytes

The physiological role of the differential STAT5 signaling arising from the structural diversity of the eJM region of ErbB4 was explored. ErbB4 JM-a induced STAT5a activation has been discovered to control mammary gland development and the expression of lactation genes (Jones et al., 1999; Long et al., 2003; Tidcombe et al., 2003). The physiological role of ErbB4 JM-b-induced STAT5b activation, however, has not been described. Since the ErbB4 JM-b isoforms are specifically expressed in the myocardium (Elenius et al., 1997a) and the NRG-1 and ErbB4 signaling has been discovered to control the development, growth, and regeneration of the myocardium (Odiete, Hill and Sawyer, 2012; De Keulenaer et al., 2019), the role of STAT5b in the NRG-1/ErbB4-induced growth processes in the myocardium was explored. First, an AAV vector construct encoding the extracellular domain of ErbB4 combined to a mouse Fc region of immunoglobulin γ (mErbB4-Fc) was generated to serve as a ligand trap for ErbB4 ligands. Mice were infected with either the AAVs encoding the mErbB4ECD-Fc (ErbB4ECD-AAV) or AAVs encoding a scrambled control vector (control AAV) and the nuclear localization of STAT5b and the expression of established STAT5b target genes were examined in the hearts of mice with immunofluorescence and real-time RT PCR (II, Fig. 1A–E; Figure 14C–D). The

degree of nuclear localization was used as a measure of STAT5b activation. The ErbB4ECD-AAV treatment significantly reduced the nuclear localization of STAT5b and the transcription of STAT5b target genes (II, Fig. 1C–E). Since the size of the cardiomyocytes was reduced in the mice injected with AAVs encoding the ErbB4ECD construct, the ErbB4ECD-AAV treatment was also concluded to reduce hypertrophic cardiomyocyte growth (II, Fig. 1A–B; Figure 14A–B). The ErbB4ECD-AAV treatment also significantly reduced the heart weight of the mice (III, Supplemental Fig. 10C–D).

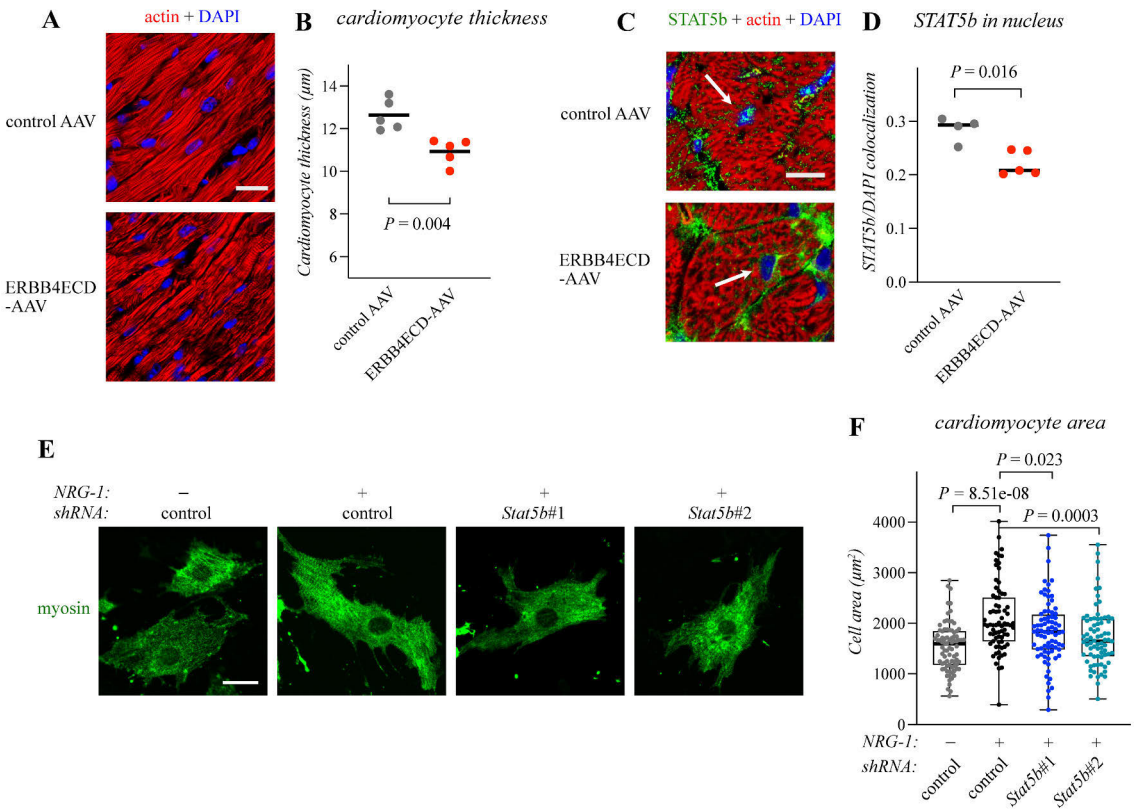

Figure 14. NRG-1/ErbB4/STAT5b signaling regulates cardiomyocyte hypertrophy in postnatal mice. **A**–**B**: Cardiomyocyte size was assessed with immunofluorescence from heart sections of control AAV and ERBB4ECD-AAV treated mice. Scale bar 20μm. **C**–**D**: Nuclear STAT5b signal was examined with immunofluorescence from heart sections of control AAV and ERBB4ECD-AAV treated mice. Scale bar 10μm. **E**–**F**: Cardiomyocyte size was assessed with immunofluorescence from NRG-1 treated or untreated and control or Stat5b shRNA treated isolated neonatal cardiomyocytes. Scale bar 20μm. DAPI: 4′,6-Diamidino-2-phenylindole dihydrochloride. AAV: adeno-associated virus. ERBB4ECD-AAV: an AAV vector construct encoding the extracellular domain of ErbB4 combined to a mouse Fc region of immunoglobulin γ.

Next, the effect of STAT5b and ErbB4 shRNA treatments on cardiomyocyte growth were explored in isolated cardiomyocytes. STAT5b shRNA treatments were discovered to reduce NRG-1-induced hypertrophic growth in isolated cardiomyocytes when assessed with immunofluorescence (II, Fig. 1F–G; Figure 14E–F). ErbB4 shRNA treatment in turn was discovered to reduce both the nuclear localization of STAT5b and the size of isolated cardiomyocytes (II, Fig. 1H–I). The treatment with both STAT5b and ErbB4 shRNAs was additionally observed to reduce the transcription of STAT5b target genes *Igf-1*, *Myc* and *Cdkn1a* when assessed with real-time RT-PCR (II, Fig. 1J).

5.2.2 STAT5b controls hyperplastic growth of the myocardium of zebrafish embryos and the activation of STAT5 in embryonic zebrafish is controlled by the NRG-1/ErbB pathway

In addition to hypertrophic growth NRG-1 is known to induce hyperplastic growth in embryonic cardiomyocytes (Zhao et al., 1998). The role of STAT5b in NRG-1/ErbB4 induced hyperplastic myocardium growth was explored in embryonic zebrafish. Pericardial injection of recombinant NRG-1 was observed to induce the activation of STAT5 and ventricular growth in embryonic zebrafish in western and immunofluorescence analyses (II, Fig. 3A–D, G–H; Figure 15A–B). The hyperplastic nature of the NRG-1 injection induced growth was confirmed by estimating the number of cardiomyocytes per ventricle area (II, Fig. 3A–B). Treatment with the ErbB inhibitors AG1478 and lapatinib reduced ventricular myocardial growth when embryonic zebrafish were assessed with live imaging (II, Fig. 4A–B; Figure 15C). Treatment with AG1478 and lapatinib also reduced Stat5 activation in western analyses (II, Fig. 4C–D, Figure 15D). Treatment with the ErbB inhibitor gefitinib in turn reduced the activation of Erk but did not significantly alter myocardial growth (II, Fig. 4A–D). None of the ErbB inhibitor treatments reduced the activation of Akt (II, Fig. 4C–D).

The *stat5b* gene of embryonic zebrafish was disrupted with CRISPR/Cas9 system resulting in the downregulation of Stat5b transcript and protein in the embryos when assessed with real time RT-PCR and immunofluorescence (II, Fig. 5A–B and EV3B). The CRISPR/Cas9 mediated knock-down of *stat5b* led to reduced ventricular growth assessed by immunofluorescence analysis and ventricular dysfunction as indicated by the reduced ejection fraction measured from the videos produced by live imaging (II, Fig. 5; Figure 16).

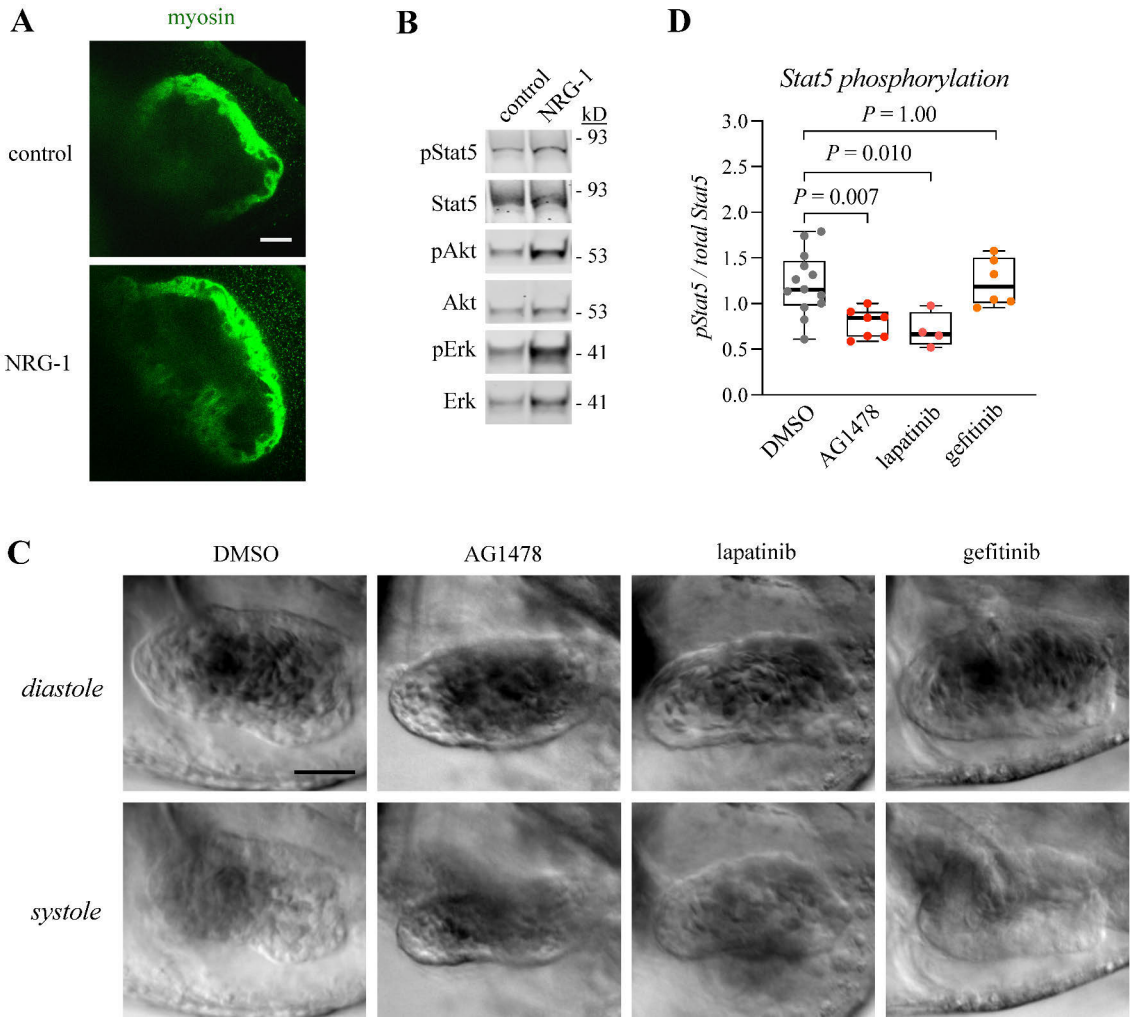

Figure 15. NRG-1/ErbB signaling regulates myocardial growth and Stat5 activation in embryonic zebrafish. **A**: Ventricle size of 4dpf zebrafish injected at 2 dpf with recombinant human NRG-1 or control substance to the pericardial sac was assessed with immunofluorescence. Scale bar 20 µm. **B**: Activation of Stat5 was assessed with western analysis from 4 dpf zebrafish embryos injected with recombinant human NRG-1 or control substance to the pericardial sac. The embryos were lysed after 20 minutes. **C**: The ventricle size was assessed with phase contrast imaging from 4dpf zebrafish embryos treated with DMSO or the ErbB inhibitors AG1478, lapatinib and gefitinib for 2 days. Scale bar 50µm. **D**: Activation of Stat5 was assessed with western analysis from 4 dpf zebrafish embryos treated with DMSO or the ErbB inhibitors AG1478, lapatinib and gefitinib for 1 hour. Dpf: days post fertilization. AG1478: ErbB1/2/4 inhibitor. Gefitinib: ErbB1 inhibitor. Lapatinib: ErbB1/2 inhibitor.

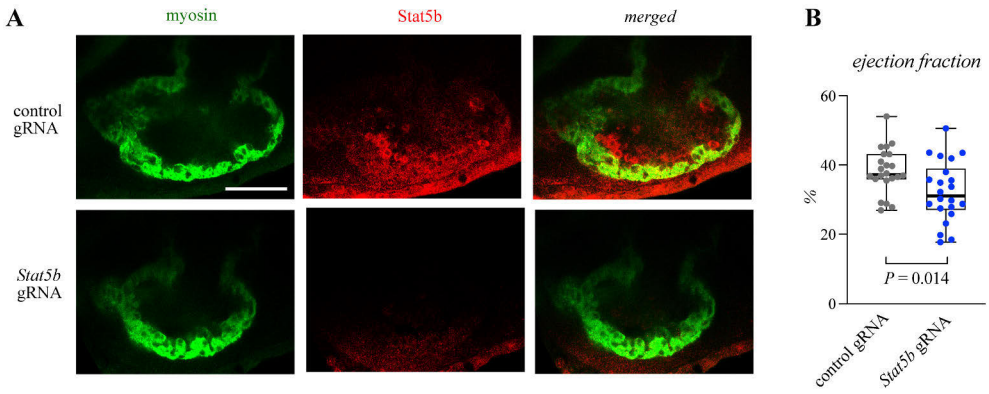

Figure 16. CRISPR/Cas9 mediated knock-down of Stat5b in zebrafish embryos results in reduced myocardial growth and ejection fraction. **A**: The ventricle size was assessed with immunofluorescence from control and Stat5b gRNA and CRISPR/Cas9 injected zebrafish embryos at 4 dpf. The injections were performed at one-cell stage. Scale bar 50µm. **B**: The ejection fraction of the zebrafish embryos treated as in A was assessed with live phase-contrast imaging. Dpf: days post fertilization.

5.2.3 Dynamin-2 controls the subcellular location of ErbB4 and STAT5b signaling in cardiomyocytes

Dynamin-2 was discovered as one of the interaction partners of ErbB4 with affinity enrichment mass spectrometry (II, Fig. EV2A). Since Dynamin-2 was additionally observed to preferentially associate with the ErbB4 JM-b isoform over the JM-a isoform in proximity ligation assays (II, Fig. EV2B-C), the role of Dynamin-2 in ErbB4 JM-b mediated STAT5b signaling was examined. Dynamin-2 is a GTPase that has been reported to regulate membrane fission in vesicle trafficking (Laiman, Lin and Liu, 2023). Inhibition of Dynamin-2 with dynasore was observed to reduce the plasma membrane location of both ErbB4 JM-isoforms when assessed with immunofluorescence (II, Fig. EV2E-F). The ErbB4 JM-b mediated activation of STAT5b and the interaction between ErbB4 JM-b and STAT5b was also observed to be Dynamin-2 dependent with the Dynamin inhibitor dynasore, Dynamin-2 siRNA treatments and western analysis (II, Fig. EV2G-I).

The role of Dynamin-2 in ErbB4 and STAT5b signaling in cardiomyocytes was determined. First, proximity ligation assay and the Dynamin inhibitor dynasore was utilized to observe whether Erbb4 and Dynamin-2 associate in isolated cardiomyocytes and whether the association is dependent on the GTPase activity of Dynamin-2 (II, Fig. 2A–B). ErbB4 and Dynamin-2 were discovered to associate in cardiomyocytes, but similar number of ErbB4/Dynamin-2 associations were observed in Dynamin inhibitor and control treated cardiomyocytes (II, Fig. 2A–D). The Dynamin inhibitor treatment, however, reduced the number of ErbB4 and Dynamin-2 associations in the cell surface (II, Fig. 2A–D).

Next, the nuclear localization of Stat5b, the transcription of Stat5b target genes and the cardiomyocyte size was assessed in Dynamin inhibitor dynasore treated and NRG-1 stimulated cardiomyocytes with immunofluorescence and real-time RT PCR (II, Fig. 2E–I). Inhibition of Dynamin-2 reduced both the nuclear localization of Stat5b and cardiomyocyte size (II, Fig. 2E–F, H–I; Figure 17A–B). The NRG-1 induced transcription of Stat5b target genes was similarly downregulated by both Dynamin-2 and ErbB receptor inhibition (II, Fig. 2G). Finally, the effect of Dynamin inhibition on the hyperplastic myocardial growth and Stat5 activation in zebrafish embryos was assessed with immunofluorescence and western analysis (II, Fig. 4E–J). Dynamin-2 inhibition reduced the myocardial growth and the Stat5 activation in embryonic zebrafish (II, Fig. 4E–F, I–J, Figure 17C).

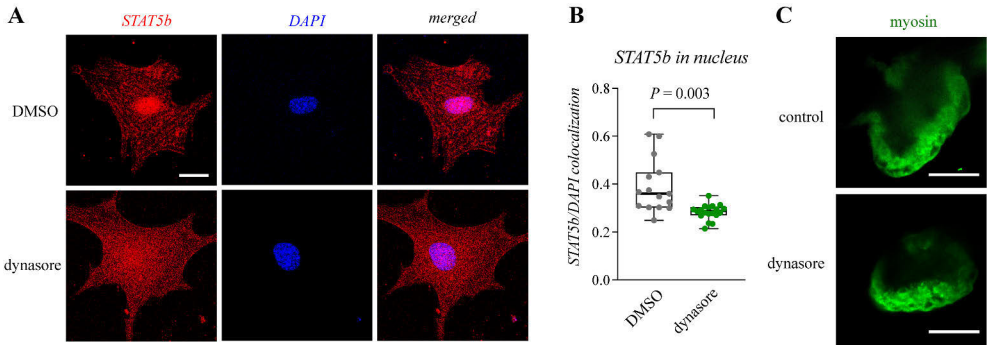

Figure 17. Dynamin-2 regulates myocardial growth and NRG-1/ErbB4 mediated activation of Stat5b in isolated cardiomyocytes and embryonic zebrafish. **A**–**B**: The nuclear accumulation of STAT5b was assessed in DMSO or Dynamin inhibitor dynasore treated isolated neonatal cardiomyocytes with immunofluorescence. Scale bar 20 µm. **C**: The ventricle size of embryonic zebrafish treated with DMSO or the Dynamin inhibitor dynasore for 2 days was assessed with immunofluorescence at 4 dpf. Scale bar 50 µm. Dpf: days post fertilization.

5.2.4 STAT5b signaling is perturbed in patients with pathological cardiac hypertrophy

The clustering of clinical samples from control and pathological hypertrophic myocardium based on the dimensionality reduced expression values of the genes in the discovered NRG-1/ErbB4/STAT5b pathway (including genes *NRG-1*, *ERBB4*, *STAT5B*, *IGF-1*, *MYC*, *DNM2*) was examined (II, Fig. 6A and EV4A). Clinical samples representing hypertrophic cardiomyopathy were statistically significantly clustered into a separate group from the normal controls in three separate independent published datasets (II, Fig. 6A and EV4A). The clustering into distinct groups indicates that the expression of the genes in the NRG-1/ErbB4/STAT5b pathway are divergent enough to separate hypertrophic and normal myocardium. The

clustering of samples from the myocardium of mice that have undergone transverse aortic constriction or sham surgery was similarly analyzed to observe whether similar group definition can be discovered in samples representing normal myocardium and pressure overload induced cardiac hypertrophy (II, Fig. 6B and EV4C). Statistically significant clustering into distinct groups representing normal myocardium and pressure overload induced hypertrophy was observed in three independent published datasets (II, Fig. 6B and EV4C).

To examine the activation of STAT5b in pathological hypertrophy, cardiac samples from patients suffering from pathological hypertrophy or noncardiac diseases were examined with immunohistochemistry (II, Fig. 6C and EV4E; Figure 18). The nuclear staining intensity for activated STAT5 was discovered to be significantly more intense in hypertrophic myocardium independent on the etiology of the hypertrophy (II, Fig. 6C).

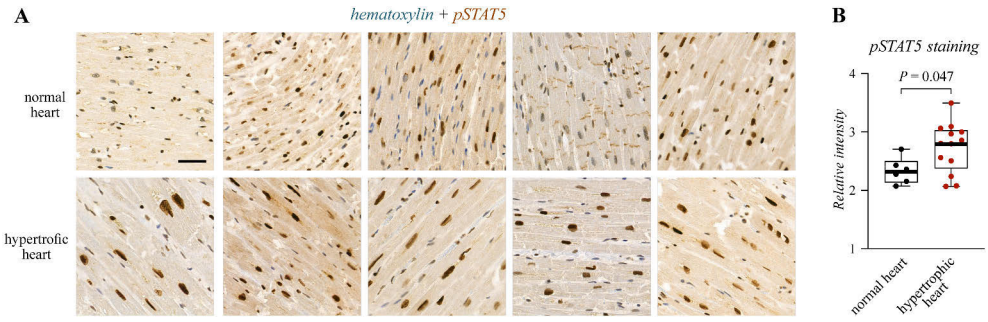

Figure 18. The staining intensity for activated STAT5 is higher in the heart sections of patients suffering from pathological hypertrophy compared to control subjects. **A**–**B**: The level of activated STAT5 in the nucleus of cardiomyocytes in heart sections of patients suffering from pathological hypertrophy or control subjects was assessed with immunohistochemistry. Scale bar 50 µm.

5.3 VEGF-B activates ErbB growth signaling in the heart (III)

Angiogenic factors such as VEGF-B can induce myocardial growth (Tirziu et al., 2007b; Karpanen et al., 2008; Jaba et al., 2013). The signaling mechanisms behind the angiogenic factor induced myocardial growth, however, have not been elucidated. Since ErbB signaling has been identified as a key regulator of myocardial growth (Odiete, Hill and Sawyer, 2012; De Keulenaer et al., 2019), the ability of the angiogenic factor VEGF-B to induce ErbB signaling in the heart was assessed. Adeno associated virus (AAV) vector constructs encoding the murine long isoform of VEGF-B (mVEGF-B186), the murine extracellular domain of ErbB4 fused to a Fc region of murine IgG (mErbB4ECD-mFc) and a scrambled control vector (control) were utilized. The AAVs encoding the mVEGF-B186 construct (AAV-

mVEGF-B186) were injected to adult mice in combination with the AAVs encoding the mErbB4ECD-mFc (AAV-mErbB4ECD-mFc) and control (AAV-control) constructs to observe whether the VEGF-B-mediated responses in the myocardium are disrupted by the mErbB4ECD-mFc ligand trap. The AAV-mVEGF-B186 treatment induced the phosphorylation of both ErbB1 and ErbB4 and increased the expression of the ErbB ligand HB-EGF in the hearts of the AAV-mVEGF-B186 treated mice in western analyses (III, Fig. 6A–B, D–G). The VEGF-B-induced phosphorylation of ErbB1 and ErbB4 was disrupted by the AAV-mErbB4ECD-mFc treatment (III, Fig. 6A, D–E; Figure 19). The AAV-mErbB4ECD-mFc treatment significantly reduced the heart weight of AAV-Control treated but had a limited effect in the hearts of AAV-mVEGF-B186 treated mice (III, Supplemental Fig. 10C-D). The limited effect in AAV-mVEGF-B186 treated mice might be due to the activation of several myocardial pathways by the AAV-mVEGF-B186 treatment.

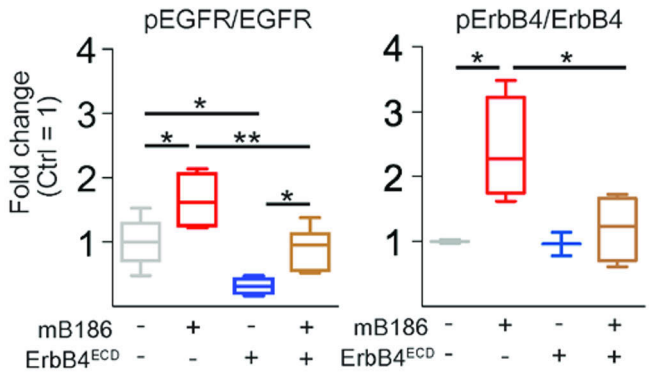

Figure 19. AAV-mediated expression of VEGF-B increases the activation of EGFR and ErbB4 in the heart. The activation of EGFR and ErbB4 was assessed with western analysis from the hearts of control AAV-treated (-), AAV-mVEGF-B186 (mB186) and AAV-mErbB4ECD-mFc ($ErbB4^{ECD}$) treated mice.

5.4 De novo multi-omics analysis (DMPA) models multi-omics data into regulatory modules and cell signaling pathways without the use of prior information (IV)

5.4.1 The association score of DMPA, the combined score, is conserved across datasets

Although the recent development of omics technologies has allowed for more comprehensive measurement of the signaling pathways of RTKs and other signaling

molecules, the tools to discover new signaling pathways and connections from multi-omics are currently inadequate. To aid in the future research of the diversity of RTK signaling a computational approach to infer cell signaling modules and pathways from multi-omics data was developed. To overcome the inherited bias from prior information, a data driven de novo approach was designed. The details of the developed approach can be found in section 4.3.5.4.1. In short, the de novo multi-omics pathway analysis (DMPA) models multi-omics data into network modules and combines them into pathways based on two association measures, the correlation and stoichiometry score that are combined to derive the combined score (IV, Fig. 1A). In the next step of the algorithm the features are assigned into modules and pathways based on common neighbors in highest scoring three feature cliques (IV, Fig. 1B-C). To validate the DMPA, the conservation of the association measures across datasets and the ability of DMPA to discover published associations were estimated. The conservation of the correlation score, stoichiometry score and the combined score in mass spectrometry derived interactome, phosphoproteome, metabolomics and protein acetylation data, RNA-seq derived transcriptome data and microarray-derived epigenetics data was assessed (IV, Fig. 2A and Supplementary Fig. 3A). A score above 0.5, the expected median score to be acquired by randomization due to ranking and adjustment steps of the association measures in DMPA, indicated conservation. The combined score was the only score that was significantly conserved in all tested omics datatypes (IV, Fig. 2A and Supplementary Fig. 3A). The stoichiometry score was conserved in interactome, phosphoproteome, metabolomics, epigenetics, and protein acetylation data while the correlation score was only conserved in protein acetylation data (IV, Fig. 2A and Supplementary Fig. 3A). The conservation of the association scores across datasets was also investigated in the multi-omics pathways inferred with DMPA (IV, Fig. 3A). The combined score was the only association score that was conserved both within and between the inferred multi-omics regulatory modules in the pathways inferred with the DMPA (IV, Fig. 3A).

5.4.2 DMPA uncovers known associations connected by a common upstream regulator

The ability of DMPA to recapitulate known associations in the network modules and multi-omics pathways and their statistical significance was assessed as described in section 4.3.5.4.2. The DMPA was run separately with settings where either the correlation score, stoichiometry score or the combined score was used as an association measure. The DMPA run with the combined score was able to consistently rediscover known protein-protein interactions, co-regulated transcripts and co-phosphorylated residues in interactome, phosphoproteome and transcriptome

data (IV, Fig. 2B–E and Supplementary Fig. 2–3). While DMPA run with the correlation and stoichiometry score were also able to discover reported associations, the performance of these variations of DMPA were highly variable based on the dataset and the omics data type (IV, Fig. 2B–E and Supplementary Fig. 2–3). The DMPA run with the combined score was also able to discover methylation sites associated with the same trait and metabolites involved in the same metabolic reaction in methylation and metabolomics data (IV, Supplementary Fig. 3B).

Cell signaling pathway discovery by DMPA was examined from multi-omics datasets. The DMPA was run with settings where the association measure for network module inference and network module combination were separately set as either the correlation, stoichiometry, or combined score (IV, Fig. 3B–C). The version of DMPA where the association measure for both regulatory module and pathway combination was set as combined score was the most consistent performer and the only DMPA version that was able to reach statistically significant models with all tested multi-omics datasets (IV, Fig. 3B–C).

5.4.3 The ranking and adjustment of association scores and three feature clique discovery increase the accuracy of DMPA

To test whether the design decisions of DMPA affect the accuracy of DMPA to discover known associations, the DMPA was run with unadjusted association scores and with a linear regulatory module combination approach. The ability of DMPA to discover known associations in the regulatory modules and their statistical significance with these settings was assessed as described in section 4.3.5.4.2. Since the P-values approached zero, the relative distance from the median value of the probability densities derived from repeated rounds of randomization was used as an accuracy measure. The ranking and adjustment of the association measures (combination, ranked) increased the accuracy of DMPA with interactome and transcriptome data compared to the combined score derived from unadjusted association measures (combination, raw) (IV, Supplementary Fig. 4A). In contrast, the ranking and adjustment step did not increase the accuracy significantly compared to the unadjusted association measures with phosphoproteome data (IV, Supplementary Fig. 4A). The ranking and adjustment step, however, did shift the median significantly away from the median of the probability distribution indicating that the step also moderately increased the accuracy of DMPA with phosphoproteome data (Wilcoxon signed rank test, $P = 0.0039$ for combination, ranked and $P = 0.6875$ for combination, raw). The three-feature clique maximization approach increased the accuracy of DMPA with interactome and phosphoproteome data compared to the linear combination approach (IV, Supplementary Fig. 4B). The

feature clique maximization approach did not, however, have a significant effect on the accuracy of DMPA with transcriptome data (IV, Supplementary Fig. 4B).

5.4.4 The accuracy of DMPA is sensitive to the zero-inflation and S parameters

The sensitivity of DMPA to parameter choice was assessed. First, the effect of the settings for the size parameters 7 and 8 described in section 4.3.5.4.1 and in the DMPA documentation available in Mendeley data (https://data.mendeley.com/datasets/m3zggn6xx9/draft?a=71c29dac-714e-497e-8109-5c324ac43ac3) to the regulatory modules inferred from published transcriptome data was examined (IV, Supplementary Fig. 5). The size parameters significantly affected the number of modules, the size of the modules and the number of transcripts included in the final modules, but had no significant effect on the accuracy of DMPA (IV, Supplementary Fig. 5).

Next, the effect of the parameter S choice was examined both with published and simulated data. The parameter S choice significantly affected the run time and the number of transcripts included in the final modules, but had no significant effect on the accuracy of DMPA with the published transcriptome data (IV, Supplementary Fig. 6). The true positive and false positive rate was assessed from simulated modules with normally, beta and negative binomially distributed feature values (IV, Supplementary Fig. 7–9). Different feature set sizes and variable number of non-associated features were explored (IV, Supplementary Fig. 7–9). Low parameter S values sensitized DMPA to false positives and high values to the loss of true positives. An optimal parameter S value range, however, was discovered (colored regions in IV, Supplementary Fig. 7–9) and a script to guide the parameter S choice was developed (IV, Supplementary Fig. 10). It is of note that the false positives always arose from the pool of non-associated features the number of which is expected to be low in real omics datasets. The effect of the parameter C was also examined and it was discovered that the parameter C should be only set based on the number of features (3 for 30-300 features in the dataset; 1 for 300< features in the dataset).

Finally, the effect of parameter that commands the zero-inflated setting of DMPA was tested with both published zero-inflated interactome data (over 30% of missing values) and non-zero-inflated transcriptome data (less than 25% of missing values). The accuracy of DMPA was discovered to be sensitive to the zero-inflation parameter (IV, Supplementary Fig. 11). The zero-inflated version of DMPA performed significantly better with the zero-inflated interactome data and the non-zero-inflated version with the non-zero-inflated transcriptome data (IV, Supplementary Fig. 11).

5.4.5 DMPA outperforms benchmark methods

DMPA was benchmarked against relevant module and network discovery and multi-omics analysis methods. The ability of WGCNA (Langfelder and Horvath, 2008), GENIE3 (Huynh-Thu et al., 2010) and LOPC (Zuo et al., 2014) to discover known associations from published transcriptome data was assessed as described in section 4.3.5.4.4. The run time and the fraction of transcripts included in the final modules or network was additionally measured. DMPA was the most consistent performer across datasets and the best performer in 6 out of 10 datasets (IV, Fig. 4A–B). WGCNA outperformed DMPA and GENIE3 in two datasets and GENIE3 outperformed DMPA and WGCNA in two datasets (IV, Fig. 4A). LOPC outperformed DMPA with only one dataset (IV, Fig. 4B). The most marked difference between DMPA and other module and network methods was discovered with datasets with low sample sizes (IV, Fig. 4C). DMPA only required 6 samples to discover known associations in contrast to the 30 required by the other methods (IV, Fig. 4C). LOPC was unable to run the datasets with low sample sizes due to the high-dimensionality problem (Ledoit and Wolf, 2004) (NA in IV, Fig. 4B).

DMPA was benchmarked against the closest analogue multi-omics integration method called TransNet (Rodrigues, Shulzhenko and Morgun, 2018). Since the aim of TransNet is to discover causal links between multi-omics modules and not multi-omics pathways, two different benchmark strategies were used as described in section 4.3.5.4.4. While TransNet was able to discover known connections between multi-omics modules (connections randomized in IV, Fig. 4D), DMPA outperformed TransNet in both multi-omics connection and pathway discovery (IV, Fig. 4D).

5.4.6 DMPA of an in-house multi-omics dataset of the signaling of the cleaved intracellular domain of the receptor tyrosine kinase TYRO3

An in-house multi-omics dataset of the signaling of the γ-secretase cleaved intracellular domain (ICD) of the RTK TYRO3 was acquired. Cleavage-resistant ΔGS and ΔADAM variants of the TYRO3 were cloned and expressed with the wild-type receptor in WM-266-4 melanoma cells where the endogenous TYRO3 had been knocked-down by lentiviral shRNA constructs (Supplementary Fig. 12A). The ΔGS variant has been described before (Merilahti et al., 2017), but the mutated cleavage sites for ADAM12 and ADAM17 in the ΔADAM variant were predicted as described in section 4.3.5.3. The functionality of the TYRO3 variants were confirmed with western and immunofluorescence analyses (IV, Supplementary Fig. 12B–E). Mass-spectrometry-derived TYRO3 interactome, phosphoproteome and total proteome and RNA-sequencing derived-transcriptome was acquired from the

cells expressing either one of the TYRO3 variants or a control construct (IV, Supplementary Fig. 12F). The interactome, phosphoproteome, total proteome and transcriptome associated with either full-length or the cleaved ICD of TYRO3 were identified with differential expression analyses (IV, Supplementary Fig. 13–18). DMPA discovered 24 and 53 interactome, 110 and 84 phosphoproteome, 46 and 45 transcriptome and 130 and 136 total proteome modules and 51 and 56 unique pathways for the full-length and cleaved TYRO3, respectively (IV, Supplementary Fig. 19–20 and Supplementary Table 1–2).

5.4.7 Prediction methods were designed to contextualize the results of DMPA

To increase the interpretability of DMPA results, prediction methods were developed to contextualize the inferred modules and pathways. Subcellular location, transcription factor and kinase prediction methods were designed for interactome, transcriptome and phosphoproteome modules. The prediction methods were applied to the modules of full-length and cleaved TYRO3. Several transcription factors and kinases known to be regulated by TYRO3 were predicted as the upstream regulators of TYRO3 transcriptome and phosphoproteome modules (IV, Supplementary Table 3,5) (Zhu et al., 2009; Guo et al., 2011; Brown et al., 2012; Fujita et al., 2018; Dufour et al., 2019; Chen et al., 2020; Tsai et al., 2020). The subcellular location prediction function for the interactome modules, in turn, was able to recapitulate the known difference in nuclear and plasma membrane location of full-length and cleaved ICD of TYRO3 (IV, Supplementary Fig. 12E and Supplementary Table 4). Interactome modules of the full-length TYRO3 were more frequently predicted to localize into the plasma membrane (33% against 9%, $P<0.0001$) and modules of the cleaved ICD to the nucleus (24% against 8%, $P=0.032$).

A function prediction method was developed for the multi-omics pathways inferred with DMPA and applied to the pathways of full-length and ICD of TYRO3. A significant difference in the predicted function and the direction of the predicted function for the pathways of full-length and cleaved TYRO3 was discovered (IV, Fig. 5 and Supplementary Fig. 21). The full-length and the ICD of TYRO3 were predicted to differentially regulate several cellular processes including cell cycle and cell growth, cell death, cell adhesion and motility, cytoskeletal arrangement, cell differentiation and immune responses (IV, Fig. 5 and Supplementary Fig. 21).

5.4.8 The function prediction approach of DMPA can predict cellular behavior

To examine whether the predicted functions of the DMPA pathways of full-length and cleaved ICD of TYRO3 reflect cellular behavior, the growth, adhesion, and morphology of WM-266-4 transfectants was explored. Cells expressing wild-type TYRO3 proliferated significantly faster than cells expressing the cleavage-resistant variants of TYRO3 when assessed with live cell imaging (IV, Fig. 6A) as expected based on the predicted functions of the ICD pathway 31 and full-length TYRO3 pathways 14,19, 28 and 10 (IV, Fig. 5A–B). The adhesion of the cells expressing the wild-type TYRO3 also adhered more strongly to fibronectin coated plates when assessed with real-time cellular impedance (IV, Fig. 6B). The stronger adhesion was predicted by the predicted functions of the ICD pathway 10 and full-length TYRO3 pathway 20 (IV, Fig. 5C). The 2-dimensional morphology of WM-266-4 transfectants was assessed from confocal images. The predicted functions of the ICD pathway 46 and the full-length pathway 9 predicted that the cell morphology is differentially regulated by the full-length and cleaved ICD of TYRO3 (IV, Fig. 5D). The convexity of the 2-dimensional shape of cells expressing wild-type TYRO3 indeed was significantly lower than the convexity of the shape of cells expressing the cleavage resistant variants of TYRO3 (IV, Fig. 6C). The cells expressing the wild-type TYRO3 additionally had more cell projections as anticipated by the predicted function of the ICD pathway 1 (IV, Fig. 5D, 6C).

6 Discussion

6.1 The discovered sequence motif reveals a new functional region in receptor tyrosine kinases that could be putatively targeted for treatment

Research into the structure-function relationship of RTKs has been instrumental in designing how to target these essential molecules as a therapy. Some structural regions such as the eJM region have received less attention. (Lemmon, Schlessinger and Ferguson, 2014). Here, a new sequence motif that associates with complex-type N-glycans in cell surface proteins in the eJM region of RTKs was identified. Both the signaling and the subcellular location of RTKs were partially defined by the presence of the motif. The RTK dependent survival of cells was dependent on the association between the motif region and the complex-type N-glycans for those cells that expressed the RTKs that contain the motif.

The fundamental differences between the signaling of the ErbB4 JM-a and JM-b isoform led to the discovery of the motif. Despite of the high homology of STAT5s (Copeland et al., 1995), the mechanism of activation of STAT5a by ErbB4 JM-a and STAT5b by ErbB4 JM-b were discovered to be markedly different. The activation of STAT5b by ErbB4 JM-b required the presence but not the kinase activity of the Janus kinase TYK2. The activation of STAT5a by ErbB4 JM-a in turn needed the association between the JM-a motif region and complex-type N-glycans coupled to cell surface proteins such as β1-integrin. Interestingly, the activation of STAT5a has been reported to be β1-integrin dependent in the mammary epithelial cells where ErbB4 JM-a has been reported to activate STAT5a (Faraldo et al., 1998; Jones et al., 1999; Long et al., 2003; Naylor et al., 2005). Thus, it is possible that β1-integrin is the N-glycosylated cell surface protein that contains the type of N-glycosylated residues that optimally associate with the motif area in ErbB4 JM-a.

The extracellular location of the sequence motif makes the motif area a more convenient target for therapy development than several other RTK regions due to easier accessibility. The physiological and clinical significance of the motif-based categorization of the RTKs, however, needs to be first explored. Cancer provides an interesting context to study the differences arising from the motif-based categorization of RTKs for two reasons. One, RTKs are well established oncogenes

that have been successfully targeted to treat cancer (Saraon et al., 2021). Two, increased β1,6 branching of complex type N-glycans has been associated with cancer progression, invasion and migration and poorer disease free and overall survival in several cancer types (de-Souza-Ferreira, Ferreira and de-Freitas-Junior, 2023). The β1,6 linkages were discovered as the preferred structural determinants of N-glycans that associate with the JM-a motif. Potentially increased β1,6 branching would promote recruitment of the RTKs that contain the sequence motif to the N-glycosylated sites. The consequence of this potential recruitment remains unclear. Scenarios where the increased recruitment would increase or decrease RTK signaling or alter the signaling pathways activated by the RTKs that contain the sequence motif are all possible. Similarly, it is unclear how the subcellular location and signaling of RTKs that do not contain the motif would be affected by the increased β1,6 branching. It is of note that annotations associated with migratory behavior such as ruffle membrane and cytoskeleton were enriched in the interactome of RTKs that contain the motif, but not of those without. Therefore, it can be hypothesized that the increased β1,6 branching would lead to increased motif-based signaling of RTKs that would lead to cancer progression. This hypothesis is supported by the discovery that β1,6 branching of N-glycans increases β1-integrin mediated migration of cancer cells (Zhao et al., 2006).

6.2 ErbB4 JM isoform-specific activation of a specific STAT5 subtype uncovers a putative candidate target for treatment of heart failure

Even with the current array of treatment options heart failure remains a high prevalence disease with high mortality (Emmons-Bell, Johnson and Roth, 2022). NRG-1/ErbB4 signaling has been established as a key regulator of growth and survival of the myocardium and recombinant NRG-1 has been investigated in clinical trials as a therapeutic agent for heart failure (De Keulenaer et al., 2019). Due to the clinical potential of NRG-1/ErbB4 signaling in the heart, the myocardium was selected as a potentially translational background to study the consequence of the differential STAT5 signaling arising from the difference in the eJM region of ErbB4 JM-isoforms. The myocardium was known to only express the ErbB4 JM-b isoform that was discovered to preferentially activate STAT5b (Elenius et al., 1997a; Veikkolainen et al., 2011). STAT5b was also discovered to be the major STAT5 subtype expressed in the heart.

STAT5b was discovered to be activated downstream of NRG-1 and ErbB4 in cardiomyocytes. STAT5b mediated both the hyperplastic and hypertrophic myocardial growth in embryonic and postnatal stages, respectively, and induced the expression of the myocardial growth genes IGF-1 and MYC in cardiomyocytes. The

NRG-1/ErbB4/STAT5b signaling pathway was also discovered to be involved in pathological hypertrophy.

While these findings do not directly prove the clinical potential of STAT5b in the treatment of myocardial diseases, they give indications that STAT5b might be involved in similar processes as NRG-1 in the myocardium. The next logical step would be to study the role of STAT5b in injury models both alone and as a potential downstream effector of NRG-1. It would be of interest to see whether the cardioprotective effect of NRG-1 is dependent on STAT5b since STAT5 has also previously been discovered to mediate the cardioprotective effect of remote ischemic preconditioning (Chen et al., 2018). Interestingly, STAT5 has been reported to regulate the activation of Akt in the heart (Chen et al., 2018; Kimura et al., 2018), which has been attributed as the downstream effector responsible for the cardioprotective effect of NRG-1 (Bersell et al., 2009; Bian et al., 2009; Fang et al., 2010). Administration of the protein product of the STAT5b target gene *IGF-1* has also been discovered to ameliorate cardiac injury in animal models and clinical trials (Welch et al., 2002; Komamura, 2017).

STAT5b inhibitors could be potentially utilized as a therapy for pathological hypertrophy, but to utilize STAT5b as target for heart failure treatment, the negative regulators of STAT5b signaling in the heart should be identified. Both phosphatases and transcriptional repressors of STAT5b could be considered as targets (Yu, Jin and Burakoff, 2000; Nakajima et al., 2001; Sefat-E-Khuda et al., 2004; Martens et al., 2005; Rigacci et al., 2008; Huang et al., 2012). The increase in proliferation in embryonic zebrafish, a species known for its regenerative capability (Poss, Wilson and Keating, 2002), could indicate that induction of STAT5b activation might have regenerative potential. The regeneration of adult myocardium is considered to mostly arise from the diploid mononuclear cardiomyocytes that are still able to proliferate (Bersell et al., 2009; Senyo et al., 2013; Patterson et al., 2017). STAT5b, however, did not affect the proliferation rate, but the survival of dividing adult cardiomyocytes (unpublished data). ErbB2 mediated cardiomyocyte re-entry to the cell cycle, however, has been reported to be mediated by the activation of STAT5 (Hirai et al., 2017). It remains to established whether STAT5b signaling only increases the survival of the cardiomyocytes in the myocardium or can also induce their regeneration.

Here, Dynamin-2 was identified as another regulator of NRG-1/ErbB4 signaling in the heart. Dynamin-2 was observed to regulate the cell surface location of ErbB4 and therefore the downstream STAT5b signaling. Dynamins have previously been reported to control the endocytosis but not the plasma membrane location of ErbB receptors (Sousa et al., 2012; Cortese et al., 2013). Since depletion of both Dynamin-2 and ErbB4 has been reported to result in heart failure (García-Rivello et al., 2005;

Li et al., 2013), it is possible that the heart failure associated with Dynamin-2 knock-down is due to downregulation of NRG-1/ErbB4 signaling in the heart.

6.3 Research into the cross-talk between angiogenic signals and myocardial growth signals reveal mechanisms of physiological myocardial growth

VEGF-B regulates the availability of VEGF-A to VEGFR-2 in endothelial cells (Olofsson et al., 1996; Hiratsuka et al., 1998; Rahimi, Dayanir and Lashkari, 2000). AAV-induced expression of VEGF-B was observed to increase physiological hypertrophy of the myocardium. To screen for a mechanism for the myocardial growth effect, VEGF-B was discovered to induce the transcription and the release of ErbB ligands HB-EGF and NRG-1 which activated the ErbB receptors ErbB1 and ErbB4 in the myocardium. The ErbB signaling was, however, probably not the only myocardial growth pathway activated by the VEGF-B expression.

These results present a mechanism for the crosstalk from the endothelial cells to the myocardium that leads to physiological myocardial growth. The mechanism of the crosstalk from the myocardium to endothelial cells, however, was not explored in this thesis. Interestingly, both NRG-1 and STAT5 have been detected to regulate the expression of VEGF-A and STAT5 dependent VEGF-A protein expression has been detected in the heart (Iivanainen et al., 2007; Chen et al., 2018). These observations could indicate that in response to the growth signals from the endothelial cells the cardiomyocytes would produce angiogenic signals to the endothelial cells via the NRG-1/ErbB4/STAT5b pathway. This reciprocal signaling could ensure that the cardiac vessels grow in tandem with the myocardium to ensure sufficient blood flow to maintain cardiac function.

6.4 DMPA discovers multi-omics modules and pathways more consistently from more diverse datasets and with lower sample sizes than previous approaches

Here, a prior data-independent multi-omics integration method was developed that is unique since it was specifically designed for cell signaling pathway discovery from multi-omics data. While some previous approaches have been proposed, their suitability to multi-omics data has not been defined and a formal analysis on the implications of the derived results from these methods is currently lacking (Acharjee et al., 2016; Zoppi et al., 2021). Prior data-independent methods are especially suited to the discovery of new cell signaling connections since these methods are unaffected

by the biases of prior knowledge (Garrido-Rodriguez et al., 2022). The discovery of new signaling connections potentially enables the discovery of new therapeutic targets.

The method proposed here, the DMPA, is based on the combination of two association measures, the combined score, that was discovered to be conserved across datasets. A level of conservation is expected from a score that represents relationships that are partially reproduced across different contexts. The three-feature maximization concept, one of the principal concepts of the DMPA, was discovered to increase the accuracy of DMPA.

The DMPA was consistently able to discover known associations and cell signaling pathways from multi-omics data. DMPA outperformed previous approaches by having a more consistent performance across datasets and by handling small sample sizes and zero-inflated data. DMPA proved to be a robust approach that can be utilized with several different omics data types.

The prediction methods of DMPA were designed to help in the interpretability of the results of DMPA. The function prediction of DMPA pathways was not only able to accurately portray the differences in cellular behavior but was also able to predict the direction of the cellular behavior. The function prediction of DMPA pathways was able to identify the fundamental difference in the regulation of cell growth, cell adhesion and cell morphology in the in-house acquired multi-omics datasets of cells expressing the cleaved and full-length TYRO3.

6.4.1 Limitations and future improvement strategies of DMPA

Due to the data drivenness of DMPA, DMPA is relatively sensitive to the quality of the omics data. High noise levels can lead to false positives in the DMPA. Non-parametric formulation was partially chosen to overcome this limitation. The multi-omics datasets that are analyzed with DMPA should be acquired from the same samples. DMPA does not support combining multi-omics data from different sources even though the datasets would represent the same tissue or cell type in the same conditions. Since DMPA was discovered to be sensitive to the parameter S that controls the cut-off limit for the combined score based on the number of features of datasets that have no true associations, incorrect parameter S choice can lead to either false positives or false negatives in the results of DMPA. A visualization technique was developed that will hopefully allow the user to select the parameter S correctly.

The current version of DMPA has been designed only to discover linear relationships and therefore misses non-linear relationships that could be discovered with mutual information-based or regression methods (Steuer et al., 2002; Margolin et al., 2006; Song, Langfelder and Horvath, 2012). DMPA also does not solve the

directionality of the relationships. A partial correlation based extra step could be implemented in the pipeline to solve the directionality of the relationships inside modules and pathways. Since the number of features inside the modules and the number of modules inside pathways are limited, the high-dimensionality problem (Ledoit and Wolf, 2004) of partial correlation-based methods should not pose an issue for solving the directionality. The partial correlation based extra step could also be utilized to better differentiate between direct and spurious connections (Werhli, Grzegorczyk and Husmeier, 2006; Zuo et al., 2014). The module combination step to pathways could be linearized to improve the interpretability of the pathways. A three-feature maximization-based scoring could be used instead of clique discovery. Finally, the applicability of DMPA to single-cell multi-omics data should be assessed. The zero-inflated nature of single cell omics data can be most likely handled by the zero-inflated version of DMPA. However, since acquiring more than one omics layer from the same single cell is still rather rare, a cell matching paradigm would need to be developed to utilize DMPA in single cell multi-omics analysis.

7 Summary/Conclusions

The mechanisms of RTK signaling diversity were examined in this thesis by studying the difference in signaling arising from the extracellular juxtamembrane region (eJM) of RTKs. To achieve this, the natural juxtamembrane isoforms of ErbB4 were utilized first to uncover a new sequence motif in the eJM region and second to understand the consequence of the differential signaling in the myocardium. To elucidate new signaling connections of RTKs and other cell signaling molecules from multi-omics data, a new prior data independent cell signaling pathway analysis method was developed. New cell signaling mechanisms were researched and methods to reveal cell signaling connections were constructed to aid in future therapeutic target candidate discovery and therapy development.

The main findings in this thesis can be concluded as follows (Figure 20):

1. A sequence motif in the extracellular juxtamembrane region of RTKs binds complex-type N-glycans in cell surface proteins. This interaction determines the cell surface location and downstream signaling of RTKs. This functional region may serve as a new approach to target RTKs for therapy.
2. ErbB4 JM-a and JM-b isoforms activate different STATs. The ErbB4 JM-b isoform-specific activation of STAT5b mediates the myocardial growth signal of NRG-1 and ErbB4 in embryonic and postnatal heart. The NRG-1/ErbB4/STAT5b pathway is involved in pathological hypertrophy. Dynamin-2 controls the activation of the NRG-1/ErbB4/STAT5b cascade in cardiomyocytes by regulating the cell surface location of ErbB4. These findings may aid in developing therapies for heart failure especially due to the previously discovered therapeutic potential of NRG-1 in clinical trials.
3. The angiogenic factor VEGF-B activates ErbB signaling in the myocardium by regulating the expression and release of NRG-1 and HB-EGF from endothelial cells. Both ErbB1 and ErbB4 are activated in the cardiomyocytes. VEGF-B signaling could be considered as a new approach to induce NRG-1/ErbB signaling as a therapy for heart failure.
4. The de novo multi-omics pathway analysis can be used to discover new cell signaling connections from multi-omics data since it is unbiased by prior

information. DMPA can handle the heterogeneity of multi-omics data, low sample sizes and zero-inflated data and outperforms previous approaches. The prediction functionalities of DMPA can help in finding new connections related to a certain cellular behavior. DMPA could be utilized in unbiased therapeutic target discovery.

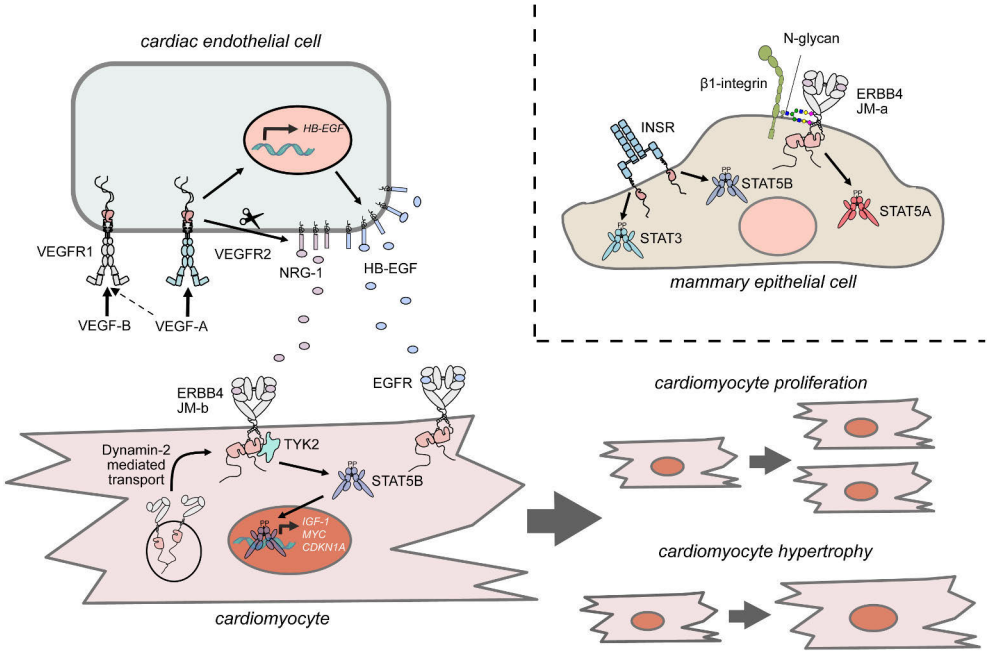

Figure 20. The molecular mechanisms of receptor tyrosine kinases uncovered in this thesis. Expression of VEGF-B controls the availability of VEGF-A to VEGFR2 in cardiac endothelial cells. Activation of VEGFR2 with VEGF-A induces the expression of HB-EGF and release of NRG-1 and HB-EGF to the extracellular space. The released NRG-1 and HB-EGF activate ERBB4 and EGFR in cardiomyocytes. In cardiomyocytes ERBB4 JM-b isoform coupled to the Janus kinase TYK2 activates STAT5b by phosphorylating its activating tyrosine residue. The activated STAT5b dimerizes and accumulates to the nucleus, where it induces the transcription of its target genes *IGF-1*, *MYC* and *CDKN1A*. Activation of the NRG-1/ERBB4/STAT5b pathway results in cardiomyocyte proliferation in prenatal and cardiomyocyte hypertrophy in postnatal myocardium. Dynamin-2 controls the translocation of ERBB4 to the plasma membrane in cardiomyocytes and in mammary epithelial cells. In the mammary epithelial cells ERBB4 JM-a and INSR localize to different membrane microdomains due to the presence or absence of a sequence motif in their eJM region. Due to the differential membrane microdomain location ERBB4 JM-a and INSR activate different STATs; ERBB4 JM-a STAT5a and INSR STAT5b and STAT3 in mammary epithelial cells. The sequence motif in the eJM region of ERBB4 JM-a isoform binds to complex type N-glycans in cell surface proteins such as β1-integrin. CDKN1A: cyclin dependent kinase inhibitor 1A. eJM: extracellular juxtamembrane. ERBB: erythroblastic leukemia viral oncogene. HB-EGF: heparin binding EGF-like growth factor. IGF-1: insulin-like growth factor 1. INSR: insulin receptor. JM: juxtamembrane. NRG-1: neuregulin-1. STAT: signal transducer and activator of transcription. TYK2: tyrosine kinase 2. VEGF: vascular endothelial growth factor. VEGFR: vascular endothelial growth factor receptor.

Acknowledgements

This thesis work was conducted in Medicity Laboratories and Institute of Biomedicine, University of Turku and Turku Bioscience Center, University of Turku and Åbo Akademi in BioCity Turku. I wish to express my gratitude to these institutions and the current and former directors Professors Klaus Elenius, Jon Eriksson, Jyrki Heino, Sirpa Jalkanen, Riitta Lahesmaa and Marko Salmi of these facilities that have provided me with an environment for efficient research work.

I am deeply grateful to my supervisor Professor Klaus Elenius who has supported me all these years and allowed me to pursue my own research paths, even when it has led me towards bioinformatics. I have really appreciated your supervision style, where advice has always been available when needed but there has also been room to grow as an independent researcher. Your contribution to my research career is invaluable.

I wish to thank the members of my thesis supervisor committee Professors Tiina Salminen and Marko Salmi who have given me excellent advice and encouragement throughout the years. Similarly, I wish to express my gratitude to the pre-examiners of this thesis book Professor Merja Heinäniemi and Professor emeritus Heikki Ruskoaho who helped me improve this thesis. I really enjoyed our correspondence and am very thankful for your quick responses and ability to carve out time to read my thesis from your busy schedules. Likewise, I am grateful to my opponent MD, PhD Tuomas Tammela who has arranged his schedule so that he can act as my opponent. I'm sure our discussion on the defense day will be interesting and beneficial to both parties. I look forward to learning from your expertise.

I wish to express my gratitude to my doctoral programme and to the former and current coordinators and directors of the Turku Doctoral Programme of Molecular Medicine (TuDMM) and University of Turku Graduate School (UTUGS) Eeva Valve, Kati Elima, Noora Kotaja and Pirjo Nuutila. Your financial support and understanding and help with the bureaucratic processes have smoothened my doctoral journey. I am grateful for the social opportunities provided by the doctoral programme that have helped me connect with my peers.

I would have been unable to conduct my doctoral research without the financial contributions of Suomen Akatemia, Syöpäsäätiö, Sigrid Juseliuksen säätiö, Turun

yliopistollinen keskussairaala, Turun yliopistosäätiö, Orionin tutkimussäätiö, K. Albin Johanssons stiftelse, Lounais-Suomalaiset syöpäsäätiöt, Maud Kuistilan muistosäätiö, Aarne Koskelon säätiö, Paulon säätiö, Emil Aaltosen säätiö, Sydäntutkimussäätiö, Paavo Nurmen säätiö, Ida Montinin säätiö, Oskar Öflunds stiftelse, Suomen kulttuurisäätiö, Suomen kulttuurisäätiön Varsinais-Suomen rahasto and Turun yliopisto. I wish to express my profound gratitude to these institutions and foundations for their support throughout the years that has allowed me to focus on research.

A special thanks goes to my collaborators without whom I wouldn't be here today. Your expertise, knowledge and contributions to my manuscripts have been paramount. I wish to thank Professor Riikka Kivelä, Professor Kari Alitalo and PhD Karthik Amudhala Hemanthakumar for allowing me to collaborate with you on your project meanwhile providing me with samples for my own project. I am very grateful for Professor Pekka Taimen for his profound knowledge on pathology, immunohistochemistry, and patient sample selection. I am deeply grateful to Professor Mark Johnson and PhD Mahlet Tamirat for their structural analyses and molecular simulations. I wish to thank Professor Markku Varjosalo and PhD Kari Salokas for sharing their RTK interactome data and for our interesting discussions. I am deeply appreciative of the improvements on my microscopy data visualization provided by the expertise of Professor Johanna Ivaska.

I am deeply grateful to the former and current members of my lab who have conducted some of the key experiments and techniques in my manuscripts. Anne, I am very grateful for your contributions from "hiirestys", to "kalahommat" to tricky pSTAT5 westerns. Your experimental work and role as my communication intermediary have been paramount for the success of my papers. Johannes, I can't express my gratitude enough for your help with cloning, mass spectrometry and bureaucratic processes in the university. You had endless patience with me even when I asked you to reanalyze the same mass spec dataset with different parameters for the 100th time. Ilkka, we have had a seamless co-operation with zebrafish work and I wish to express my gratitude for your invaluable help in also designing these experiments. Juho and Veera, I am grateful for your contributions in zebrafish data analysis and cell line production and help in editing the manuscripts. Anna, Maria, Ville and Elli, while the papers I've been working with you are not included in this thesis, I am grateful to have had the opportunity to work with you during my years in the Elenius lab.

On top of my co-authors, I am also grateful to all the current and former members of the Elenius lab: Kaisa Aalto, Sini Ahonen, Deepankar Chakroborty, Iman Farahani, Nelli Heiskanen, Juho Heliste, Maria Helkkula, Anne Jokilammi, Mahtab Karbasian, Anna Khudarayova, Peppi Kirjalainen, Anna Knittle, Kari Kurppa, Johannes Merilahti, Matias Mäenpää, Elli Narvi, Veera Ojala, Ilkka Paatero, Meri

Pelkonen, Arto Pulliainen, Fred Saarinen, Minna Santanen, Mika Savisalo, Farid Siddiqui, Maria Sundvall, Jori Torkkila, Maria Tuominen, Ville Veikkolainen, and the Heino and Kurppa lab who we share lab space and lab meetings with: Nikol Dibus, Johanna Jokinen, Meija Honkanen, Marjaana Ojalill, Marjaana Parikainen, Anna-Brita Puranen, Maria Salmela, Kalle Sipilä, Elina Siljamäki, Zejia Song, Salli Talvi, Sarang Talwelkar, Mari Tienhaara, Noora Virtanen and Kamal Wahid. You have created a lovely atmosphere to work in and I am grateful to you for providing me with an environment where I can always find a sympathetic ear. For excellent technical assistance Maria Tuominen, Minna Santanen, Mika Savisalo, Nea Konttinen, Merja Lakkisto and Sinikka Kollanius are acknowledged. For their help in the bureaucratic processes of the university, I wish to express my gratitude to Päivi Aalto, Outi Irjala, Katri Kulmala, Rakel Mattson, Kristiina Nuutila, Pia Tahvanainen and Hanna Tuominen.

I have been fortunate enough to be born into a family with a lot of siblings and to meet wonderful people during my lifetime that I can call friends. I am very grateful to my parents Harri and Teija, who have taught me persistence and emphasized the value of education. I do not only owe you my physical existence, but also some of the key traits of my personality that made me complete this thesis that I wouldn't have developed if you were not my parents. I am very grateful to my siblings Riina, Henri and Janne, without whom my life growing up would have been empty. I can't imagine how I would have turned out as an only child and I'm grateful for your lifelong support. I also wish to extend my gratitude to my extended family, to my grandparents, aunts and uncles, cousins, nieces, and nephews who have been there throughout the years.

I owe deep gratitude to my circle of friends, acquaintances and generally the people in the research community for helping me to take my mind of work and to enjoy life. I wish to thank Loimaan plikat, my friends from TerBio times, my friends from Aalto times, the members of the book club and the numerous friends I've met through my years as a PhD student for bringing laughter, joy and good conversation to my life. Finally, I wish to extend my gratitude to my partner Sina who has been with me most of my PhD journey for his support, advice and for allowing me to share my day-to-day burdens with him.

November 2023
Katri Vaparanta

References

Abascal, F., Acosta, R., Addleman, N.J., Adrian, J., Afzal, V., Aken, B., Akiyama, J.A., Jammal, O. Al, Amrhein, H., Anderson, S.M., Andrews, G.R., Antoshechkin, I., Ardlie, K.G., Armstrong, J., Astley, M., Banerjee, B., Barkal, A.A., Barnes, I.H.A., Barozzi, I., Barrell, D., Barson, G., Bates, D., Baymuradov, U.K., Bazile, C., Beer, M.A., Beik, S., Bender, M.A., Bennett, R.,..., and Zimmerman, J., 2020. Expanded encyclopaedias of DNA elements in the human and mouse genomes. *Nature*, 583(7818).

Acharjee, A., Ament, Z., West, J.A., Stanley, E. and Griffin, J.L., 2016. Integration of metabolomics, lipidomics and clinical data using a machine learning method. *BMC Bioinformatics*, 17.

Albuquerque, R.J.C., Hayashi, T., Cho, W.G., Kleinman, M.E., Dridi, S., Takeda, A., Baffi, J.Z., Yamada, K., Kaneko, H., Green, M.G., Chappell, J., Wilting, J., Weich, H.A., Yamagami, S., Amano, S., Mizuki, N., Alexander, J.S., Peterson, M.L., Brekken, R.A., Hirashima, M., Capoor, S., Usui, T., Ambati, B.K. and Ambati, J., 2009. Alternatively spliced VEGF receptor-2 is an essential endogenous inhibitor of lymphatic vessels. *Nature medicine*, 15(9), p.1023.

Alitalo, K., Karkkainen, M.J., Haiko, P., Sainio, K., Partanen, J., Taipale, J., Petrova, T. V, Jeltsch, M., Jackson, D.G., Talikka, M., Rauvala, H. and Betsholtz, C., 2004. Vascular endothelial growth factor C is required for sprouting of the first lymphatic vessels from embryonic veins. *Nature immunology*, 5(1), pp.74–80.

Alitalo, R., Aprelikova, O., Korhonen, J., Kaipainen, A., Alitalo, K. and Pertovaara, L., 1992. FLT4 Receptor Tyrosine Kinase Contains Seven Immunoglobulin-like Loops and Is Expressed in Multiple Human Tissues and Cell Lines. *Cancer Research*, 52(20).

Alkass, K., Panula, J., Westman, M., Wu, T.-D., Guerquin-Kern, J.-L. and Bergmann, O., 2015. No Evidence for Cardiomyocyte Number Expansion in Preadolescent Mice. *Cell*, 163(4), pp.1026–1036.

Alvarez, C. V., Shon, K.J., Miloso, M. and Beguinot, L., 1995. Structural Requirements of the Epidermal Growth Factor Receptor for Tyrosine Phosphorylation of eps8 and eps15, Substrates Lacking Src SH2 Homology Domains. *Journal of Biological Chemistry*, 270(27), pp.16271–16276.

Amato, G., Carella, C., Fazio, S., La Montagna, G., Cittadini, A., Sabatini, D., Marciano-Mone, C., Sacca, L. and Bellastella, A., 1993. Body composition, bone metabolism, and heart structure and function in growth hormone (GH)-deficient adults before and after GH replacement therapy at low doses. *The Journal of Clinical Endocrinology & Metabolism*, 77(6), pp.1671–1676.

Amit, I., Wides, R. and Yarden, Y., 2007. Evolvable signaling networks of receptor tyrosine kinases: relevance of robustness to malignancy and to cancer therapy. *Molecular Systems Biology*, 3(1), p.151.

Arkhipov, A., Shan, Y., Das, R., Endres, N.F., Eastwood, M.P., Wemmer, D.E., Kuriyan, J. and Shaw, D.E., 2013. Architecture and membrane interactions of the EGF receptor. *Cell*, 152(3), pp.557–569.

Ashburner, M., Ball, C.A., Blake, J.A., Botstein, D., Butler, H., Cherry, J.M., Davis, A.P., Dolinski, K., Dwight, S.S., Eppig, J.T., Harris, M.A., Hill, D.P., Issel-Tarver, L., Kasarskis, A., Lewis, S.,

Matese, J.C., Richardson, J.E., Ringwald, M., Rubin, G.M. and Sherlock, G., 2000. Gene Ontology: tool for the unification of biology. *Nature Genetics*, 25(1), pp.25–29.

Bader, G.D. and Hogue, C.W.V., 2003. An automated method for finding molecular complexes in large protein interaction networks. *BMC Bioinformatics*, 4.

Baldwin, M.E., Halford, M.M., Roufail, S., Williams, R.A., Hibbs, M.L., Grail, D., Kubo, H., Stacker, S.A. and Achen, M.G., 2005. Vascular Endothelial Growth Factor D Is Dispensable for Development of the Lymphatic System. *Molecular and Cellular Biology*, 25(6), pp.2441–2449.

Baliga, R.R., Pimental, D.R., Zhao, Y.Y., Simmons, W.W., Marchionni, M.A., Sawyer, D.B. and Kelly, R.A., 1999. NRG-1-induced cardiomyocyte hypertrophy. Role of PI-3-kinase, p70(S6K), and MEK-MAPK-RSK. *American Journal of Physiology - Heart and Circulatory Physiology*, 277(5 46-5).

Bansal, P., Morgat, A., Axelsen, K.B., Muthukrishnan, V., Coudert, E., Aimo, L., Hyka-Nouspikel, N., Gasteiger, E., Kerhornou, A., Neto, T.B., Pozzato, M., Blatter, M.C., Ignatchenko, A., Redaschi, N. and Bridge, A., 2022. Rhea, the reaction knowledgebase in 2022. *Nucleic Acids Research*, 50(D1), p.D693.

Barbier, A.J., Poppleton, H.M., Yigzaw, Y., Mullenix, J.B., Wiepz, G.J., Bertics, P.J. and Patel, T.B., 1999. Transmodulation of Epidermal Growth Factor Receptor Function by Cyclic AMP-dependent Protein Kinase*. https://doi.org/10.1074/jbc.274.20.14067.

Barkai, N., Ihmels, J., Friedlander, G., Bergmann, S., Sarig, O. and Ziv, Y., 2002. Revealing modular organization in the yeast transcriptional network. *Nature genetics*, 31(4), pp.370–377.

Bateman, A., Martin, M.J., Orchard, S., Magrane, M., Agivetova, R., Ahmad, S., Alpi, E., Bowler-Barnett, E.H., Britto, R., Bursteinas, B., Bye-A-Jee, H., Coetzee, R., Cukura, A., da Silva, A., Denny, P., Dogan, T., Ebenezer, T.G., Fan, J., Castro,…, and Teodoro, D., 2021. UniProt: the universal protein knowledgebase in 2021. *Nucleic acids research*, 49(D1), pp.D480–D489.

Batth, T.S., Papetti, M., Pfeiffer, A., Tollenaere, M.A.X., Francavilla, C. and Olsen, J. V., 2018. Large-Scale Phosphoproteomics Reveals Shp-2 Phosphatase-Dependent Regulators of Pdgf Receptor Signaling. *Cell Reports*, 22(10), pp.2784–2796. https://doi.org/10.1016/j.celrep.2018.02.038.

Belmonte, J.C.I., Jopling, C., Sleep, E., Raya, M., Martí, M. and Raya, A., 2010. Zebrafish heart regeneration occurs by cardiomyocyte dedifferentiation and proliferation. *Nature (London)*, 464(7288), pp.606–609.

van den Berg, G., Abu-Issa, R., de Boer, B.A., Hutson, M.R., de Boer, P.A.J., Soufan, A.T., Ruijter, J.M., Kirby, M.L., van den Hoff, M.J.B. and Moorman, A.F.M., 2009. A caudal proliferating growth center contributes to both poles of the forming heart tube. *Circulation research*, 104(2), pp.179–188.

Bergmann, O., Zdunek, S., Felker, A., Salehpour, M., Alkass, K., Bernard, S., Sjostrom, S.L., Szewczykowska, M., Jackowska, T., Dos Remedios, C., Malm, T., Andrä, M., Jashari, R., Nyengaard, J.R., Possnert, G., Jovinge, S., Druid, H. and Frisén, J., 2015. Dynamics of Cell Generation and Turnover in the Human Heart. *Cell*, 161(7), pp.1566–1575.

Van Berlo, J.H., Kanisicak, O., Maillet, M., Vagnozzi, R.J., Karch, J., Lin, S.-C.J., Middleton, R.C., Marbán, E. and Molkentin, J.D., 2014. C-kit cells minimally contribute cardiomyocytes to the heart. *Nature (London)*, 509(7500), pp.337–341.

Bernal, V., Bischoff, R., Horvatovich, P., Guryev, V. and Grzegorczyk, M., 2021. The 'un-shrunk' partial correlation in Gaussian graphical models. *BMC Bioinformatics*, 22(1).

Bersell, K., Arab, S., Haring, B. and Kühn, B., 2009. Neuregulin1/ErbB4 Signaling Induces Cardiomyocyte Proliferation and Repair of Heart Injury. *Cell*, 138(2), pp.257–270.

Bhattacharya, S., Eckner, R., Grossman, S., Oldread, E., Arany, Z., D'Andrea, A. and Livingston, D.M., 1996. Cooperation of Stat2 and p300/CBP in signalling induced by interferon-α. *Nature 1996 383:6598*, 383(6598), pp.344–347.

Bian, Y., Sun, M., Silver, M., Ho, K.K.L., Marchionni, M.A., Caggiano, A.O., Stone, J.R., Amende, I., Hampton, T.G., Morgan, J.P. and Yan, X., 2009. Neuregulin-1 attenuated doxorubicin-induced

decrease in cardiac troponins. *American Journal of Physiology - Heart and Circulatory Physiology*, 297(6), pp.1974–1983.

Binder, J.X., Pletscher-Frankild, S., Tsafou, K., Stolte, C., O'Donoghue, S.I., Schneider, R. and Jensen, L.J., 2014. COMPARTMENTS: unification and visualization of protein subcellular localization evidence. *Database*, 2014(0), pp.bau012–bau012.

Birges, R.B., Fajardot, J.E., Mayerll, B.J. and Hanafusall, H., 1992. THE JOURNAL OF BIOLOGICAL CHEMISTRY Tyrosine-phosphorylated Epidermal Growth Factor Receptor and Cellular p130 Provide High Affinity Binding Substrates to Analyze Crk-Phosphotyrosine-dependent Interactions in Vitro*. *Journal of Biological Chemistry*, 267(15), pp.10588–10595.

de Boer, B.A., van den Berg, G., de Boer, P.A.J., Moorman, A.F.M. and Ruijter, J.M., 2012. Growth of the developing mouse heart: An interactive qualitative and quantitative 3D atlas. *Developmental biology*, 368(2), pp.203–213.

Bolger, A.M., Lohse, M. and Usadel, B., 2014. Trimmomatic: A flexible trimmer for Illumina sequence data. *Bioinformatics*, 30(15).

Bolli, R., Stein, A.B., Guo, Y., Wang, O.L., Rokosh, G., Dawn, B., Molkentin, J.D., Sanganalmath, S.K., Zhu, Y. and Xuan, Y.T., 2011. A murine model of inducible, cardiac-specific deletion of STAT3: Its use to determine the role of STAT3 in the upregulation of cardioprotective proteins by ischemic preconditioning. *Journal of Molecular and Cellular Cardiology*, 50(4).

Bonnet, E., Calzone, L. and Michoel, T., 2015. Integrative multi-omics module network inference with Lemon-Tree. *PLoS computational biology*, 11(2).

Borlaug, B.A., 2020. Evaluation and management of heart failure with preserved ejection fraction. *Nature reviews cardiology*, 17(9), pp.559–573. https://doi.org/10.1038/s41569-020-0363-2.

Bost, F., McKay, R., Dean, N. and Mercola, D., 1997. The JUN Kinase/Stress-activated Protein Kinase Pathway Is Required for Epidermal Growth Factor Stimulation of Growth of Human A549 Lung Carcinoma Cells. *Journal of Biological Chemistry*, 272(52), pp.33422–33429.

Bouyain, S., Longo, P.A., Li, S., Ferguson, K.M. and Leahy, D.J., 2005. The extracellular region of ErbB4 adopts a tethered conformation in the absence of ligand. *Proceedings of the National Academy of Sciences of the United States of America*, 102(42), pp.15024–15029.

Bowles, E.J.A., Wellman, R., Feigelson, H.S., Onitilo, A.A., Freedman, A.N., Delate, T., Allen, L.A., Nekhlyudov, L., Goddard, K.A.B., Davis, R.L., Habel, L.A., Yood, M.U., McCarty, C., Magid, D.J. and Wagner, E.H., 2012. Risk of heart failure in breast cancer patients after anthracycline and trastuzumab treatment: a retrospective cohort study. *Journal of the National Cancer Institute*, 104(17), pp.1293–1305.

Bray, N.L., Pimentel, H., Melsted, P. and Pachter, L., 2016. Near-optimal probabilistic RNA-seq quantification. *Nature Biotechnology*, 34(5).

Brown, J.E., Krodel, M., Pazos, M., Lai, C. and Prieto, A.L., 2012. Cross-phosphorylation, signaling and proliferative functions of the Tyro3 and Axl receptors in Rat2 cells. *PLoS ONE*, 7(5), pp.1–11.

Brüel, A., Christoffersen, T.E.H. and Nyengaard, J.R., 2007. Growth hormone increases the proliferation of existing cardiac myocytes and the total number of cardiac myocytes in the rat heart. *Cardiovascular research*, 76(3), pp.400–408.

Bryant, K.L., Antonyak, M.A., Cerione, R.A., Baird, B. and Holowka, D., 2013. Mutations in the Polybasic Juxtamembrane Sequence of Both Plasma Membrane- and Endoplasmic Reticulum-localized Epidermal Growth Factor Receptors Confer Ligand-independent Cell Transformation. *The Journal of Biological Chemistry*, 288(48), p.34930.

Buckingham, M., Meilhac, S. and Zaffran, S., 2005. Building the mammalian heart from two sources of myocardial cells. *Nature reviews. Genetics*, 6(11), pp.826–837.

Caescu, C.I., Jeschke, G.R. and Turk, B.E., 2009. Active-site determinants of substrate recognition by the metalloproteinases TACE and ADAM10. *Biochemical Journal*, 424(1).

Cantini, L., Zakeri, P., Hernandez, C., Naldi, A., Thieffry, D., Remy, E. and Baudot, A., 2021. Benchmarking joint multi-omics dimensionality reduction approaches for the study of cancer. *Nature Communications 2021 12:1*, 12(1), pp.1–12.

Carmeliet, P., Ferreira, V., Breier, G., Pollefeyt, S., Kieckens, L., Gertsenstein, M., Fahrig, M., Vandenhoeck, A., Harpal, K., Eberhardt, C., Declercq, C., Pawling, J., Moons, L., Collen, D., Risau, W. and Nagy, A., 1996. Abnormal blood vessel development and lethality in embryos lacking a single VEGF allele. *Nature (London)*, 380(6573), pp.435–439.

Carmeliet, P., Moons, L., Luttun, A., Vincenti, V., Compernolle, V., De Mol, M., Wu, Y., Bono, F., Devy, L., Beck, H., Scholz, D., Acker, T., DiPalma, T., Dewerchin, M., Noel, A., Stalmans, I., Barra, A., Blacher, S., Vandendriessche, T., Ponten, A., Eriksson, U., Plate, K.H., Foidart, J.-M., Schaper, W., Charnock-Jones, D.S., Hicklin, D.J., Herbert, J.-M., Collen, D. and Persico, M.G., 2001. Synergism between vascular endothelial growth factor and placental growth factor contributes to angiogenesis and plasma extravasation in pathological conditions. *Nature medicine*, 7(5), pp.575–583.

Carpenter, C.D., Ingraham, H.A., Cochet, C., Walton, G.M., Lazar, C.S., Sowadski, J.M., Rosenfeld, M.G. and Gill, G.N., 1991. Structural analysis of the transmembrane domain of the epidermal growth factor receptor. *Journal of Biological Chemistry*, 266(9), pp.5750–5755.

Carraway, K.L., Sliwkowski, M.X., Akita, R., Platko, J. V., Guy, P.M., Nuijens, A., John Diamonti, A., Vandlen, R.L., Cantley, L.C. and Cerione, R.A., 1994. The erbB3 gene product is a receptor for heregulin. *The Journal of biological chemistry*, 269(19), pp.14303–14306.

Carraway, K.L., Weber, J.L., Unger, M.J., Ledesma, J., Yu, N., Gassmann, M. and Lai, C., 1997. Neuregulin-2, a new ligand of ErbB3/ErbB4-receptor tyrosine kinases. *Nature*, 387(6632), pp.512–516.

Carter, A.N. and Downes, C.P., 1992. Phosphatidylinositol 3-kinase is activated by nerve growth factor and epidermal growth factor in PC12 cells. *Journal of Biological Chemistry*, 267(21), pp.14563–14567.

Cerami, E.G., Gross, B.E., Demir, E., Rodchenkov, I., Babur, Ö., Anwar, N., Schultz, N., Bader, G.D. and Sander, C., 2011. Pathway Commons, a web resource for biological pathway data. *Nucleic Acids Research*, 39(SUPPL. 1), pp.685–690.

Chang, H., Riese, D.J., Gilbert, W., Stern, D.F. and McMahan, U.J., 1997. Ligands for ErbB-family receptors encoded by a neuregulin-like gene. *Nature*, 387(6632), pp.509–512.

Chen, D., Liu, Q., Cao, G. and Zhang, W., 2020. TYRO3 facilitates cell growth and metastasis via activation of the Wnt/β-catenin signaling pathway in human gastric cancer cells. *Aging*, 12(3), pp.2261–2274.

Chen, H., Chédotal, A., He, Z., Goodman, C.S. and Tessier-Lavigne, M., 1997. Neuropilin-2, a Novel Member of the Neuropilin Family, Is a High Affinity Receptor for the Semaphorins Sema E and Sema IV but Not Sema III. *Neuron*, 19(3), pp.547–559.

Chen, H., Jing, X.Y., Shen, Y.J., Wang, T.L., Ou, C., Lu, S.F., Cai, Y., Li, Q., Chen, X., Ding, Y.J., Yu, X.C. and Zhu, B.M., 2018. Stat5-dependent cardioprotection in late remote ischaemia preconditioning. *Cardiovascular Research*, 114(5), pp.679–689.

Cho, H.S. and Leahy, D.J., 2002. Structure of the extracellular region of HER3 reveals an interdomain tether. *Science*, 297(5585), pp.1330–1333.

Cho, H.S., Mason, K., Ramyar, K.X., Stanley, A.M., Gabelli, S.B., Denney, D.W. and Leahy, D.J., 2003. Structure of the extracellular region of HER2 alone and in complex with the Herceptin Fab. *Nature*, 421(6924), pp.756–760.

Christoffels, V.M., Habets, P.E.M.H., Franco, D., Campione, M., de Jong, F., Lamers, W.H., Bao, Z.-Z., Palmer, S., Biben, C., Harvey, R.P. and Moorman, A.F.M., 2000. Chamber Formation and Morphogenesis in the Developing Mammalian Heart. *Developmental biology*, 223(2), pp.266–278.

Cohen, S., 1962. Isolation of a Mouse Submaxillary Gland Protein Accelerating Incisor Eruption and Eyelid Opening in the New-born Animal*. *Journal of Biological Chemistry*, 237(6), pp.1555–1562.

Copeland, N.G., Gilbert, D.J., Schindler, C., Zhong, Z., Wen, Z., Darnell, J.E., Mui, A.L.F., Miyajima, A., Quelle, F.W., Ihle, J.N. and Jenkins, N.A., 1995. Distribution of the Mammalian Stat Gene Family in Mouse Chromosomes. *Genomics*, 29(1), pp.225–228.

Cortese, K., Howes, M.T., Lundmark, R., Tagliatti, E., Bagnato, P., Petrelli, A., Bono, M., McMahon, H.T., Parton, R.G. and Tacchetti, C., 2013. The HSP90 inhibitor geldanamycin perturbs endosomal structure and drives recycling ErbB2 and transferrin to modified MVBs/lysosomal compartments. *Molecular Biology of the Cell*, 24(2).

Coskun, Ü., Grzybek, M., Drechsel, D. and Simons, K., 2011. Regulation of human EGF receptor by lipids. *Proceedings of the National Academy of Sciences of the United States of America*, 108(22), pp.9044–9048.

Cote, G.M., Miller, T.A., LeBrasseur, N.K., Kuramochi, Y. and Sawyer, D.B., 2005. Neuregulin-1α and β isoform expression in cardiac microvascular endothelial cells and function in cardiac myocytes in vitro. *Experimental Cell Research*, 311(1), pp.135–146.

Coussens, L., Yang-Feng, T.L., Liao, Y.C., Chen, E., Gray, A., McGrath, J., Seeburg, P.H., Libermann, T.A., Schlessinger, J., Francke, U., Levinson, A. and Ullrich, A., 1985. Tyrosine kinase receptor with extensive homology to EGF receptor shares chromosomal location with neu oncogene. *Science (New York, N.Y.)*, 230(4730), pp.1132–1139.

Cox, J. and Mann, M., 2008. MaxQuant enables high peptide identification rates, individualized p.p.b.-range mass accuracies and proteome-wide protein quantification. *Nature Biotechnology 2008 26:12*, 26(12), pp.1367–1372.

Crone, S.A., Zhao, Y.Y., Fan, L., Gu, Y., Minamisawa, S., Liu, Y., Peterson, K.L., Chen, J., Kahn, R., Condorelli, G., Ross, J., Chien, K.R. and Lee, K.F., 2002. ErbB2 is essential in the prevention of dilated cardiomyopathy. *Nature Medicine*, 8(5), pp.459–465.

Dai, X. and Shen, L., 2022. Advances and Trends in Omics Technology Development. *Frontiers in Medicine*, 9, p.1546.

David, M., Wong, L., Flavell, R., Thompson, S.A., Wells, A., Larner, A.C. and Johnson, G.R., 1996. STAT Activation by Epidermal Growth Factor (EGF) and Amphiregulin. *Journal of Biological Chemistry*, 271(16), pp.9185–9188.

Davis, R.J., 1988. Independent mechanisms account for the regulation by protein kinase C of the epidermal growth factor receptor affinity and tyrosine-protein kinase activity. *Journal of Biological Chemistry*, 263(19), pp.9462–9469.

Dawson, J.P., Berger, M.B., Lin, C.-C., Schlessinger, J., Lemmon, M.A. and Ferguson, K.M., 2005. Epidermal Growth Factor Receptor Dimerization and Activation Require Ligand-Induced Conformational Changes in the Dimer Interface. *Molecular and Cellular Biology*, 25(17), p.7734.

Delaughter, M.C., Taffet, G.E., Fiorotto, M.L., Entman, M.L. and Schwartz, R.J., 1999. Local insulin-like growth factor I expression induces physiologic, then pathologic, cardiac hypertrophy in transgenic mice. *The FASEB Journal*, 13(14), pp.1923–1929. https://doi.org/10.1096/FASEBJ.13.14.1923.

del-Toro, N., Dumousseau, M., Orchard, S., Jimenez, R.C., Galeota, E., Launay, G., Goll, J., Breuer, K., Ono, K., Salwinski, L. and Hermjakob, H., 2013. A new reference implementation of the PSICQUIC web service. *Nucleic Acids Research*, 41(W1), pp.W601–W606.

Dennis, G., Sherman, B.T., Hosack, D.A., Yang, J., Gao, W., Lane, H.C. and Lempicki, R.A., 2003. DAVID: Database for Annotation, Visualization, and Integrated Discovery. *Genome biology*, 4(5).

DeRisi, J.L., Iyer, V.R. and Brown, P.O., 1997. Exploring the Metabolic and Genetic Control of Gene Expression on a Genomic Scale. *Science (American Association for the Advancement of Science)*, 278(5338), pp.680–686.

de-Souza-Ferreira, M., Ferreira, É.E. and de-Freitas-Junior, J.C.M., 2023. *Aberrant N-glycosylation in cancer: MGAT5 and β1,6-GlcNAc branched N-glycans as critical regulators of tumor development and progression*. *Cellular Oncology*, https://doi.org/10.1007/s13402-023-00770-4.

Doerner, A., Scheck, R. and Schepartz, A., 2015. Growth Factor Identity Is Encoded by Discrete Coiled-Coil Rotamers in the EGFR Juxtamembrane Region. *Chemistry & Biology*, 22(6), pp.776–784.

Doherty, R., MacLeod, B.L., Nelson, M.M., Ibrahim, M.M.H., Borges, B.C., Jaradat, N.W., Finneran, M.C., Giger, R.J. and Corfas, G., 2022. Identification of in vivo roles of ErbB4-JMa and its direct nuclear signaling using a novel isoform-specific knock out mouse. *Scientific reports*, 12(1), pp.17267–17267.

Dufour, F., Silina, L., Neyret-Kahn, H., Moreno-Vega, A., Krucker, C., Karboul, N., Dorland-Galliot, M., Maillé, P., Chapeaublanc, E., Allory, Y., Stransky, N., Haegel, H., Menguy, T., Duong, V., Radvanyi, F. and Bernard-Pierrot, I., 2019. TYRO3 as a molecular target for growth inhibition and apoptosis induction in bladder cancer. *British Journal of Cancer*, 120(5), pp.555–564.

Dugourd, A., Kuppe, C., Sciacovelli, M., Gjerga, E., Gabor, A., Emdal, K.B., Vieira, V., Bekker-Jensen, D.B., Kranz, J., Bindels, Eric.M.J., Costa, A.S.H., Sousa, A., Beltrao, P., Rocha, M., Olsen, J. V., Frezza, C., Kramann, R. and Saez-Rodriguez, J., 2021. Causal integration of multi-omics data with prior knowledge to generate mechanistic hypotheses. *Molecular Systems Biology*, 17(1), p.e9730.

Dull, T., Zufferey, R., Kelly, M., Mandel, R.J., Nguyen, M., Trono, D. and Naldini, L., 1998. A third-generation lentivirus vector with a conditional packaging system. *Journal of virology*, 72(11), pp.8463–71.

Dumont, D.J., Jussila, L., Taipale, J., Lymboussaki, A., Mustonen, T., Pajusola, K., Breitman, M. and Alitalo, K., 1998. Cardiovascular Failure in Mouse Embryos Deficient in VEGF Receptor-3. *Science (American Association for the Advancement of Science)*, 282(5390), pp.946–949.

D'uva, G., Aharonov, A., Lauriola, M., Kain, D., Yahalom-Ronen, Y., Carvalho, S., Weisinger, K., Bassat, E., Rajchman, D., Yifa, O., Lysenko, M., Konfino, T., Hegesh, J., Brenner, O., Neeman, M., Yarden, Y., Leor, J., Sarig, R., Harvey, R.P. and Tzahor, E., 2015. ERBB2 triggers mammalian heart regeneration by promoting cardiomyocyte dedifferentiation and proliferation. *NATURE CELL BIOLOGY*, 17, p.627.

Ebos, J.M.L., Bocci, G., Man, S., Thorpe, P.E., Hicklin, D.J., Zhou, D., Jia, X. and Kerbel, R.S., 2004. A Naturally Occurring Soluble Form of Vascular Endothelial Growth Factor Receptor 2 Detected in Mouse and Human Plasma. *Molecular Cancer Research*, 2(6), pp.315–326.

Edgar, R., Domrachev, M. and Lash, A.E., 2002. Gene Expression Omnibus: NCBI gene expression and hybridization array data repository. *Nucleic acids research*, 30(1), pp.207–210.

Elenius, K., Choi, C.J., Paul, S., Santiestevan, E., Nishi, E. and Klagsbrun, M., 1999. Characterization of a naturally occurring ErbB4 isoform that does not bind or activate phosphatidyl inositol 3-kinase. *Oncogene 1999 18:16*, 18(16), pp.2607–2615.

Elenius, K., Corfas, G., Paul, S., Choi, C.J., Rio, C., Plowman, G.D. and Klagsbrun, M., 1997a. A Novel Juxtamembrane Domain Isoform of HER4/ErbB4: ISOFORM-SPECIFIC TISSUE DISTRIBUTION AND DIFFERENTIAL PROCESSING IN RESPONSE TO PHORBOL ESTER. *Journal of Biological Chemistry*, 272(42), pp.26761–26768..

Elenius, K., Paul, S., Allison, G., Sun, J. and Klagsbrun, M., 1997b. Activation of HER4 by heparin-binding EGF-like growth factor stimulates chemotaxis but not proliferation. *The EMBO journal*, 16(6), pp.1268–1278.

Emmons-Bell, S., Johnson, C. and Roth, G., 2022. *Prevalence, incidence and survival of heart failure: A systematic review*. *Heart*. https://doi.org/10.1136/heartjnl-2021-320131.

Endres, N.F., Das, R., Smith, A.W., Arkhipov, A., Kovacs, E., Huang, Y., Pelton, J.G., Shan, Y., Shaw, D.E., Wemmer, D.E., Groves, J.T. and Kuriyan, J., 2013. Conformational coupling across the plasma membrane in activation of the EGF receptor. *Cell*, 152(3), pp.543–556.

Ennis S Lamon, D.J., Rian Eyland -j Ones, B.L., Teven Hak, S.S., Ank Uchs, H.F., Irginia Aton, V.P., Harm, P.D., Lex Ajamonde, A.B., Homas Leming, T.F., Olfgang Iermann, W.E., Anet Olter, J.W., Ark Egram, M.P., Ose Aselga, J.B. and Arry Orton, L.N., 2001. Use of Chemotherapy plus a

Monoclonal Antibody against HER2 for Metastatic Breast Cancer That Overexpresses HER2. *https://doi.org/10.1056/NEJM200103153441101*, 344(11), pp.783–792.

Eschenhagen, T., Bolli, R., Braun, T., Field, L.J., Fleischmann, B.K., Frisén, J., Giacca, M., Hare, J.M., Houser, S., Lee, R.T., Marbán, E., Martin, J.F., Molkentin, J.D., Murry, C.E., Riley, P.R., Ruiz-Lozano, P., Sadek, H.A., Sussman, M.A. and Hill, J.A., 2017a. Cardiomyocyte regeneration: A consensus statement. *Circulation*, 136(7).

Eschenhagen, T., Bolli, R., Braun, T., Field, L.J., Fleischmann, B.K., Frisén, J., Giacca, M., Hare, J.M., Houser, S., Lee, R.T., Marbán, E., Martin, J.F., Molkentin, J.D., Murry, C.E., Riley, P.R., Ruiz-Lozano, P., Sadek, H.A., Sussman, M.A. and Hill, J.A., 2017b. Cardiomyocyte Regeneration: A Consensus Statement. *Circulation*, 136(7), pp.680–686.

Faith, J.J., Hayete, B., Thaden, J.T., Mogno, I., Wierzbowski, J., Cottarel, G., Kasif, S., Collins, J.J. and Gardner, T.S., 2007. Large-Scale Mapping and Validation of Escherichia coli Transcriptional Regulation from a Compendium of Expression Profiles. *PLOS Biology*, 5(1), p.e8.

Fang, S.J., Wu, X.S., Han, Z.H., Zhang, X.X., Wang, C.M., Li, X.Y., Lu, L.Q. and Zhang, J.L., 2010. Neuregulin-1 preconditioning protects the heart against ischemia/reperfusion injury through a PI3K/Akt-dependent mechanism. *Chinese Medical Journal*, 123(24), pp.3597–3604.

Faraldo, M.M., Deugnier, M.A., Lukashev, M., Thiery, J.P. and Glukhova, M.A., 1998. Perturbation of β1-integrin function alters the development of murine mammary gland. *EMBO Journal*, 17(8), pp.2139–2147.

Feng, S.-M., Muraoka-Cook, R.S., Hunter, D., Sandahl, M.A., Caskey, L.S., Miyazawa, K., Atfi, A. and H. Shelton Earp, I., 2009. The E3 Ubiquitin Ligase WWP1 Selectively Targets HER4 and Its Proteolytically Derived Signaling Isoforms for Degradation. *Molecular and Cellular Biology*, 29(3), p.892.

Feracci, M., Pimentel, C., Bornet, O., Roche, P., Salaun, D., Badache, A. and Guerlesquin, F., 2011. MEMO associated with an ErbB2 receptor phosphopeptide reveals a new phosphotyrosine motif. *FEBS Letters*, 585(17), pp.2688–2692.

Ferguson, K.M., 2008. A structure-based view of Epidermal Growth Factor Receptor regulation. *Annual review of biophysics*, 37, p.353.

Ferguson, K.M., Berger, M.B., Mendrola, J.M., Cho, H.S., Leahy, D.J. and Lemmon, M.A., 2003. EGF activates its receptor by removing interactions that autoinhibit ectodomain dimerization. *Molecular Cell*, 11(2), pp.507–517.

Fernandes, H., Cohen, S. and Bishayee, S., 2001. Glycosylation-induced conformational modification positively regulates receptor-receptor association: A study with an aberrant epidermal growth factor receptor (EGFRvIII/ΔEGFR) expressed in cancer cells. *Journal of Biological Chemistry*, 276(7), pp.5375–5383.

Ferrara, N. and Henzel, W.J., 1989. Pituitary follicular cells secrete a novel heparin-binding growth factor specific for vascular endothelial cells. *Biochemical and biophysical research communications*, 161(2), pp.851–858.

Fleming, N.D., Samsa, L.A., Hassel, D., Qian, L. and Liu, J., 2018. Rapamycin attenuates pathological hypertrophy caused by an absence of trabecular formation. *Scientific Reports*, 8(1).

Fong, G.H., Rossant, J., Gertsenstein, M. and Breitman, M.L., 1995. Role of the Flt-1 receptor tyrosine kinase in regulating the assembly of vascular endothelium. *Nature 1995 376:6535*, 376(6535), pp.66–70.

Fong, G.H., Zhang, L., Bryce, D.M. and Peng, J., 1999. Increased hemangioblast commitment, not vascular disorganization, is the primary defect in flt-1 knock-out mice. *Development*, 126(13), pp.3015–3025.

Friedman, J., Hastie, T. and Tibshirani, R., 2008. Sparse inverse covariance estimation with the graphical lasso. *Biostatistics*, 9(3).

Friedman, N., Linial, M., Nachman, I. and Pe'er, D., 2000. Using Bayesian networks to analyze expression data. In: *Proceedings of the Annual International Conference on Computational Molecular Biology, RECOMB*.

Fuglesteg, B.N., Suleman, N., Tiron, C., Kanhema, T., Lacerda, L., Andreasen, T. V., Sack, M.N., Jonassen, A.K., Mjøs, O.D., Opie, L.H. and Lecour, S., 2008. Signal transducer and activator of transcription 3 is involved in the cardioprotective signalling pathway activated by insulin therapy at reperfusion. *Basic Research in Cardiology*, 103(5).

Fuh, G., Garcia, K.C. and de Vos, A.M., 2000. The Interaction of Neuropilin-1 with Vascular Endothelial Growth Factor and Its Receptor Flt-1. *Journal of Biological Chemistry*, 275(35), pp.26690–26695.

Fujio, Y., Nguyen, T., Wencker, D., Kitsis, R.N. and Walsh, K., 2000. Akt Promotes Survival of Cardiomyocytes In Vitro and Protects Against Ischemia-Reperfusion Injury in Mouse Heart. *Circulation*, 101(6), pp.660–667.

Fujita, K., Chen, X., Homma, H., Tagawa, K., Amano, M., Saito, A., Imoto, S., Akatsu, H., Hashizume, Y., Kaibuchi, K., Miyano, S. and Okazawa, H., 2018. Targeting Tyro3 ameliorates a model of PGRN-mutant FTLD-TDP via tau-mediated synaptic pathology. *Nature Communications*, 9(1).

Fukuzawa, J., Booz, G.W., Hunt, R.A., Shimizu, N., Karoor, V., Baker, K.M. and Dostal, D.E., 2000. Cardiotrophin-1 Increases Angiotensinogen mRNA in Rat Cardiac Myocytes Through STAT3. *Hypertension*, 35(6), pp.1191–1196.

Galindo, C.L., Kasasbeh, E., Murphy, A., Ryzhov, S., Lenihan, S., Ahmad, F.A., Williams, P., Nunnally, A., Adcock, J., Song, Y., Harrell, F.E., Tran, T.-L., Parry, T.J., Iaci, J., Ganguly, A., Feoktistov, I., Stephenson, M.K., Caggiano, A.O., Sawyer, D.B. and Cleator, J.H., 2014. Anti-Remodeling and Anti-Fibrotic Effects of the Neuregulin-1b Glial Growth Factor 2 in a Large Animal Model of Heart Failure. *Journal of the American Heart Association*, 3(5), p.e000773.

Gao, R., Zhang, J., Cheng, L., Wu, X., Dong, W., Yang, X., Li, T., Liu, X., Xu, Y., Li, X. and Zhou, M., 2010. A Phase II, randomized, double-blind, multicenter, based on standard therapy, placebo-controlled study of the efficacy and safety of recombinant human neuregulin-1 in patients with chronic heart failure. *Journal of the American College of Cardiology*, 55(18), pp.1907–1914.

Gao, R., Zhang, J., Liu, H., Wang, L., Pang, X., Fu, L., Meng, F. and Zhou, M., 2018. A PHASE III, RANDOMIZED, DOUBLE-BLIND, MULTICENTER, PLACEBO-CONTROLLED STUDY OF THE EFFICACY AND SAFETY OF NEUCARDIN™ IN PATIENTS WITH CHRONIC HEART FAILURE. *Journal of the American College of Cardiology*, 71(11), p.A668.

Garcia-Martinez, V. and Schoenwolf, G.C., 1993. Primitive-Streak Origin of the Cardiovascular System in Avian Embryos. *Developmental biology*, 159(2), pp.706–719.

García-Rivello, H., Taranda, J., Said, M., Cabeza-Meckert, P., Vila-Petroff, M., Scaglione, J., Ghio, S., Chen, J., Lai, C., Laguens, R.P., Lloyd, K.C. and Hertig, C.M., 2005. Dilated cardiomyopathy in Erb-b4-deficient ventricular muscle. *American Journal of Physiology - Heart and Circulatory Physiology*, 289(3 58-3).

Garrett, T.P.J., McKern, N.M., Lou, M., Elleman, T.C., Adams, T.E., Lovrecz, G.O., Kofler, M., Jorissen, R.N., Nice, E.C., Burgess, A.W. and Ward, C.W., 2003. The crystal structure of a truncated ErbB2 ectodomain reveals an active conformation, poised to interact with other ErbB receptors. *Molecular cell*, 11(2), pp.495–505.

Garrett, T.P.J., McKern, N.M., Lou, M., Elleman, T.C., Adams, T.E., Lovrecz, G.O., Zhu, H.J., Walker, F., Frenkel, M.J., Hoyne, P.A., Jorissen, R.N., Nice, E.C., Burgess, A.W. and Ward, C.W., 2002. Crystal structure of a truncated epidermal growth factor receptor extracellular domain bound to transforming growth factor α. *Cell*, 110(6), pp.763–773.

Garrido-Rodriguez, M., Zirngibl, K., Ivanova, O., Lobentanzer, S. and Saez-Rodriguez, J., 2022. Integrating knowledge and omics to decipher mechanisms via large-scale models of signaling networks. *Molecular Systems Biology*, 18(7).

Gassmann, M., Casagranda, F., Orloli, D., Simon, H., Lai, C., Kleint, R. and Lemke, G., 1995. Aberrant neural and cardiac development in mice lacking the ErbB4 neuregulin receptor. *Nature 1995 378:6555*, 378(6555), pp.390–394.

Gemberling, M., Karra, R., Dickson, A.L. and Poss, K.D., 2015. Nrg1 is an injury-induced cardiomyocyte mitogen for the endogenous heart regeneration program in zebrafish. *eLife*, 2015(4).

Gerber, D., Sal-Man, N. and Shai, Y., 2004. Two Motifs within a Transmembrane Domain, One for Homodimerization and the Other for Heterodimerization. *Journal of Biological Chemistry*, 279(20), pp.21177–21182.

Gessulat, S., Schmidt, T., Zolg, D.P., Samaras, P., Schnatbaum, K., Zerweck, J., Knaute, T., Rechenberger, J., Delanghe, B., Huhmer, A., Reimer, U., Ehrlich, H.C., Aiche, S., Kuster, B. and Wilhelm, M., 2019. Prosit: proteome-wide prediction of peptide tandem mass spectra by deep learning. *Nature Methods*, 16(6).

Gilmore-Hebert, M., Ramabhadran, R. and Stern, D.F., 2010. Interactions of ErbB4 and Kap1 connect the growth factor and DNA damage response pathways. *Molecular cancer research : MCR*, 8(10), pp.1388–1398.

Goldberger, J., Roweis, S., Hinton, G. and Salakhutdinov, R., 2005. Neighbourhood components analysis. In: *Advances in Neural Information Processing Systems*.

González-Rosa, J.M., Sharpe, M., Field, D., Soonpaa, M.H., Field, L.J., Burns, C.E. and Burns, C.G., 2018. Myocardial Polyploidization Creates a Barrier to Heart Regeneration in Zebrafish. *Developmental cell*, 44(4), pp.433-446.e7.

Grimley, P.M., Dong, F. and Rui, H., 1999. Stat5a and Stat5b: fraternal twins of signal transduction and transcriptional activation. *Cytokine & Growth Factor Reviews*, 10(2), pp.131–157.

Gu, X., Liu, X., Xu, D., Li, X., Yan, M., Qi, Y., Yan, W., Wang, W., Pan, J., Xu, Y., Xi, B., Cheng, L., Jia, J., Wang, K., Ge, J. and Zhou, M., 2010. Cardiac functional improvement in rats with myocardial infarction by up-regulating cardiac myosin light chain kinase with neuregulin. *Cardiovascular research*, 88(2), pp.334–343.

Guo, H., Barrett, T.M., Zhong, Z., Fernndez, J.A., Griffin, J.H., Freeman, R.S. and Zlokovic, B. V., 2011. Protein S blocks the extrinsic apoptotic cascade in tissue plasminogen activator/N-methyl D-aspartate-treated neurons via Tyro3-Akt-FKHRL1 signaling pathway. *Molecular Neurodegeneration*, 6(1).

Guo, H.H., Jing, X.Y., Chen, H., Xu, H.X. and Zhu, B.M., 2021. STAT3 but Not STAT5 Contributes to the Protective Effect of Electroacupuncture Against Myocardial Ischemia/Reperfusion Injury in Mice. *Frontiers in medicine*, 8.

Guo, Y.F., Zhang, X.X., Liu, Y., Duan, H.Y., Jie, B.Z. and Wu, X.S., 2012. Neuregulin-1 attenuates mitochondrial dysfunction in a rat model of heart failure. *Chinese Medical Journal*, 125(5), pp.807–814.

Guy, P.M., Platko, J. V., Cantley, L.C., Cerione, R.A. and Carraway, K.L., 1994. Insect cell-expressed p180erbB3 possesses an impaired tyrosine kinase activity. *Proceedings of the National Academy of Sciences of the United States of America*, 91(17), pp.8132–8136.

Haghverdi, L., Lun, A.T.L., Morgan, M.D. and Marioni, J.C., 2018. Batch effects in single-cell RNA-sequencing data are corrected by matching mutual nearest neighbors. *Nature Biotechnology*, 36(5).

Halim, K.B.A., Koldsø, H. and Sansom, M.S.P., 2015. Interactions of the EGFR juxtamembrane domain with PIP2-containing lipid bilayers: Insights from multiscale molecular dynamics simulations. *Biochimica et Biophysica Acta*, 1850(5), p.1017.

Hammal, F., De Langen, P., Bergon, A., Lopez, F. and Ballester, B., 2022. ReMap 2022: A database of Human, Mouse, Drosophila and Arabidopsis regulatory regions from an integrative analysis of DNA-binding sequencing experiments. *Nucleic Acids Research*, 50(D1).

Han, J., Ye, S., Zou, C., Chen, T., Wang, J., Li, J., Jiang, L., Xu, J., Huang, W., Wang, Y. and Liang, G., 2018. Angiotensin II causes biphasic STAT3 activation through TLR4 to initiate cardiac remodeling. *Hypertension*, 72(6), pp.1301–1311.

Harari, D., Tzahar, E., Romano, J., Shelly, M., Pierce, J.H., Andrews, G.C. and Yarden, Y., 1999. Neuregulin-4: a novel growth factor that acts through the ErbB-4 receptor tyrosine kinase. *Oncogene*, 18(17), pp.2681–2689.

Haug, K., Cochrane, K., Nainala, V.C., Williams, M., Chang, J., Jayaseelan, K.V. and O'Donovan, C., 2020. MetaboLights: a resource evolving in response to the needs of its scientific community. *Nucleic Acids Research*, 48(D1), pp.D440–D444.

Haury, A.-C., Mordelet, F., Vera-Licona, P. and Vert, J.-P., 2012. TIGRESS: Trustful Inference of Gene REgulation using Stability Selection. *BMC systems biology*, 6(1), pp.145–145.

Heusch, G., Musiolik, J., Kottenberg, E., Peters, J., Jakob, H. and Thielmann, M., 2012. STAT5 activation and cardioprotection by remote ischemic preconditioning in humans: short communication. *Circulation research*, 110(1), pp.111–115.

Hill, M.F., Patel, A. V., Murphy, A., Smith, H.M., Galindo, C.L., Pentassuglia, L., Peng, X., Lenneman, C.G., Odiete, O., Friedman, D.B., Kronenberg, M.W., Zheng, S., Zhao, Z., Song, Y., Harrell, F.E., Srinivas, M., Ganguly, A., Iaci, J., Parry, T.J., Caggiano, A.O. and Sawyer, D.B., 2013. Intravenous Glial Growth Factor 2 (GGF2) Isoform of Neuregulin-1β Improves Left Ventricular Function, Gene and Protein Expression in Rats after Myocardial Infarction. *PLOS ONE*, 8(2), p.e55741.

Hinton, G. and Roweis, S., 2003. Stochastic neighbor embedding. In: *Advances in Neural Information Processing Systems*.

Hirai, M., Arita, Y., McGlade, C.J., Lee, K.F., Chen, J. and Evans, S.M., 2017. Adaptor proteins NUMB and NUMBL promote cell cycle withdrawal by targeting ERBB2 for degradation. *The Journal of Clinical Investigation*, 127(2), pp.569–582.

Hiratsuka, S., Minowa, O., Kuno, J., Noda, T. and Shibuya, M., 1998. Flt-1 lacking the tyrosine kinase domain is sufficient for normal development and angiogenesis in mice. *Proceedings of the National Academy of Sciences of the United States of America*, 95(16), pp.9349–9354.

Horie, T., Ono, K., Nishi, H., Nagao, K., Kinoshita, M., Watanabe, S., Kuwabara, Y., Nakashima, Y., Takanabe-Mori, R., Nishi, E., Hasegawa, K., Kita, T. and Kimura, T., 2010. Acute doxorubicin cardiotoxicity is associated with miR-146a-induced inhibition of the neuregulin-ErbB pathway. *Cardiovascular Research*, 87(4), pp.656–664.

Hornbeck, P. V., Kornhauser, J.M., Latham, V., Murray, B., Nandhikonda, V., Nord, A., Skrzypek, E., Wheeler, T., Zhang, B. and Gnad, F., 2019. 15 years of PhosphoSitePlus ®: Integrating post-translationally modified sites, disease variants and isoforms. *Nucleic Acids Research*, 47(D1), pp.D433–D441.

Horvath, C.M., Stark, G.R., Kerr, I.M. and Darnell, J.E., 1996. Interactions between STAT and non-STAT proteins in the interferon-stimulated gene factor 3 transcription complex. *Molecular and cellular biology*, 16(12), pp.6957–6964.

Horvath, C.M., Wen, Z. and Darnell, J.E., 1995. A STAT protein domain that determines DNA sequence recognition suggests a novel DNA-binding domain. *Genes & development*, 9(8), pp.984–994.

Hosack, D.A., Dennis, G., Sherman, B.T., Lane, H.C. and Lempicki, R.A., 2003. Identifying biological themes within lists of genes with EASE. *Genome biology*, 4(10).

Huang, C., Jacobson, K. and Schaller, M.D., 2004. MAP kinases and cell migration. *Journal of Cell Science*, 117(20), pp.4619–4628. https://doi.org/10.1242/JCS.01481.

Huang, C.Y., Lin, Y.C., Hsiao, W.Y., Liao, F.H., Huang, P.Y. and Tan, T.H., 2012. DUSP4 deficiency enhances CD25 expression and CD4+ T-cell proliferation without impeding T-cell development. *European Journal of Immunology*, 42(2), pp.476–488.

Huang, Y., Ognjenović, J., Karandur, D., Miller, K., Merk, A., Subramaniam, S. and Kuriyan, J., 2021. A molecular mechanism for the generation of Ligand-dependent differential outputs by the epidermal growth factor receptor. *eLife*, 10. https://doi.org/10.7554/ELIFE.73218.

Hunter, T., Lingt, N. and Cooper, J.A., 1980. Protein kinase C phosphorylation of the EGF receptor at a threonine residue close to the cytoplasmic face of the plasma membrane. *J. M. Proc. natn. Acad. Sci. U.S.A*, 155, pp.521–527.

Huusko, J., Lottonen, L., Merentie, M., Gurzeler, E., Anisimov, A., Miyanohara, A., Alitalo, K., Tavi, P. and Ylä-Herttuala, S., 2012. AAV9-mediated VEGF-B Gene Transfer Improves Systolic Function in Progressive Left Ventricular Hypertrophy. *Molecular therapy*, 20(12), pp.2212–2221.

Huynh-Thu, V.A., Irrthum, A., Wehenkel, L. and Geurts, P., 2010. Inferring regulatory networks from expression data using tree-based methods. *PloS one*, 5(9), p.e12776. https://doi.org/10.1371/journal.pone.0012776.

Hynes, N.E. and Author, C., 2016. ErbB2: From an EGFR Relative to a Central Target for Cancer Therapy. *Cancer Research*, 76(13), pp.3659–3662.

Icli, B., Bharti, A., Pentassuglia, L., Peng, X. and Sawyer, D.B., 2012. ErbB4 localization to cardiac myocyte nuclei, and its role in myocyte DNA damage response. *Biochemical and Biophysical Research Communications*, 418(1), p.116.

Iivanainen, E., Paatero, I., Heikkinen, S.M., Junttila, T.T., Cao, R., Klint, P., Jaakkola, P.M., Cao, Y. and Elenius, K., 2007. Intra- and extracellular signaling by endothelial neuregulin-1. *Experimental Cell Research*, 313(13).

Iwamoto, R., Yamazaki, S., Asakura, M., Takashima, S., Hasuwa, H., Miyado, K., Adachi, S., Kitakaze, M., Hashimoto, K., Raab, G., Nanba, D., Higashiyama, S., Hori, M., Klagsbrun, M. and Mekada, E., 2003. Heparin-binding EGF-like growth factor and ErbB signaling is essential for heart function. *Proceedings of the National Academy of Sciences of the United States of America*, 100(6), pp.3221–3226.

Jaba, I.M., Zhuang, Z.W., Li, N., Jiang, Y., Martin, K.A., Sinusas, A.J., Papademetris, X., Simons, M., Sessa, W.C., Young, L.H. and Tirziu, D., 2013. No triggers rgs4 degradation to coordinate angiogenesis and cardiomyocyte growth. *The Journal of clinical investigation*, 123(4), pp.1718–1731.

Jabbour, A., Hayward, C.S., Keogh, A.M., Kotlyar, E., McCrohon, J.A., England, J.F., Amor, R., Liu, X., Li, X.Y., Zhou, M.D., Graham, R.M. and MacDonald, P.S., 2011. Parenteral administration of recombinant human neuregulin-1 to patients with stable chronic heart failure produces favourable acute and chronic haemodynamic responses. *European Journal of Heart Failure*, 13(1), pp.83–92.

Jackson, L.F., Qiu, T.H., Sunnarborg, S.W., Chang, A., Zhang, C., Patterson, C. and Lee, D.C., 2003. Defective valvulogenesis in HB-EGF and TACE-null mice is associated with aberrant BMP signaling. *The EMBO Journal*, 22(11), pp.2704–2716.

Jacoby, J.J., Kalinowski, A., Liu, M.G., Zhang, S.S.M., Gao, Q., Chai, G.X., Ji, L., Iwamoto, Y., Li, E., Schneider, M., Russell, K.S. and Fu, X.Y., 2003. Cardiomyocyte-restricted knockout of STAT3 results in higher sensitivity to inflammation, cardiac fibrosis, and heart failure with advanced age. *Proceedings of the National Academy of Sciences of the United States of America*, 100(22).

Jin, G., Wang, L. and Ma, J., 2022. Inhibiting STAT5 significantly attenuated Ang II-induced cardiac dysfunction and inflammation. *European Journal of Pharmacology*, 915, p.174689.

Jingjing, L., Xue, Y., Agarwal, N. and Roque, R.S., 1999. Human Muller cells express VEGF183, a novel spliced variant of vascular endothelial growth factor. *Investigative Ophthalmology and Visual Science*, 40(3).

John, S., Vinkemeier, U., Soldaini, E., Darnell, J.E. and Leonard, W.J., 1999. The significance of tetramerization in promoter recruitment by Stat5. *Molecular and cellular biology*, 19(3), pp.1910–1918.

Jones, F.E., Welte, T., Fu, X.Y., Stern, D.F. and Sato, N., 1999. ErbB4 signaling in the mammary gland is required for lobuloalveolar development and Stat5 activation during lactation\rInduction of the hair growth phase in postnatal mice by localized transient expression of Sonic hedgehog. *Journal of Cell Biology*, 147(1), pp.77–88.

Joukov, V., Pajusola, K., Kaipainen, A., Chilov, D., Lahtinen, I., Kukk, E., Saksela, O., Kalkkinen, N. and Alitalo, K., 1996. A novel vascular endothelial growth factor, VEGF-C, is a ligand for the Flt4 (VEGFR-3) and KDR (VEGFR-2) receptor tyrosine kinases. *The EMBO Journal*, 15(2), pp.290–298.

Jura, N., Endres, N.F., Engel, K., Deindl, S., Das, R., Lamers, M.H., Wemmer, D.E., Zhang, X. and Kuriyan, J., 2009a. Mechanism for activation of the EGF receptor catalytic domain by the juxtamembrane segment. *Cell*, 137(7), pp.1293–1307.

Jura, N., Endres, N.F., Engel, K., Deindl, S., Das, R., Lamers, M.H., Wemmer, D.E., Zhang, X. and Kuriyan, J., 2009b. Mechanism for activation of the EGF receptor catalytic domain by the juxtamembrane segment. *Cell*, 137(7), pp.1293–1307.

Kainulainen, V., Sundvall, M., Määttä, J.A., Santiestevan, E., Klagsbrun, M. and Elenius, K., 2000. A natural ErbB4 isoform that does not activate phosphoinositide 3-kinase mediates proliferation but not survival or chemotaxis. *The Journal of biological chemistry*, 275(12), pp.8641–8649.

Kajstura, J., Cheng, W., Reiss, K. and Anversa, P., 1994. The IGF-1-IGF-1 Receptor System Modulates Myocyte Proliferation but Not Myocyte Cellular Hypertrophy in Vitro. *Experimental cell research*, 215(2), pp.273–283.

Kaminuma, O., Deckert, M., Elly, C., Liu, Y.-C. and Altman, A., 2001. Vav-Rac1-Mediated Activation of the c-Jun N-Terminal Kinase/c-Jun/AP-1 Pathway Plays a Major Role in Stimulation of the Distal NFAT Site in the Interleukin-2 Gene Promoter. *Molecular and Cellular Biology*, 21(9), p.3126.

Karayel, Ö., Xu, P., Bludau, I., Velan Bhoopalan, S., Yao, Y., Ana Rita, F.C., Santos, A., Schulman, B.A., Alpi, A.F., Weiss, M.J. and Mann, M., 2020. Integrative proteomics reveals principles of dynamic phosphosignaling networks in human erythropoiesis. *Molecular Systems Biology*, 16(12), pp.1–22.

Karczewski, K.J. and Snyder, M.P., 2018. Integrative omics for health and disease. *Nature reviews. Genetics*, 19(5), pp.299–310.

Karpanen, T., Bry, M., Ollila, H.M., Seppänen-Laakso, T., Liimatta, E., Leskinen, H., Kivelä, R., Helkamaa, T., Merentie, M., Jeltsch, M., Paavonen, K., Andersson, L.C., Mervaala, E., Hassinen, I.E., Ylä-Herttuala, S., Orešič, M. and Alitalo, K., 2008. Overexpression of Vascular Endothelial Growth Factor-B in Mouse Heart Alters Cardiac Lipid Metabolism and Induces Myocardial Hypertrophy. *Circulation Research*, 103(9), pp.1018–1026.

Karpanen, T., Heckman, C.A., Keskitalo, S., Jeltsch, M., Ollila, H., Neufeld, G., Tamagnone, L. and Alitalo, K., 2006. Functional interaction of VEGF-C and VEGF-D with neuropilin receptors. *The FASEB Journal*, 20(9), pp.1462–1472.

Kashles, O., Szapary, D., Bellot, F., Ullrich, A., Schlessinger, J. and Schmidt, A., 1988. Ligand-induced stimulation of epidermal growth factor receptor mutants with altered transmembrane regions. *Proceedings of the National Academy of Sciences*, 85(24), pp.9567–9571.

Kaszuba, K., Grzybek, M., Orłowski, A., Danne, R., Róg, T., Simons, K., Coskun, Ü. and Vattulainen, I., 2015. N-Glycosylation as determinant of epidermal growth factor receptor conformation in membranes. *Proceedings of the National Academy of Sciences of the United States of America*, 112(14), pp.4334–4339.

Kawashima, N., Yoon, S.J., Itoh, K. and Nakayama, K.I., 2009. Tyrosine kinase activity of epidermal growth factor receptor is regulated by GM3 binding through carbohydrate to carbohydrate interactions. *Journal of Biological Chemistry*, 284(10), pp.6147–6155.

Keenan, A.B., Torre, D., Lachmann, A., Leong, A.K., Wojciechowicz, M.L., Utti, V., Jagodnik, K.M., Kropiwnicki, E., Wang, Z. and Ma'ayan, A., 2019. ChEA3: transcription factor enrichment analysis by orthogonal omics integration. *Nucleic Acids Research*, 47(W1).

Kendall, R.L. and Thomas, K.A., 1993. Inhibition of vascular endothelial cell growth factor activity by an endogenously encoded soluble receptor. *Proceedings of the National Academy of Sciences of the United States of America*, 90(22), pp.10705–10709.

Keppel, T.R., Sarpong, K., Murray, E.M., Monsey, J., Zhu, J. and Bose, R., 2017. Biophysical Evidence for Intrinsic Disorder in the C-terminal Tails of the Epidermal Growth Factor Receptor (EGFR) and HER3 Receptor Tyrosine Kinases. *The Journal of biological chemistry*, 292(2), pp.597–610.

De Keulenaer, G.W., Feyen, E., Dugaucquier, L., Shakeri, H., Shchendrygina, A., Belenkov, Y.N., Brink, M., Vermeulen, Z. and Segers, V.F.M., 2019. Mechanisms of the Multitasking Endothelial

Protein NRG-1 as a Compensatory Factor during Chronic Heart Failure. *Circulation: Heart Failure*, 12(10), p.6288.

Kiavue, N., Cabel, L., Melaabi, S., Bataillon, G., Callens, C., Lerebours, F., Pierga, J.Y. and Bidard, F.C., 2019. ERBB3 mutations in cancer: biological aspects, prevalence and therapeutics. *Oncogene 2019 39:3*, 39(3), pp.487–502.

Kimura, A., Ishida, Y., Furuta, M., Nosaka, M., Kuninaka, Y., Taruya, A., Mukaida, N. and Kondo, T., 2018. Protective Roles of Interferon-γ in Cardiac Hypertrophy Induced by Sustained Pressure Overload. *Journal of the American Heart Association: Cardiovascular and Cerebrovascular Disease*, 7(6).

Knittle, A.M., Helkkula, M., Johnson, M.S., Sundvall, M. and Elenius, K., 2017. SUMOylation regulates nuclear accumulation and signaling activity of the soluble intracellular domain of the ErbB4 receptor tyrosine kinase. *The Journal of biological chemistry*, 292(48), pp.19890–19904.

Kodama, H., Fukuda, K., Pan, J., Makino, S., Baba, A., Hori, S. and Ogawa, S., 1997. Leukemia inhibitory factor, a potent cardiac hypertrophic cytokine, activates the JAK/STAT pathway in rat cardiomyocytes. *Circulation research*, 81(5), pp.656–663.

Koh, H.W.L., Fermin, D., Vogel, C., Choi, K.P., Ewing, R.M. and Choi, H., 2019. iOmicsPASS: network-based integration of multiomics data for predictive subnetwork discovery. *npj Systems Biology and Applications5*, 5(22).

Koivisto, M. and Sood, K., 2004. Exact Bayesian structure discovery in Bayesian networks. *Journal of Machine Learning Research*, 5.

Kolodkin, A.L., Levengood, D. V., Rowe, E.G., Tai, Y.T., Giger, R.J. and Ginty, D.D., 1997. Neuropilin Is a Semaphorin III Receptor. *Cell*, 90(4), pp.753–762.

Komamura, K., 2017. Recombinant insulin-like growth factor-1 improves cardiac function and symptoms in the patients on the waiting list for heart transplantation with end-stage dilated cardiomyopathy. *European Heart Journal*, 38(suppl_1). https://doi.org/10.1093/eurheartj/ehx502.p1105.

Komuro, A., Nagai, M., Navin, N.E. and Sudol, M., 2003. WW Domain-containing Protein YAP Associates with ErbB-4 and Acts as a Co-transcriptional Activator for the Carboxyl-terminal Fragment of ErbB-4 That Translocates to the Nucleus. *Journal of Biological Chemistry*, 278(35), pp.33334–33341.

Kornblum, H.I., Hussain, R., Wiesen, J., Miettinen, P., Zurcher, S.D., Chow, K., Derynck, R. and Werb, Z., 1998. Abnormal Astrocyte Development and Neuronal Death in Mice Lacking the Epidermal Growth Factor Receptor. 53, pp.697–717.

Korpelainen, E.I., Kärkkäinen, M., Gunji, Y., Vikkula, M. and Alitalo, K., 1999. Endothelial receptor tyrosine kinases activate the STAT signaling pathway: mutant Tie-2 causing venous malformations signals a distinct STAT activation response. *Oncogene 1999 18:1*, 18(1), pp.1–8.

Kovacs, E., Das, R., Wang, Q., Collier, T.S., Cantor, A., Huang, Y., Wong, K., Mirza, A., Barros, T., Grob, P., Jura, N., Bose, R. and Kuriyan, J., 2015. Analysis of the Role of the C-Terminal Tail in the Regulation of the Epidermal Growth Factor Receptor. *Molecular and Cellular Biology*, 35(17), p.3083.

Kraus, M.H., Issing, W., Miki, T., Popescu, N.P. and Aaronson, S.A., 1989. Isolation and characterization of ERBB3, a third member of the ERBB/epidermal growth factor receptor family: evidence for overexpression in a subset of human mammary tumors. *Proceedings of the National Academy of Sciences of the United States of America*, 86(23), pp.9193–9197.

Küffner, R., Petri, T., Tavakkolkhah, P., Windhager, L. and Zimmer, R., 2012. Inferring gene regulatory networks by ANOVA. 28(10), pp.1376–1382.

Kunisada, K., Negoro, S., Tone, E., Funamoto, M., Osugi, T., Yamada, S., Okabe, M., Kishimoto, T. and Yamauchi-Takihara, K., 2000. Signal transducer and activator of transcription 3 in the heart transduces not only a hypertrophic signal but a protective signal against doxorubicin-induced cardiomyopathy. *Proceedings of the National Academy of Sciences of the United States of America*, 97(1), pp.315–319.

Kunisada, K., Tone, E., Fujio, Y., Matsui, H., Yamauchi-Takihara, K. and Kishimoto, T., 1998. Activation of gp130 transduces hypertrophic signals via STAT3 in cardiac myocytes. *Circulation*, 98(4), pp.346–352.

Kuramochi, Y., Guo, X. and Sawyer, D.B., 2006. Neuregulin activates erbB2-dependent src/FAK signaling and cytoskeletal remodeling in isolated adult rat cardiac myocytes. *Journal of molecular and cellular cardiology*, 41(2), p.228.

Lachmann, A., Torre, D., Keenan, A.B., Jagodnik, K.M., Lee, H.J., Wang, L., Silverstein, M.C. and Ma'ayan, A., 2018. Massive mining of publicly available RNA-seq data from human and mouse. *Nature Communications*, 9(1).

Lai, D., Liu, X., Forrai, A., Wolstein, O., Michalicek, J., Ahmed, I., Garratt, A.N., Birchmeier, C., Zhou, M., Hartley, L., Robb, L., Feneley, M.P., Fatkin, D. and Harvey, R.P., 2010. Neuregulin 1 sustains the gene regulatory network in both trabecular and nontrabecular myocardium. *Circulation Research*, 107(6), pp.715–727.

Laiman, J., Lin, S.-S. and Liu, Y.-W., 2023. Dynamins in human diseases: differential requirement of dynamin activity in distinct tissues.

Landau, M. and Ben-Tal, N., 2008. Dynamic equilibrium between multiple active and inactive conformations explains regulation and oncogenic mutations in ErbB receptors. *Biochimica et biophysica acta*, 1785(1), pp.12–31.

Lange, T., Guttmann-Raviv, N., Baruch, L., Machluf, M. and Neufeld, G., 2003. VEGF162, a new heparin-binding vascular endothelial growth factor splice form that is expressed in transformed human cells. *Journal of Biological Chemistry*, 278(19).

Langfelder, P. and Horvath, S., 2008. WGCNA: An R package for weighted correlation network analysis. *BMC bioinformatics*, 9(1), pp.559–559.

Leaman, D.W., Pisharody, S., Flickinger, T.W., Commane, M.A., Schlessinger, J., Kerr, I.M., Levy, D.E. and Stark, G.R., 1996. Roles of JAKs in activation of STATs and stimulation of c-fos gene expression by epidermal growth factor. *Molecular and cellular biology*, 16(1), pp.369–375.

Ledoit, O. and Wolf, M., 2004. A well-conditioned estimator for large-dimensional covariance matrices. *Journal of multivariate analysis*, 88(2), pp.365–411.

Lee, J., Gray, A., Yuan, J., Luoh, S.M., Avraham, H. and Wood, W.I., 1996. Vascular endothelial growth factor-related protein: a ligand and specific activator of the tyrosine kinase receptor Flt4. *Proceedings of the National Academy of Sciences*, 93(5), pp.1988–1992.

Lee, K.F., Simon, H., Chen, H., Bates, B., Hung, M.C. and Hauser, C., 1995. Requirement for neuregulin receptor erbB2 in neural and cardiac development. *Nature 1995 378:6555*, 378(6555), pp.394–398.

Lee, N.Y., Hazlett, T.L. and Koland, J.G., 2006. Structure and dynamics of the epidermal growth factor receptor C-terminal phosphorylation domain. *Protein Science : A Publication of the Protein Society*, 15(5), p.1142.

Lee, N.Y. and Koland, J.G., 2005. Conformational changes accompany phosphorylation of the epidermal growth factor receptor C-terminal domain. *Protein Science : A Publication of the Protein Society*, 14(11), p.2793.

Legland, D., Arganda-Carreras, I. and Andrey, P., 2016. MorphoLibJ: Integrated library and plugins for mathematical morphology with ImageJ. *Bioinformatics*, 32(22).

Lemmens, K., Doggen, K. and De Keulenaer, G.W., 2011. Activation of the neuregulin/ErbB system during physiological ventricular remodeling in pregnancy. *Am J Physiol Heart Circ Physiol*, 300, pp.931–942.

Lemmens, K., Segers, V.F.M., Demolder, M. and De Keulenaer, G.W., 2006. Role of Neuregulin-1/ErbB2 Signaling in Endothelium-Cardiomyocyte Cross-talk. *Journal of Biological Chemistry*, 281(28), pp.19469–19477.

Lemmon, M.A., 2009. Ligand-induced ErbB receptor dimerization. *Experimental cell research*, 315(4), p.638.

Lemmon, M.A. and Schlessinger, J., 2010. Cell signaling by receptor tyrosine kinases. *Cell*, 141(7), pp.1117–34.

Lemmon, M.A., Schlessinger, J. and Ferguson, K.M., 2014. The EGFR family: Not so prototypical receptor tyrosine kinases. *Cold Spring Harbor Perspectives in Biology*, 6(4).

Lemmon, M.A., Treutlein, H.R., Adams, P.D., Brünger, A.T. and Engelman, D.M., 1994. A dimerization motif for transmembrane alpha-helices. *Nature structural biology*, 1(3), pp.157–163.

Lenihan, D.J., Anderson, S.A., Lenneman, C.G., Brittain, E., Muldowney, J.A.S., Mendes, L., Zhao, P.Z., Iaci, J., Frohwein, S., Zolty, R., Eisen, A., Sawyer, D.B. and Caggiano, A.O., 2016. A Phase I, Single Ascending Dose Study of Cimaglermin Alfa (Neuregulin 1β3) in Patients With Systolic Dysfunction and Heart Failure. *JACC: Basic to Translational Science*, 1(7), p.576.

Levkowitz, G., Waterman, H., Zamir, E., Kam, Z., Oved, S., Langdon, W.Y., Beguinot, L., Geiger, B. and Yarden, Y., 1998. c-Cbl/Sli-1 regulates endocytic sorting and ubiquitination of the epidermal growth factor receptor. *Genes & Development*, 12(23), p.3663.

Levy, D.E. and Darnell, J.E., 2002. STATS: TRANSCRIPTIONAL CONTROL AND BIOLOGICAL IMPACT.

Li, B., Zheng, Z., Wei, Y., Wang, M., Peng, J., Kang, T., Huang, X., Xiao, J., Li, Y. and Li, Z., 2011. Therapeutic effects of neuregulin-1 in diabetic cardiomyopathy rats. *Cardiovascular Diabetology*, 10(1), pp.1–8.

Li, F., Wang, X., Capasso, J.M. and Gerdes, A.M., 1996. Rapid Transition of Cardiac Myocytes from Hyperplasia to Hypertrophy During Postnatal Development. *Journal of molecular and cellular cardiology*, 28(8), pp.1737–1746.

Li, J., Zhang, D.S., Ye, J.C., Li, C.M., Qi, M., Liang, D.D., Xu, X.R., Xu, L., Liu, Y., Zhang, H., Zhang, Y.Y., Deng, F.F., Feng, J., Shi, D., Chen, J.J., Li, L., Chen, G., Sun, Y.F., Peng, L.Y. and Chen, Y.H., 2013. Dynamin-2 mediates heart failure by modulating Ca2 +-dependent cardiomyocyte apoptosis. *International Journal of Cardiology*, 168(3), pp.2109–2119.

Li, P., Zhang, C., Perkins, E.J., Gong, P. and Deng, Y., 2007. Comparison of probabilistic Boolean network and dynamic Bayesian network approaches for inferring gene regulatory networks. In: *BMC Bioinformatics*.

Li, Y.J., Zhang, C., Martincuks, A., Herrmann, A. and Yu, H., 2023. *STAT proteins in cancer: orchestration of metabolism*. *Nature Reviews Cancer*, https://doi.org/10.1038/s41568-022-00537-3.

Liberzon, A., Subramanian, A., Pinchback, R., Thorvaldsdóttir, H., Tamayo, P. and Mesirov, J.P., 2011. Molecular signatures database (MSigDB) 3.0. *Bioinformatics*, 27(12), pp.1739–1740.

Lin, W., Sanchez, H.B., Deerinckt, T., Morris, J.K., Ellisman, M. and Lee, K.F., 2000. Aberrant development of motor axons and neuromuscular synapses in erbB2-deficient mice. *Proceedings of the National Academy of Sciences of the United States of America*, 97(3), pp.1299–1304.

Linggi, B. and Carpenter, G., 2006. ErbB-4 s80 intracellular domain abrogates ETO2-dependent transcriptional repression. *The Journal of biological chemistry*, 281(35), pp.25373–25380.

Liu, A., Trairatphisan, P., Gjerga, E., Didangelos, A., Barratt, J. and Saez-Rodriguez, J., 2019. From expression footprints to causal pathways: contextualizing large signaling networks with CARNIVAL. *npj Systems Biology and Applications*, 5(40).

Liu, J., Bressan, M., Hassel, D., Huisken, J., Staudt, D., Kikuchi, K., Poss, K.D., Mikawa, T. and Stainier, D.Y.R., 2010. A dual role for ErbB2 signaling in cardiac trabeculation. *Development*, 137(22), pp.3867–3875.

Liu, L., McBride, K.M. and Reich, N.C., 2005. STAT3 nuclear import is independent of tyrosine phosphorylation and mediated by importin-alpha3. *Proceedings of the National Academy of Sciences of the United States of America*, 102(23), pp.8150–8155.

Liu, X., Gallego, M.I., Smith, G.H., Robinson, G.W. and Hennighausen, L., 1998. Functional rescue of Stat5a-null mammary tissue through the activation of compensating signals including Stat5b. *Cell growth & differentiation : the molecular biology journal of the American Association for Cancer Research.*, 9(9), pp.795–803.

Liu, X., Gu, X., Li, Z., Li, X., Li, H., Chang, J., Chen, P., Jin, J., Xi, B., Chen, D., Lai, D., Graham, R.M. and Zhou, M., 2006. Neuregulin-1/erbB-activation improves cardiac function and survival in models of ischemic, dilated, and viral cardiomyopathy. *Journal of the American College of Cardiology*, 48(7), pp.1438–1447.

Long, W., Wagner, K.-U., Lloyd, K.C.K., Binart, N., Shillingford, J.M., Hennighausen, L. and Jones, F.E., 2003. Impaired differentiation and lactational failure of Erbb4-deficient mammary glands identify ERBB4 as an obligate mediator of STAT5. *Development*, 130(21), pp.5257–5268.

Louch, W.E., Sheehan, K.A. and Wolska, B.M., 2011. Methods in cardiomyocyte isolation, culture, and gene transfer. *Journal of Molecular and Cellular Cardiology*, 51(3), pp.288–298.

Love, M.I., Huber, W. and Anders, S., 2014. Moderated estimation of fold change and dispersion for RNA-seq data with DESeq2. *Genome Biology*, 15(12).

Lu, C., Mi, L.-Z., Grey, M.J., Zhu, J., Graef, E., Yokoyama, S. and Springer, T.A., 2010. Structural Evidence for Loose Linkage between Ligand Binding and Kinase Activation in the Epidermal Growth Factor Receptor. *Molecular and Cellular Biology*, 30(22), p.5432.

Lucas, L.M., Dwivedi, V., Senfeld, J.I., Cullum, R.L., Mill, C.P., Piazza, J.T., Bryant, I.N., Cook, L.J., Miller, S.T., Lott, J.H., Kelley, C.M., Knerr, E.L., Markham, J.A., Kaufmann, D.P., Jacobi, M.A., Shen, J. and Riese, D.J., 2022. The Yin and Yang of ERBB4: Tumor Suppressor and Oncoprotein. *Pharmacological Reviews*, 74(1), pp.18–47.

Lund, F.W., Jensen, M.L. V., Christensen, T., Nielsen, G.K., Heegaard, C.W. and Wüstner, D., 2014. SpatTrack: An Imaging Toolbox for Analysis of Vesicle Motility and Distribution in Living Cells. *Traffic*, 15(12), pp.1406–1429.

Luxán, G., D'Amato, G., MacGrogan, D. and De La Pompa, J.L., 2016. Endocardial Notch Signaling in Cardiac Development and Disease. *Circulation Research*, 118(1), pp.e1–e18.

MacLean, B., Tomazela, D.M., Shulman, N., Chambers, M., Finney, G.L., Frewen, B., Kern, R., Tabb, D.L., Liebler, D.C. and MacCoss, M.J., 2010. Skyline: An open source document editor for creating and analyzing targeted proteomics experiments. *Bioinformatics*, 26(7).

Maeda, R., Sato, T., Okamoto, K., Yanagawa, M. and Sako, Y., 2018. Lipid-Protein Interplay in Dimerization of Juxtamembrane Domains of Epidermal Growth Factor Receptor. *Biophysical journal*, 114(4), pp.893–903.

Maetschke, S.R., Madhamshettiwar, P.B., Davis, M.J. and Ragan, M.A., 2014. Supervised, semi-supervised and unsupervised inference of gene regulatory networks. *Briefings in Bioinformatics*, 15(2).

Maglione, D., Guerriero, V., Viglietto, G., Delli-Bovit, P. and Graziella Persico, M., 1991. Isolation of a human placenta cDNA coding for a protein related to the vascular permeability factor. *Proc. Natl. Acad. Sci. USA*, 88, pp.9267–9271.

Maglione, D., Guerriero, V., Viglietto, G., Grazia Ferraro, M., Aprelikova, O., Alitalo, K., Del Vecchio, S., Lei, K.J., Yang Chou, J. and Persico, M.G., 1993. Two alternative mRNAs coding for the angiogenic factor, placenta growth factor (PlGF), are transcribed from a single gene of chromosome 14. *Oncogene*, 8(4), pp.925–931.

Mao, G., Zeng, R., Peng, J., Zuo, K., Pang, Z. and Liu, J., 2022. Reconstructing gene regulatory networks of biological function using differential equations of multilayer perceptrons. *BMC Bioinformatics*, 23(1).

Marbach, D., Costello, J.C., Küffner, R., Vega, N.M., Prill, R.J., Camacho, D.M., Allison, K.R., Kellis, M., Collins, J.J., Aderhold, A., Stolovitzky, G., Bonneau, R., Chen, Y., Cordero, F., Crane, M., Dondelinger, F., Drton, M., Esposito, R., Foygel, R., De La Fuente, A., Gertheiss, J., Geurts, P., Greenfield, A., Grzegorczyk, M., Haury, A.-C., Holmes, B., Hothorn, T., Husmeier, D., Huynh-Thu, V.A., Irrthum, A., Karlebach, G., Lèbre, S., De Leo, V., Madar, A., Mani, S., Mordelet, F., Ostrer, H., Ouyang, Z., Pandya, R., Petri, T., Pinna, A., Poultney, C.S., Rezny, S., Ruskin, H.J., Saeys, Y., Shamir, R., Sîrbu, A., Song, M., Soranzo, N., Statnikov, A., Vega, N., Vera-Licona, P., Vert, J.-P., Visconti, A., Wang, H., Wehenkel, L., Windhager, L., Zhang, Y. and Zimmer, R., 2012. Wisdom of crowds for robust gene network inference. *Nature methods*, 9(8), pp.796–804..

Marbach, D., Prill, R.J., Schaffter, T., Mattiussi, C., Floreano, D. and Stolovitzky, G., 2010. Revealing strengths and weaknesses of methods for gene network inference. *Proceedings of the National Academy of Sciences of the United States of America*, 107(14).

Margolin, A.A., Nemenman, I., Basso, K., Wiggins, C., Stolovitzky, G., Favera, R.D. and Califano, A., 2006. ARACNE: An algorithm for the reconstruction of gene regulatory networks in a mammalian cellular context. *BMC bioinformatics*, 7(1), pp.S7–S7.

Margolis, B., Rhee, S.G., Felder, S., Mervic, M., Lyall, R., Levitzki, A., Ullrich, A., Zilberstein, A. and Schlessinger, J., 1989. EGF induces tyrosine phosphorylation of phospholipase C-II: a potential mechanism for EGF receptor signaling. *Cell*, 57(7), pp.1101–1107.

Martens, N., Uzan, G., Wery, M., Hooghe, R., Hooghe-Peters, E.L. and Gertler, A., 2005. Suppressor of cytokine signaling 7 inhibits prolactin, growth hormone, and leptin signaling by interacting with STAT5 or STAT3 and attenuating their nuclear translocation. *The Journal of biological chemistry*, 280(14), pp.13817–13823.

Matsui, T., Li, L., Del Monte, F., Fukui, Y., Franke, T.F., Hajjar, R.J. and Rosenzweig, A., 1999. Adenoviral Gene Transfer of Activated Phosphatidylinositol 3′-Kinase and Akt Inhibits Apoptosis of Hypoxic Cardiomyocytes In Vitro. *Circulation*, 100(23), pp.2373–2379.

Matthews, W., Jordan, C.T., Gavin, M., Jenkins, N.A., Copeland, N.G. and Lemischka, I.R., 1991. A receptor tyrosine kinase cDNA isolated from a population of enriched primitive hematopoietic cells and exhibiting close genetic linkage to c-kit. *Proceedings of the National Academy of Sciences of the United States of America*, 88(20). https://doi.org/10.1073/pnas.88.20.9026.

Mayer, B.J., 2015. *The discovery of modular binding domains: Building blocks of cell signalling*. *Nature Reviews Molecular Cell Biology*, https://doi.org/10.1038/nrm4068.

McBride, K.M., Banninger, G., McDonald, C. and Reich, N.C., 2002. Regulated nuclear import of the STAT1 transcription factor by direct binding of importin-α. *EMBO Journal*, 21(7), pp.1754–1763.

McKay, M.M. and Morrison, D.K., 2007. Integrating signals from RTKs to ERK/MAPK. *Oncogene 2007 26:22*, 26(22), pp.3113–3121.

McWhinney, C.D., Dostal, D. and Baker, K., 1998. Angiotensin II activates Stat5 through Jak2 kinase in cardiac myocytes. *Journal of Molecular and Cellular Cardiology*, 30(4), pp.751–761.

Mendrola, J.M., Berger, M.B., King, M.C. and Lemmon, M.A., 2002. The single transmembrane domains of ErbB receptors self-associate in cell membranes. *Journal of Biological Chemistry*, 277(7), pp.4704–4712.

Merilahti, J.A.M., Ojala, V.K., Knittle, A.M., Pulliainen, A.T. and Elenius, K., 2017. Genome-wide screen of gamma-secretase–mediated intramembrane cleavage of receptor tyrosine kinases. *Molecular Biology of the Cell*, 28(22), pp.3123–3131.

Merkhofer, E.C., Cogswell, P. and Baldwin, A.S., 2010. Her2 activates NF-κB and induces invasion through the canonical pathway involving IKKα *Oncogene*, 29, pp.1238–1248.

Merola, B., Cittadini, A., Colao, A., Longobardi, S., Fazio, S., Sabatini, D., Saccà, L. and Lombardi, G., 1993. Cardiac structural and functional abnormalities in adult patients with growth hormone deficiency. *The Journal of Clinical Endocrinology & Metabolism*, 77(6), pp.1658–1661.

Meyer, D. and Birchmeier, C., 1995. Multiple essential functions of neuregulin in development. *Nature*, 378(6555), pp.386–390.

Meyer, D., Yamaal, T., Garratt, A., Riethmacher-Sonnenberg, E., Kane, D., Theill, L.E. and Birchmeier, C., 1997. Isoform-specific expression and function of neuregulin. *Development (Cambridge)*, 124(18), pp.3575–3586. https://doi.org/10.1242/dev.124.18.3575.

Millikin, R.J., Solntsev, S.K., Shortreed, M.R. and Smith, L.M., 2018. Ultrafast Peptide Label-Free Quantification with FlashLFQ. *Journal of Proteome Research*, 17(1), pp.386–391.

Mirza, B., Wang, W., Wang, J., Choi, H., Chung, N.C. and Ping, P., 2019. *Machine learning and integrative analysis of biomedical big data*. *Genes*, https://doi.org/10.3390/genes10020087.

Mohr, J.D., Wagenknecht-Wiesner, A., Holowka, D.A. and Baird, B.A., 2020. Basic amino acids within the juxtamembrane domain of the epidermal growth factor receptor regulate receptor dimerization and auto-phosphorylation. *The protein journal*, 39(5), p.476.

Mollova, M., Bersell, K., Walsh, S., Savla, J., Das, L.T., Park, S.Y., Silberstein, L.E., Dos Remedios, C.G., Graham, D., Colan, S. and Kühn, B., 2013. Cardiomyocyte proliferation contributes to heart growth in young humans. *Proceedings of the National Academy of Sciences of the United States of America*, 110(4), pp.1446–1451.

Montero, J.C., Yuste, L., Díaz-Rodríguez, E., Esparís-Ogando, A. and Pandiella, A., 2000. Differential Shedding of Transmembrane Neuregulin Isoforms by the Tumor Necrosis Factor-α-Converting Enzyme. *Molecular and Cellular Neuroscience*, 16(5), pp.631–648.

Muhl, L., Moessinger, C., Adzemovic, M.Z., Dijkstra, M.H., Nilsson, I., Zeitelhofer, M., Hagberg, C.E., Huusko, J., Falkevall, A., Ylä-Herttuala, S. and Eriksson, U., 2016. Expression of vascular endothelial growth factor (VEGF)-B and its receptor (VEGFR1) in murine heart, lung and kidney. *Cell and Tissue Research*, 365(1).

Mui, A.L.F., Wakao, H., O'Farrell, A.M., Harada, N. and Miyajima, A., 1995. Interleukin-3, granulocyte-macrophage colony stimulating factor and interleukin-5 transduce signals through two STAT5 homologs. *The EMBO journal*, 14(6), pp.1166–1175.

Muraoka-Cook, R.S., Sandahl, M., Hunter, D., Miraglia, L. and Earp, H.S., 2008. Prolactin and ErbB4/HER4 Signaling Interact via Janus Kinase 2 to Induce Mammary Epithelial Cell Gene Expression Differentiation. *Molecular Endocrinology*, 22(10), p.2307.

Muraoka-Cook, R.S., Sandahl, M., Husted, C., Hunter, D., Miraglia, L., Feng, S., Elenius, K. and Earp, H.S., 2006. The Intracellular Domain of ErbB4 Induces Differentiation of Mammary Epithelial Cells. *Molecular Biology of the Cell*, 17(9), pp.4118–4129.

Muraoka-Cook, R.S., Sandahl, M.A., Strunk, K.E., Miraglia, L.C., Husted, C., Hunter, D.M., Elenius, K., Chodosh, L.A. and Earp III, H.S., 2009. ErbB4 Splice Variants Cyt1 and Cyt2 Differ by 16 Amino Acids and Exert Opposing Effects on the Mammary Epithelium In Vivo. *Molecular and Cellular Biology*, 29(18), pp.4935–4948.

Murphy, S.P., Ibrahim, N.E. and Januzzi, J.L., 2020. Heart Failure With Reduced Ejection Fraction: A Review. *JAMA : the journal of the American Medical Association*, 324(5), pp.488–504. https://doi.org/10.1001/jama.2020.10262.

Nakajima, H., Brindle, P.K., Handa, M. and Ihle, J.N., 2001. Functional interaction of STAT5 and nuclear receptor co-repressor SMRT: implications in negative regulation of STAT5-dependent transcription. *The EMBO Journal*, 20(23), pp.6836–6844. https://doi.org/10.1093/EMBOJ/20.23.6836.

Nakamura, M. and Sadoshima, J., 2018. Mechanisms of physiological and pathological cardiac hypertrophy. *Nature reviews cardiology*, 15(7), pp.387–407

Naylor, M.J., Li, N., Cheung, J., Lowe, E.T., Lambert, E., Marlow, R., Wang, P., Schatzmann, F., Wintermantel, T., Schüetz, G., Clarke, A.R., Mueller, U., Hynes, N.E. and Streuli, C.H., 2005. Ablation of β1 integrin in mammary epithelium reveals a key role for integrin in glandular morphogenesis and differentiation. *Journal of Cell Biology*, 171(4), pp.717–728.

Ni, C.-Y., Murphy, M.P., Golde, T.E. and Carpenter, G., 2001. gamma -Secretase Cleavage and Nuclear Localization of ErbB-4 Receptor Tyrosine Kinase. *Science*, 294(5549), pp.2179–2181.

Oates, C.J., Dondelinger, F., Bayani, N., Korkola, J., Gray, J.W. and Mukherjee, S., 2014. Causal network inference using biochemical kinetics. In: *Bioinformatics*.

Obana, M., Miyamoto, K., Murasawa, S., Iwakura, T., Hayama, A., Yamashita, T., Shiragaki, M., Kumagai, S., Miyawaki, A., Takewaki, K., Matsumiya, G., Maeda, M., Yoshiyama, M., Nakayama, H. and Fujio, Y., 2012. Therapeutic administration of IL-11 exhibits the postconditioning effects against ischemia-reperfusion injury via STAT3 in the heart. *American Journal of Physiology - Heart and Circulatory Physiology*, 303(5).

Obeng, E.O., Rusciano, I., Marvi, M.V., Fazio, A., Ratti, S., Follo, M.Y., Xian, J., Manzoli, L., Billi, A.M., Mongiorgi, S., Ramazzotti, G. and Cocco, L., 2020. Phosphoinositide-Dependent Signaling in Cancer: A Focus on Phospholipase C Isozymes. *International journal of molecular sciences*, 21(7).

Odiete, O., Hill, M.F. and Sawyer, D.B., 2012. Neuregulin in Cardiovascular Development and Disease. *Circulation research*, 111(10), p.1376.

Ogiso, H., Ishitani, R., Nureki, O., Fukai, S., Yamanaka, M., Kim, J.H., Saito, K., Sakamoto, A., Inoue, M., Shirouzu, M. and Yokoyama, S., 2002. Crystal structure of the complex of human epidermal growth factor and receptor extracellular domains. *Cell*, 110(6), pp.775–787.

Ojala, V.K., Knittle, A.M., Kirjalainen, P., Merilahti, J.A.M., Kortesoja, M., Tvorogov, D., Vaparanta, K., Lin, S., Kast, J., Pulliainen, A.T., Kurppa, K.J. and Elenius, K., 2020. The guanine nucleotide exchange factor VAV3 participates in ERBB4-mediated cancer cell migration. *The Journal of biological chemistry*, 295(33), pp.11559–11571.

Okamoto, K. and Sako, Y., 2018. Single-Molecule Fö rster Resonance Energy Transfer Measurement Reveals the Dynamic Partially Ordered Structure of the Epidermal Growth Factor Receptor C-Tail Domain.

Olayioye, M.A., Beuvink, I., Horsch, K., Daly, J.M. and Hynes, N.E., 1999. ErbB receptor-induced activation of Stat transcription factors is mediated by Src tyrosine kinases. *Journal of Biological Chemistry*, 274(24), pp.17209–17218.

Olofsson, B., Pajusola, K., Kaipainen, A., Von Euler, G., Joukov, V., Saksela, O., Orpana, A., Pettersson, R.F., Alitalo, K. and Eriksson, U., 1996. Vascular endothelial growth factor B, a novel growth factor for endothelial cells. *Proceedings of the National Academy of Sciences of the United States of America*, 93(6).

Olson, M.F., Pasteris, N.G., Gorski, J.L. and Hall, A., 1996. Faciogenital dysplasia protein (FGD1) and Vav, two related proteins required for normal embryonic development, are upstream regulators of Rho GTPases. *Current Biology*, 6(12), pp.1628–1633.

Olsson, A.K., Dimberg, A., Kreuger, J. and Claesson-Welsh, L., 2006. *VEGF receptor signalling - In control of vascular function*. *Nature Reviews Molecular Cell Biology*,

Orlandini, M., Marconcini, L., Ferruzzi, R. and Oliviero, S., 1996. Identification of a c-fos-induced gene that is related to the platelet-derived growth factor/vascular endothelial growth factor family. *Proceedings of the National Academy of Sciences of the United States of America*, 93(21), p.11675.

Oved, S., Mosesson, Y., Zwang, Y., Santonico, E., Shtiegman, K., Marmor, M.D., Kochupurakkal, B.S., Katz, M., Lavi, S., Cesareni, G. and Yarden, Y., 2006. Conjugation to Nedd8 Instigates Ubiquitylation and Down-regulation of Activated Receptor Tyrosine Kinases. *Journal of Biological Chemistry*, 281(31), pp.21640–21651.

Özcelik, C., Erdmann, B., Pilz, B., Wettschureck, N., Britsch, S., Hübner, N., Chien, K.R., Birchmeier, C. and Garratt, A.N., 2002. Conditional mutation of the ErbB2 (HER2) receptor in cardiomyocytes leads to dilated cardiomyopathy. *Proceedings of the National Academy of Sciences of the United States of America*, 99(13), pp.8880–8885.

Paatero, I., Jokilammi, A., Heikkinen, P.T., Iljin, K., Kallioniemi, O.P., Jones, F.E., Jaakkola, P.M. and Elenius, K., 2012. Interaction with ErbB4 promotes hypoxia-inducible factor-1α signaling. *The Journal of biological chemistry*, 287(13), pp.9659–9671.

Packham, S., Lin, Y., Zhao, Z., Warsito, D., Rutishauser, D. and Larsson, O., 2015. The Nucleus-Localized Epidermal Growth Factor Receptor is SUMOylated. *Biochemistry*, 54(33), pp.5157–5166.

Palshikar, M.G., Min, X., Crystal, A., Meng, J., Hilchey, S.P., Zand, M.S. and Thakar, J., 2023. Executable Network Models of Integrated Multiomics Data.

Pan, J., Fukuda, K., Kodama, H., Makino, S., Takahashi, T., Sano, M., Hori, S. and Ogawa, S., 1997. Role of Angiotensin II in Activation of the JAK/STAT Pathway Induced by Acute Pressure Overload in the Rat Heart. *Circulation research*, 81(4), pp.611–617. https://doi.org/10.1161/01.RES.81.4.611.

Pan, J., Fukuda, K., Saito, M., Matsuzaki, J., Kodama, H., Sano, M., Takahashi, T., Kato, T. and Ogawa, S., 1999. Mechanical Stretch Activates the JAK/STAT Pathway in Rat Cardiomyocytes.

Pan, J., Sano, M., Takahashi, T., Makino, S., Kato, T., Manabe, T., HorF, S. and Ogawa, S., 1998. Involvement of gpl30-mediated signaling in pressure overload-induced activation of the JAK/STAT pathway in rodent heart. *Heart Vessels*, 13, pp.199–208.

Pandey, A., Podtelejnikov, A. V., Blagoev, B., Bustelo, X.R., Mann, M. and Lodish, H.F., 2000. Analysis of receptor signaling pathways by mass spectrometry: Identification of Vav-2 as a substrate of the epidermal and platelet-derived growth factor receptors. *Proceedings of the National Academy of Sciences*, 97(1), pp.179–184.

Park, J.J., Yi, J.Y., Jin, Y.B., Lee, Y.J., Lee, J.S., Lee, Y.S., Ko, Y.G. and Lee, M., 2012. Sialylation of epidermal growth factor receptor regulates receptor activity and chemosensitivity to gefitinib in colon cancer cells. *Biochemical Pharmacology*, 83(7), pp.849–857.

Patterson, M., Barske, L., Van Handel, B., Rau, C.D., Gan, P., Sharma, A., Parikh, S., Denholtz, M., Huang, Y., Yamaguchi, Y., Shen, H., Allayee, H., Crump, J.G., Force, T.I., Lien, C.-L., Makita, T., Lusis, A.J., Kumar, S.R. and Sucov, H.M., 2017. Frequency of mononuclear diploid cardiomyocytes underlies natural variation in heart regeneration. *Nature genetics*, 49(9), pp.1346–1353.

Paull, E.O., Carlin, D.E., Niepel, M., Sorger, P.K., Haussler, D. and Stuart, J.M., 2013. Discovering causal pathways linking genomic events to transcriptional states using Tied Diffusion Through Interacting Events (TieDIE). *Bioinformatics*, 29(21).

Peles, E., Ben Levy, R., Or, E., Ullrich, A. and Yarden, Y., 1991. Oncogenic forms of the neu/HER2 tyrosine kinase are permanently coupled to phospholipase C gamma. *The EMBO journal*, 10(8), pp.2077–2086.

Peng, Y., Zhou, B., Wang, Y., Chen, Y., Li, H., Song, Y., Zhang, L. and Rao, L., 2012. Association between polymorphisms in the signal transducer and activator of transcription and dilated cardiomyopathy in the Chinese Han population. *Molecular and Cellular Biochemistry*, 360(1–2), pp.197–203.

Pentassuglia, L., Timolati, F., Seifriz, F., Abudukadier, K., Suter, T.M. and Zuppinger, C., 2007. Inhibition of ErbB2/neuregulin signaling augments paclitaxel-induced cardiotoxicity in adult ventricular myocytes. *Experimental Cell Research*, 313(8), pp.1588–1601.

Philips, R.L., Wang, Y., Cheon, H.J., Kanno, Y., Gadina, M., Sartorelli, V., Horvath, C.M., Darnell, J.E., Stark, G.R. and O'Shea, J.J., 2022. The JAK-STAT pathway at 30: Much learned, much more to do. *Cell*, 185(21), pp.3857–3876.

Plowman, G.D., Culouscou, J.M., Whitney, G.S., Green, J.M., Carlton, G.W., Foy, L., Neubauer, M.G. and Shoyab, M., 1993a. Ligand-specific activation of HER4/p180erbB4, a fourth member of the epidermal growth factor receptor family. *Proceedings of the National Academy of Sciences of the United States of America*, 90(5), pp.1746–1750.

Plowman, G.D., Green, J.M., Culouscou, J.M., Carlton, G.W., Rothwell, V.M. and Buckley, S., 1993b. Heregulin induces tyrosine phosphorylation of HER4/p180erbB4. *Nature*, 366(6454), pp.473–475.

Poitras, L., Jean, S., Islam, N. and Moss, T., 2003. PAK interacts with NCK and MLK2 to regulate the activation of jun N-terminal kinase. *FEBS Letters*, 543(1–3), pp.129–135.

Poltorak, Z., Cohen, T., Sivan, R., Kandelis, Y., Spira, G., Vlodavsky, I., Keshet, E. and Neufeld, G., 1997. VEGF145, a secreted vascular endothelial growth factor isoform that binds to extracellular matrix. *Journal of Biological Chemistry*, 272(11).

Poss, K.D., Wilson, L.G. and Keating, M.T., 2002. Heart regeneration in zebrafish. *Science*, 298(5601), pp.2188–2190.

Prill, R.J., Marbach, D., Saez-Rodriguez, J., Sorger, P.K., Alexopoulos, L.G., Xue, X., Clarke, N.D., Altan-Bonnet, G. and Stolovitzky, G., 2010. Towards a rigorous assessment of systems biology models: The DREAM3 challenges. *PloS one*, 5(2), pp.e9202–e9202.

Qiu, C., Tarrant, M.K., Choi, S.H., Sathyamurthy, A., Bose, R., Banjade, S., Pal, A., Bornmann, W.G., Lemmon, M.A., Cole, P.A. and Leahy, D.J., 2008. Mechanism of Activation and Inhibition of the HER4/ErbB4 Kinase. *Structure (London, England : 1993)*, 16(3), p.460.

Rahimi, N., Dayanir, V. and Lashkari, K., 2000. Receptor chimeras indicate that the vascular endothelial growth factor receptor-1 (VEGFR-1) modulates mitogenic activity of VEGFR-2 in endothelial cells. *The Journal of biological chemistry*, 275(22), pp.16986–16992.

Rasouli, S.J. and Stainier, D.Y.R., 2017. Regulation of cardiomyocyte behavior in zebrafish trabeculation by Neuregulin 2a signaling. *Nature Communications 2017 8:1*, 8(1), pp.1–11.

Rebsamen, M.C., Arrighi, J.-F., Juge-Aubry, C.E., Vallotton, M.B. and Lang, U., 2000. Epidermal Growth Factor Induces Hypertrophic Responses and Stat5 Activation in Rat Ventricular Cardiomyocytes. *Journal of molecular and cellular cardiology*, 32(4), pp.599–610.

Red Brewer, M., Choi, S.H., Alvarado, D., Moravcevic, K., Pozzi, A., Lemmon, M.A. and Carpenter, G., 2009. The Juxtamembrane Region of the EGF Receptor Functions as an Activation Domain. *Molecular cell*, 34(6), p.641.

Regmi, R., Srinivasan, S., Latham, A.P., Kukshal, V., Cui, W., Zhang, B., Bose, R. and Schlau-Cohen, G.S., 2020. Phosphorylation-dependent Conformations of the Disordered Carboxyl-terminus Domain in the Epidermal Growth Factor Receptor. *The journal of physical chemistry letters*, 11(23), p.10037.

Reiss, K., Cheng, W., Ferber, A., Kajstura, J., Li, P., Li, B., Olivetti, G., Homcy, C.J., Baserga, R. and Anversa, P., 1996. Overexpression of Insulin-Like Growth Factor-1 in the Heart is Coupled with Myocyte Proliferation in Transgenic Mice. *Proceedings of the National Academy of Sciences - PNAS*, 93(16), pp.8630–8635. https://doi.org/10.1073/pnas.93.16.8630.

Rice, J.J., Tu, Y. and Stolovitzky, G., 2005. Reconstructing biological networks using conditional correlation analysis. *BIOINFORMATICS*, 21(6), pp.765–773.

Riese, D.J., Bermingham, Y., Van Raaij, T.M., Buckley, S., Plowman, G.D. and Stern, D.F., 1996a. Betacellulin activates the epidermal growth factor receptor and erbB-4, and induces cellular response patterns distinct from those stimulated by epidermal growth factor or neuregulin-beta. *Oncogene*, 12(2), pp.345–353. Available at: <https://pubmed.ncbi.nlm.nih.gov/8570211/> [Accessed 15 March 2023].

Riese, D.J., Kim, E.D., Elenius, K., Buckley, S., Klagsbrun, M., Plowman, G.D. and Stern, D.F., 1996b. The epidermal growth factor receptor couples transforming growth factor-alpha, heparin-binding epidermal growth factor-like factor, and amphiregulin to Neu, ErbB-3, and ErbB-4. *The Journal of biological chemistry*, 271(33), pp.20047–20052.

Riese, D.J., Komurasaki, T., Plowman, G.D. and Stern, D.F., 1998. Activation of ErbB4 by the bifunctional epidermal growth factor family hormone epiregulin is regulated by ErbB2. *The Journal of biological chemistry*, 273(18), pp.11288–11294.

Riethmacher, D., Sonnenberg-Riethmacher, E., Brinkmann, V., Yamaai, T., Lewin, G.R. and Birchmeier, C., 1997. Severe neuropathies in mice with targeted mutations in the ErbB3 receptor. *Nature*, 389(6652), pp.725–730.

Rigacci, S., Guidotti, V., Parri, M. and Berti, A., 2008. Articles Modulation of STAT5 Interaction with LMW-PTP during Early Megakaryocyte Differentiation.

Rio, C., Buxbaum, J.D., Peschon, J.J. and Corfas, G., 2000. Tumor necrosis factor-alpha-converting enzyme is required for cleavage of erbB4/HER4. *The Journal of biological chemistry*, 275(14), pp.10379–87.

Robinson, D.R., Wu, Y.M. and Lin, S.F., 2000. The protein tyrosine kinase family of the human genome. *Oncogene 2000 19:49*, 19(49), pp.5548–5557.

Rodrigues, R.R., Shulzhenko, N. and Morgun, A., 2018. Transkingdom Networks: A Systems Biology Approach to Identify Causal Members of Host–Microbiota Interactions. *Methods in Molecular Biology*, 1849, pp.227–242.

Rohrbach, S., Niemann, B., Silber, R.E. and Holtz, J., 2005. Neuregulin receptors erbB2 and erbB4in failing human myocardium. Depressed expression and attenuated activation. *Basic Research in Cardiology*, 100(3), pp.240–249.

Rohrbach, S., Yan, X., Weinberg, E.O., Hasan, F., Bartunek, J., Marchionni, M.A. and Lorell, B.H., 1999. Neuregulin in Cardiac Hypertrophy in Rats With Aortic Stenosis. *Circulation*, 100(4), pp.407–412.

Runkle, K.B., Kharbanda, A., Stypulkowski, E., Cao, X.J., Wang, W., Garcia, B.A. and Witze, E.S., 2016. Inhibition of DHHC20 mediated EGFR palmitoylation creates a dependence on EGFR signaling. *Molecular cell*, 62(3), p.385.

Salokas, K., Liu, X., Öhman, T., Chowdhury, I., Gawriyski, L., Keskitalo, S. and Varjosalo, M., 2022. Physical and functional interactome atlas of human receptor tyrosine kinases. *EMBO reports*, 23(6), pp.e54041-n/a.

Saraon, P., Pathmanathan, S., Snider, J., Lyakisheva, A., Wong, V. and Stagljar, I., 2021. *Receptor tyrosine kinases and cancer: oncogenic mechanisms and therapeutic approaches*. *Oncogene*,

Sardi, S.P., Murtie, J., Koirala, S., Patten, B.A. and Corfas, G., 2006. Presenilin-dependent ErbB4 nuclear signaling regulates the timing of astrogenesis in the developing brain. *Cell*, 127(1), pp.185–197.

Sartorio, A., Ferrero, S., Conti, A., Bragato, R., Malfatto, G., Leonetti, G. and Faglia, G., 1997. Adults with childhood-onset growth hormone deficiency: effects fo growth harmone treatment on cardiac structure. *Journal of Internal Medicine*, 241(6), pp.515–520.

Savarese, G., Stolfo, D., Sinagra, G. and Lund, L.H., 2022. Heart failure with mid-range or mildly reduced ejection fraction. *Nature reviews cardiology*, 19(2), pp.100–116.

Sawyer, D.B., Zuppinger, C., Miller, T.A., Eppenberger, H.M. and Suter, T.M., 2002. Modulation of Anthracycline-Induced Myofibrillar Disarray in Rat Ventricular Myocytes by Neuregulin-1β and Anti-erbB2. *Circulation*, 105(13), pp.1551–1554.

Scheck, R.A., Lowder, M.A., Appelbaum, J.S. and Schepartz, A., 2012. Bipartite Tetracysteine Display Reveals Allosteric Control of Ligand-Specific EGFR Activation. *ACS chemical biology*, 7(8), p.1367.

Schena, M., Shalon, D., Davis, R.W. and Brown, P.O., 1995. Quantitative Monitoring of Gene Expression Patterns with a Complementary DNA Microarray. *Science (American Association for the Advancement of Science)*, 270(5235), pp.467–470.

Schindelin, J., Arganda-Carreras, I., Frise, E., Kaynig, V., Longair, M., Pietzsch, T., Preibisch, S., Rueden, C., Saalfeld, S., Schmid, B., Tinevez, J.Y., White, D.J., Hartenstein, V., Eliceiri, K., Tomancak, P. and Cardona, A., 2012. Fiji: an open-source platform for biological-image analysis. *Nature Methods 2012 9:7*, 9(7), pp.676–682.

Schindler, C., Shuai, K., Prezioso, V.R. and Darnell, J.E., 1992. Interferon-dependent tyrosine phosphorylation of a latent cytoplasmic transcription factor. *Science (New York, N.Y.)*, 257(5071), pp.809–813. https://doi.org/10.1126/SCIENCE.1496401.

Schlessinger, J., 2014. Receptor tyrosine kinases: Legacy of the first two decades. *Cold Spring Harbor Perspectives in Biology*, 6(3).

Schmieder, R. and Edwards, R., 2011. Quality control and preprocessing of metagenomic datasets. *Bioinformatics*, 27(6), pp.863–864.

Schulze, W.X., Deng, L. and Mann, M., 2005. Phosphotyrosine interactome of the ErbB-receptor kinase family. *Molecular systems biology*, 1, p.2005.0008.

Schunkert, H., Dzau, V.J., Tang, S.S., Hirsch, A.T., Apstein, C.S. and Lorell, B.H., 1990. Increased rat cardiac angiotensin converting enzyme activity and mRNA expression in pressure overload left ventricular hypertrophy. Effects on coronary resistance, contractility, and relaxation. *Journal of Clinical Investigation*, 86(6), p.1913.

Sefat-E-Khuda, Yoshida, M., Xing, Y., Shimasaki, T., Takeya, M., Kuwahara, K. and Sakaguchi, N., 2004. The Sac3 Homologue shd1 Is Involved in Mitotic Progression in Mammalian Cells. *Journal of Biological Chemistry*, 279(44), pp.46182–46190.

Segers, V.F.M., Dugaucquier, L., Feyen, E., Shakeri, H. and De Keulenaer, G.W., 2020. The role of ErbB4 in cancer. *Cellular oncology (Dordrecht)*, 43(3), pp.335–352.

Senyo, S.E., Steinhauser, M.L., Pizzimenti, C.L., Yang, V.K., Cai, L., Wang, M., Wu, T.-D., Guerquin-Kern, J.-L., Lechene, C.P. and Lee, R.T., 2013. Mammalian heart renewal by pre-existing cardiomyocytes. *Nature (London)*, 493(7432), pp.433–436.

Sepp-Lorenzino, L., Eberhard, I., Ma, Z., Cho, C., Serve, H., Liu, F., Rosen, N. and Lupu, R., 1996. Signal transduction pathways induced by heregulin in MDA-MB-453 breast cancer cells. *Oncogene.*, 12(8), pp.1679–1687.

Shalaby, F., Rossant, J., Yamaguchi, T.P., Gertsenstein, M., Wu, X.-F., Breitman, M.L. and Schuh, A.C., 1995. Failure of blood-island formation and vasculogenesis in Flk-1-deficient mice. *Nature (London)*, 376(6535), pp.62–66. https://doi.org/10.1038/376062a0.

Shen, B., Coruzzi, G. and Shasha, D., 2023. EnsInfer: a simple ensemble approach to network inference outperforms any single method. *BMC Bioinformatics*, 24(1).

Shi, F., Telesco, S.E., Liu, Y., Radhakrishnan, R. and Lemmona, M.A., 2010. ErbB3/HER3 intracellular domain is competent to bind ATP and catalyze autophosphorylation. *Proceedings of the National Academy of Sciences of the United States of America*, 107(17), pp.7692–7697.

Shibuya, M., Yamaguchi, S., Yamane, A., Ikeda, T., Tojo, A., Matsushime, H. and Sato, M., 1990. Nucleotide sequence and expression of a novel human receptor-type tyrosine kinase gene (flt) closely relatd to the fms family. *Oncogene*, 5(4).

Shmulevich, I., Dougherty, E.R., Kim, S. and Zhang, W., 2002. Probabilistic Boolean networks: A rule-based uncertainty model for gene regulatory networks. *Bioinformatics*, 18(2).

Shostak, K. and Chariot, A., 2015. EGFR and NF-kB: partners in cancer.

Shuai, K., Horvath, C.M., Huang, L.H.T., Qureshi, S.A., Cowburn, D. and Darnell, J.E., 1994. Interferon activation of the transcription factor Stat91 involves dimerization through SH2-phosphotyrosyl peptide interactions. *Cell*, 76(5), pp.821–828.

Shuai, K., Schindler, C., Prezioso, V.R. and Darnell, J.E., 1992. Activation of transcription by IFN-gamma: tyrosine phosphorylation of a 91-kD DNA binding protein. *Science (New York, N.Y.)*, 258(5089), pp.1808–1812.

Shuai, K., Stark, G.R., Kerr, I.M. and Darnell, J.E., 1993. A single phosphotyrosine residue of Stat91 required for gene activation by interferon-gamma. *Science (New York, N.Y.)*, 261(5129), pp.1744–1746.

Sibilia, M., Steinbach, J.P., Stingl, L., Aguzzi, A. and Wagner, E.F., 1998. A strain-independent postnatal neurodegeneration in mice lacking the EGF receptor. *The EMBO journal*, 17(3), pp.719–731.

Sibilia, M., Wagner, B., Hoebertz, A., Elliott, C., Marino, S., Jochum, W. and Wagner, E.F., 2003. Mice humanised for the EGF receptor display hypomorphic phenotypes in skin, bone and heart. *Development*, 130(19), pp.4515–4525.

Sibilia, M. and Wagner, E.F., 1995. Strain-Dependent Epithelial Defects in Mice Lacking the EGF Receptor. *Science*, 269(5221), pp.234–238.

Sinclair, J.K.L., Walker, A.S., Doerner, A.E. and Schepartz, A., 2018. Mechanism of Allosteric Coupling into and through the Plasma Membrane by EGFR. *Cell chemical biology*, 25(7), pp.857-870.e7.

Skirzewski, M., Cronin, M.E., Murphy, R., Buonanno, A., Fobbs, W. and Kravitz, A. V., 2020. ErbB4 Null Mice Display Altered Mesocorticolimbic and Nigrostriatal Dopamine Levels as well as Deficits in Cognitive and Motivational Behaviors. *eNeuro*, 7(3).

Sławek, J. and Arodź, T., 2012. ADANET: Inferring gene regulatory networks using ensemble classifiers. In: *2012 ACM Conference on Bioinformatics, Computational Biology and Biomedicine, BCB 2012*.

Slawek, J. and Arodz, T., 2013. ENNET: Inferring large gene regulatory networks from expression data using gradient boosting. *BMC systems biology*, 7(1), pp.106–106.

Soker, S., Takashima, S., Miao, H.Q., Neufeld, G. and Klagsbrun, M., 1998. Neuropilin-1 is expressed by endothelial and tumor cells as an isoform-specific receptor for vascular endothelial growth factor. *Cell*, 92(6), pp.735–745.

Solntsev, S.K., Shortreed, M.R., Frey, B.L. and Smith, L.M., 2018. Enhanced Global Post-translational Modification Discovery with MetaMorpheus. *Journal of Proteome Research*, 17(5), pp.1844–1851.

Soltoff, S.P., Carraway Iii, K.L., Prigent, S.A., Gullick, W.G. and Cantley', L.C., 1994. ErbB3 Is Involved in Activation of Phosphatidylinositol 3-Kinase by Epidermal Growth Factor. *MOLECULAR AND CELLULAR BIOLOGY*, 14(6), pp.3550–3558.

Song, H., Li, C.W., Labaff, A.M., Lim, S.O., Li, L.Y., Kan, S.F., Chen, Y., Zhang, K., Lang, J., Xie, X., Wang, Y., Huo, L.F., Hsu, S.C., Chen, X., Zhao, Y. and Hung, M.C., 2011. Acetylation of EGF receptor contributes to tumor cell resistance to histone deacetylase inhibitors. *Biochemical and biophysical research communications*, 404(1), pp.68–73.

Song, L., Langfelder, P. and Horvath, S., 2012. Comparison of co-expression measures: Mutual information, correlation, and model based indices. *BMC bioinformatics*, 13(1), pp.328–328.

Song, M., Greenbaum, J., Luttrell, J., Zhou, W., Wu, C., Shen, H., Gong, P., Zhang, C. and Deng, H.W., 2020. *A Review of Integrative Imputation for Multi-Omics Datasets*. *Frontiers in Genetics*,

Soonpaa, M.H., Kim, K.K., Pajak, L., Franklin, M. and Field, L.J., 1996. Cardiomyocyte DNA synthesis and binucleation during murine development. *American journal of physiology. Heart and circulatory physiology*, 271(5), pp.H2183–H2189.

Sorokin, A., 1995. Activation of the EGF receptor by insertional mutations in its juxtamembrane regions. *Oncogene*, 11(8), pp.1531–1540.

Soufan, A.T., van den Berg, G., Ruijter, J.M., de Boer, P.A.J., van den Hoff, M.J.B. and Moorman, A.F.M., 2006. Regionalized sequence of myocardial cell growth and proliferation characterizes early chamber formation. *Circulation research*, 99(5), pp.545–552.

Sousa, L.P., Lax, I., Shen, H., Ferguson, S.M., De Camilli, P. and Schlessinger, J., 2012. Suppression of EGFR endocytosis by dynamin depletion reveals that EGFR signaling occurs primarily at the plasma membrane. *Proceedings of the National Academy of Sciences of the United States of America*, 109(12).

Sriram, G., Jankowski, W., Kasikara, C., Reichman, C., Saleh, T., Nguyen, K.Q., Li, J., Hornbeck, P., Machida, K., Liu, T., Li, H., Kalodimos, C.G. and Birge, R.B., 2014. Iterative tyrosine phosphorylation controls non-canonical domain utilization in Crk. *Oncogene 2014 34:32*, 34(32), pp.4260–4269.

Stansfield, W.E., Ranek, M., Pendse, A., Schisler, J.C., Wang, S., Pulinilkunnil, T. and Willis, M.S., 2014. The Pathophysiology of Cardiac Hypertrophy and Heart Failure. In: *Cellular and Molecular Pathobiology of Cardiovascular Disease*.

Stein, R.A. and Staros, J. V., 2006. Insights into the evolution of the ErbB receptor family and their ligands from sequence analysis. *BMC evolutionary biology*, 6.

Steuer, R., Kurths, J., Daub, C.O., Weise, J. and Selbig, J., 2002. The mutual information: Detecting and evaluating dependencies between variables. In: *Bioinformatics*.

Stover, D.R., Becker, M., Liebetanz, J. and Lydon, N.B., 1995. Src Phosphorylation of the Epidermal Growth Factor Receptor at Novel Sites Mediates Receptor Interaction with Src and P85α. *Journal of Biological Chemistry*, 270(26), pp.15591–15597.

Strachan, L., Murison, J.G., Prestidge, R.L., Sleeman, M.A., Watson, J.D. and Kumble, K.D., 2001. Cloning and biological activity of epigen, a novel member of the epidermal growth factor superfamily. *The Journal of biological chemistry*, 276(21), pp.18265–18271.

Strehlow, I. and Schindler, C., 1998. Amino-terminal signal transducer and activator of transcription (STAT) domains regulate nuclear translocation and STAT deactivation. *Journal of*

Subramanian, A., Tamayo, P., Mootha, V.K., Mukherjee, S., Ebert, B.L., Gillette, M.A., Paulovich, A., Pomeroy, S.L., Golub, T.R., Lander, E.S. and Mesirov, J.P., 2005. Gene set enrichment analysis: A knowledge-based approach for interpreting genome-wide expression profiles. *Proceedings of the National Academy of Sciences of the United States of America*, 102(43), pp.15545–15550.

Sucov, H.M., Gu, Y., Thomas, S., Li, P. and Pashmforoush, M., 2009. Epicardial control of myocardial proliferation and morphogenesis. *Pediatric Cardiology*, 30(5), pp.617–625.

Sultana, N., Zhang, L., Yan, J., Chen, J., Cai, W., Razzaque, S., Jeong, D., Sheng, W., Bu, L., Xu, M., Huang, G.-Y., Hajjar, R.J., Zhou, B., Moon, A. and Cai, C.-L., 2015. Resident c-kit + cells in the heart are not cardiac stem cells. *Nature communications*, 6(1), pp.8701–8701.

Sun, W., Wei, X., Kesavan, K., Garrington, T.P., Fan, R., Mei, J., Anderson, S.M., Gelfand, E.W. and Johnson, G.L., 2003. MEK Kinase 2 and the Adaptor Protein Lad Regulate Extracellular Signal-Regulated Kinase 5 Activation by Epidermal Growth Factor via Src. *Molecular and Cellular Biology*, 23(7), p.2298.

Sundvall, M., Korhonen, A., Paatero, I., Gaudio, E., Melino, G., Croce, C.M., Aqeilan, R.I. and Elenius, K., 2008. Isoform-specific monoubiquitination, endocytosis, and degradation of alternatively spliced ErbB4 isoforms. *Proceedings of the National Academy of Sciences of the United States of America*, 105(11), pp.4162–4167.

Sundvall, M., Korhonen, A., Vaparanta, K., Anckar, J., Halkilahti, K., Salah, Z., Aqeilan, R.I., Palvimo, J.J., Sistonen, L. and Elenius, K., 2012. Protein Inhibitor of Activated STAT3 (PIAS3) Protein Promotes SUMOylation and Nuclear Sequestration of the Intracellular Domain of ErbB4 Protein. *Journal of Biological Chemistry*, 287(27), pp.23216–23226.

Sundvall, M., Veikkolainen, V., Kurppa, K., Salah, Z., Tvorogov, D., van Zoelen, E.J., Aqeilan, R. and Elenius, K., 2010. Cell death or survival promoted by alternative isoforms of ErbB4. *Molecular biology of the cell*, 21(23), pp.4275–86. https://doi.org/10.1091/mbc.E10-04-0332.

Sysa-Shah, P., Xu, Y., Guo, X., Belmonte, F., Kang, B., Bedja, D., Pin, S., Tsuchiya, N. and Gabrielson, K., 2012. Cardiac-specific over-expression of epidermal growth factor receptor 2 (ErbB2) induces pro-survival pathways and hypertrophic cardiomyopathy in mice. *PloS one*, 7(8), p.e42805.

Szklarczyk, D., Gable, A.L., Lyon, D., Junge, A., Wyder, S., Huerta-Cepas, J., Simonovic, M., Doncheva, N.T., Morris, J.H., Bork, P., Jensen, L.J. and Von Mering, C., 2019. STRING v11: Protein-protein association networks with increased coverage, supporting functional discovery in genome-wide experimental datasets. *Nucleic Acids Research*, 47(D1), pp.D607–D613.

Takahashi, M., Yokoe, S., Asahi, M., Lee, S.H., Li, W., Osumi, D., Miyoshi, E. and Taniguchi, N., 2008. N-glycan of ErbB family plays a crucial role in dimer formation and tumor promotion. *Biochimica et Biophysica Acta (BBA) - General Subjects*, 1780(3), pp.520–524.

Takishima, K., Griswold-Prenner, I., Ingebritsen, T. and Rosner, M.R., 1991. Epidermal growth factor (EGF) receptor T669 peptide kinase from 3T3-L1 cells is an EGF-stimulated 'MAP' kinase. *Proceedings of the National Academy of Sciences of the United States of America*, 88(6), p.2520.

Tam, P.P., Parameswaran, M., Kinder, S.J. and Weinberger, R.P., 1997. The allocation of epiblast cells to the embryonic heart and other mesodermal lineages: the role of ingression and tissue movement during gastrulation. *Development (Cambridge)*, 124(9), pp.1631–1642.

Tamayo, P., Slonim, D., Mesirov, J., Zhu, Q., Kitareewan, S., Dmitrovsky, E., Lander, E.S. and Golub, T.R., 1999. Interpreting Patterns of Gene Expression with Self-Organizing Maps: Methods and Application to Hematopoietic Differentiation. *Proceedings of the National Academy of Sciences - PNAS*, 96(6), pp.2907–2912. https://doi.org/10.1073/pnas.96.6.2907.

Tanos, B. and Pendergast, A.M., 2006. Abl tyrosine kinase regulates endocytosis of the epidermal growth factor receptor. *The Journal of biological chemistry*, 281(43), pp.32714–32723.

Tarazona, S., Arzalluz-Luque, A. and Conesa, A., 2021. *Undisclosed, unmet and neglected challenges in multi-omics studies*. *Nature Computational Science*, https://doi.org/10.1038/s43588-021-00086-z.

Terman, B.I., Carrion, M.E., Kovacs, E., Rasmussen, B.A., Eddy, R.L. and Shows, T.B., 1991. Identification of a new endothelial cell growth factor receptor tyrosine kinase. *Oncogene*, 6(9).

Terman, B.I., Dougher-Vermazen, M., Carrion, M.E., Dimitrov, D., Armellino, D.C., Gospodarowicz, D. and Böhlen, P., 1992. Identification of the KDR tyrosine kinase as a receptor for vascular endothelial cell growth factor. *Biochemical and biophysical research communications*, 187(3), pp.1579–1586.

Terveyden ja hyvinvoinnin laitos, 2023. *https://thl.fi/*. Sydän- ja verisuonitautien yleisyys.

Theroux, S.J., Taglienti-Sian, C., Nair, N., Countaway, J.L., Robinson, H.L. and Davis, R.J., 1992. Increased oncogenic potential of ErbB is associated with the loss of a COOH-terminal domain serine phosphorylation site. *Journal of Biological Chemistry*, 267(12), pp.7967–7970.

Thiel, K.W. and Carpenter, G., 2007. Epidermal growth factor receptor juxtamembrane region regulates allosteric tyrosine kinase activation. *Proceedings of the National Academy of Sciences of the United States of America*, 104(49), p.19238.

Threadgill, D.W., Dlugosz, A.A., Hansen, L.A., Tennenbaum, T., Lichti, U., Yee, D., LaMantia, C., Mourton, T., Herrup, K., Harris, R.C., Barnard, J.A., Yuspa, S.H., Coffey, R.J. and Magnuson, T., 1995. Targeted Disruption of Mouse EGF receptor: Effect of Genetic Background on Mutant Phenotype. *Science*, 269(5221), pp.230–234.

Tian, Y., Zhang, W., Xia, D., Modi, P., Liang, D. and Wei, M., 2011. Postconditioning inhibits myocardial apoptosis during prolonged reperfusion via a JAK2-STAT3-Bcl-2 pathway. *Journal of Biomedical Science*, 18(1), pp.1–8.

Tidcombe, H., Jackson-Fisher, A., Mathers, K., Stern, D.F., Gassmann, M. and Golding, J.P., 2003. Neural and mammary gland defects in ErbB4 knockout mice genetically rescued from embryonic lethality. *Proceedings of the National Academy of Sciences of the United States of America*, 100(14), pp.8281–6.

Tirziu, D., Chorianopoulos, E., Moodie, K.L., Palac, R.T., Zhuang, Z.W., Tjwa, M., Roncal, C., Eriksson, U., Fu, Q., Elfenbein, A., Hall, A.E., Carmeliet, P., Moons, L. and Simons, M., 2007a. Myocardial hypertrophy in the absence of external stimuli is induced by angiogenesis in mice. *The Journal of clinical investigation*, 117(11), pp.3188–3197.

Tirziu, D., Chorianopoulos, E., Moodie, K.L., Palac, R.T., Zhuang, Z.W., Tjwa, M., Roncal, C., Eriksson, U., Fu, Q., Elfenbein, A., Hall, A.E., Carmeliet, P., Moons, L. and Simons, M., 2007b. Myocardial hypertrophy in the absence of external stimuli is induced by angiogenesis in mice. *The Journal of clinical investigation*, 117(11), pp.3188–3197.

Tischer, E., Mitchell, R., Hartman, T., Silva, M., Gospodarowicz, D., Fiddes, J.C. and Abraham, J.A., 1991. The human gene for vascular endothelial growth factor: Multiple protein forms are encoded through alternative exon splicing. *Journal of Biological Chemistry*, 266(18).

Tsai, C.L., Chang, J.S., Yu, M.C., Lee, C.H., Chen, T.C., Chuang, W.Y., Kuo, W.L., Lin, C.C., Lin, S.M. and Hsieh, S.Y., 2020. Functional genomics identifies hepatitis-induced STAT3-TyrO3-STAT3 signaling as a potential therapeutic target of hepatoma. *Clinical Cancer Research*, 26(5), pp.1185–1197.

Tsuda, T., Ikeda, Y. and Taniguchi, N., 2000. The Asn-420-linked Sugar Chain in Human Epidermal Growth Factor Receptor Suppresses Ligand-independent Spontaneous Oligomerization. *Journal of Biological Chemistry*, 275(29), pp.21988–21994.

Tucher, J., Linke, D., Koudelka, T., Cassidy, L., Tredup, C., Wichert, R., Pietrzik, C., Becker-Pauly, C. and Tholey, A., 2014. LC–MS Based Cleavage Site Profiling of the Proteases ADAM10 and ADAM17 Using Proteome-Derived Peptide Libraries. *Journal of Proteome Research*, 13(4), pp.2205–2214.

Udy, G.B., Towers, R.P., Snell, R.G., Wilkins, R.J., Park, S.-H., Ram, P.A., Waxman, D.J. and Davey, H.W., 1997. Requirement of STAT5b for Sexual Dimorphism of Body Growth Rates and Liver Gene Expression. *Proceedings of the National Academy of Sciences - PNAS*, 94(14), pp.7239–7244.

Ullrich, A., Coussens, L., Hayflick, J.S., Dull, T.J., Gray, A., Tam, A.W., Lee, J., Yarden, Y., Libermann, T.A., Schlessinger, J., Downward, J., Mayes, E.L.V., Whittle, N., Waterfield, M.D. and Seeburg, P.H., 1984. Human epidermal growth factor receptor cDNA sequence and aberrant expression of the amplified gene in A431 epidermoid carcinoma cells. *Nature*, 309(5967), pp.418–425.

Uribe, M.L., Marrocco, I. and Yarden, Y., 2021. EGFR in Cancer: Signaling Mechanisms, Drugs, and Acquired Resistance. *Cancers*, 13(11)..

Ushiro, H. and Cohens, S., 1980. Identification of Phosphotyrosine as a Product of Epidermal Growth Factor-activated Protein Kinase in A-431 Cell Membranes*. *Journal of Biological Chemistry*, 255(18), pp.8363–8365.

Vahabi, N. and Michailidis, G., 2022. Unsupervised Multi-Omics Data Integration Methods: A Comprehensive Review. *Frontiers in Genetics*, 13.

Vasaikar, S. V., Straub, P., Wang, J. and Zhang, B., 2018. LinkedOmics: Analyzing multi-omics data within and across 32 cancer types. *Nucleic Acids Research*, 46(D1), pp.D956–D963.

Vaske, C.J., Benz, S.C., Sanborn, J.Z., Earl, D., Szeto, C., Zhu, J., Haussler, D. and Stuart, J.M., 2010. Inference of patient-specific pathway activities from multi-dimensional cancer genomics data using PARADIGM. *Bioinformatics (Oxford, England)*, 26(12).

Vecchi, M., Baulida, J. and Carpenter, G., 1996. Selective cleavage of the heregulin receptor ErbB-4 by protein kinase C activation. *The Journal of biological chemistry*, 271(31), pp.18989–18995.

Veikkolainen, V., Naillat, F., Railo, A., Chi, L., Manninen, A., Hohenstein, P., Hastie, N., Vainio, S. and Elenius, K., 2012. ErbB4 modulates tubular cell polarity and lumen diameter during kidney development. *Journal of the American Society of Nephrology*, 23(1), pp.112–122.

Veikkolainen, V., Vaparanta, K., Halkilahti, K., Iljin, K., Sundvall, M. and Elenius, K., 2011. Function of ERBB4 is determined by alternative splicing. *Cell Cycle*, 10(16), pp.2647–2657.

Vidal, G.A., Naresh, A., Marrero, L. and Jones, F.E., 2005. Presenilin-dependent gamma-secretase processing regulates multiple ERBB4/HER4 activities. *The Journal of biological chemistry*, 280(20), pp.19777–83.

Villalta, J.I., Galli, S., Iacaruso, M.F., Antico Arciuch, V.G., Poderoso, J.J., Jares-Erijman, E.A. and Pietrasanta, L.I., 2011. New Algorithm to Determine True Colocalization in Combination with Image Restoration and Time-Lapse Confocal Microscopy to Map Kinases in Mitochondria. *PLoS ONE*, 6(4), p.e19031.

Villarino, A. V., Kanno, Y. and O'Shea, J.J., 2017. Mechanisms and consequences of Jak–STAT signaling in the immune system. *Nature Immunology 2017 18:4*, 18(4), pp.374–384.

Vinkemeier, U., Moarefi, I., Darnell, J.E. and Kuriyan, J., 1998. Structure of the amino-terminal protein interaction domain of STAT-4. *Science (New York, N.Y.)*, 279(5353), pp.1048–1052.

De Vries, C., Escobedo, J.A., Ueno, H., Houck, K., Ferrara, N. and Williams, L.T., 1992. The fms-Like Tyrosine Kinase, a Receptor for Vascular Endothelial Growth Factor. *Science (American Association for the Advancement of Science)*, 255(5047), pp.989–991.

Wadhwa, D., Fallah-Rad, N., Grenier, D., Krahn, M., Fang, T., Ahmadie, R., Walker, J.R., Lister, D., Arora, R.C., Barac, I., Morris, A. and Jassal, D.S., 2009. Trastuzumab mediated cardiotoxicity in the setting of adjuvant chemotherapy for breast cancer: a retrospective study. *Breast cancer research and treatment*, 117(2), pp.357–364.

Wagner, B., Natarajan, A., Grünaug, S., Kroismayr, R., Wagner, E.F. and Sibilia, M., 2006. Neuronal survival depends on EGFR signaling in cortical but not midbrain astrocytes. *The EMBO journal*, 25(4), pp.752–762.

Wakao, H., Gouilleux, F. and Groner, B., 1995. Mammary gland factor (MGF) is a novel member of the cytokine regulated transcription factor gene family and confers the prolactin response. *The EMBO journal*, 14(4), pp.854–855.

Wali, V.B., Gilmore-Hebert, M., Mamillapalli, R., Haskins, J.W., Kurppa, K.J., Elenius, K., Booth, C.J. and Stern, D.F., 2014. Overexpression of ERBB4 JM-a CYT-1 and CYT-2 isoforms in transgenic mice reveals isoform-specific roles in mammary gland development and carcinogenesis. *Breast cancer research : BCR*, 16(6), p.501.

Walsh, S., Pontén, A., Fleischmann, B.K. and Jovinge, S., 2010. Cardiomyocyte cell cycle control and growth estimation in vivo--an analysis based on cardiomyocyte nuclei. *Cardiovascular research*, 86(3), pp.365–373.

Walton, G.M., Chen, W.S., Rosenfeld, M.G. and Gill, G.N., 1990. Analysis of deletions of the carboxyl terminus of the epidermal growth factor receptor reveals self-phosphorylation at tyrosine 992 and

enhanced in vivo tyrosine phosphorylation of cell substrates. *Journal of Biological Chemistry*, 265(3), pp.1750–1754.

Wang, K., Yamamoto, H., Chin, J.R., Werb, Z. and Vu, T.H., 2004. Epidermal growth factor receptor-deficient mice have delayed primary endochondral ossification because of defective osteoclast recruitment. *The Journal of biological chemistry*, 279(51), pp.53848–53856.

Wang, L., Audenaert, P. and Michoel, T., 2019. High-Dimensional Bayesian Network Inference From Systems Genetics Data Using Genetic Node Ordering. *Frontiers in Genetics*, 10.

Wang, Y., Gao, J., Guo, X., Tong, T., Shi, X., Li, L., Qi, M., Wang, Y., Cai, M., Jiang, J., Xu, C., Ji, H. and Wang, H., 2014. Regulation of EGFR nanocluster formation by ionic protein-lipid interaction. *Cell research*, 24(8), pp.959–976.

Wang, Y., Zhang, Y., An, T., Zhang, R., Zhao, X., Liu, N., Yin, S., Gan, T., Liang, T., Huang, Y., Zhou, Q. and Zhang, J., 2016. ErbB4 Gene Polymorphism Is Associated With the Risk and Prognosis of Congestive Heart Failure in a Northern Han Chinese Population. *Journal of Cardiac Failure*, 22(9), pp.700–709.

Wang, Y.H., Pinet, L., Assrir, N., Elantak, L., Guerlesquin, F., Badache, A., Lescop, E. and van Heijenoort, C., 2018. 1H, 13C and 15N assignments of the C-terminal intrinsically disordered cytosolic fragment of the receptor tyrosine kinase ErbB2. *Biomolecular NMR Assignments*, 12(1), pp.23–26.

Wang, Z., Chan, H.W., Gambarotta, G., Smith, N.J., Purdue, B.W., Pennisi, D.J., Porrello, E.R., O'Brien, S.L., Reichelt, M.E., Thomas, W.G. and Paravicini, T.M., 2021. Stimulation of the four isoforms of receptor tyrosine kinase ErbB4, but not ErbB1, confers cardiomyocyte hypertrophy. *Journal of Cellular Physiology*, 236(12), pp.8160–8170.

Ward, M.D. and Leahy, D.J., 2015. Kinase Activator-Receiver Preference in ErbB Heterodimers Is Determined by Intracellular Regions and Is Not Coupled to Extracellular Asymmetry. *The Journal of Biological Chemistry*, 290(3), p.1570.

Welch, S., Plank, D., Witt, S., Glascock, B., Schaefer, E., Chimenti, S., Andreoli, A.M., Limana, F., Leri, A., Kajstura, J., Anversa, P. and Sussman, M.A., 2002. Cardiac-specific IGF-1 expression attenuates dilated cardiomyopathy in tropomodulin-overexpressing transgenic mice. *Circulation research*, 90(6), pp.641–648.

Werhli, A. V., Grzegorczyk, M. and Husmeier, D., 2006. Comparative evaluation of reverse engineering gene regulatory networks with relevance networks, graphical gaussian models and bayesian networks. *Bioinformatics*, 22(20).

Wheeler, D.L. and Yarden, Y., 2015. *Receptor tyrosine kinases : structure, functions and role in human disease*. 1st ed. 2015. ed. New York, NY: Humana Press.

Williams, C.C., Allison, J.G., Vidal, G.A., Burow, M.E., Beckman, B.S., Marrero, L. and Jones, F.E., 2004. The ERBB4/HER4 receptor tyrosine kinase regulates gene expression by functioning as a STAT5A nuclear chaperone. *The Journal of Cell Biology*, 167(3), p.469.

Wodicka, L. (Affymetrix, Dong, H., Mittmann, M., Ho, M.H. and Lockhart, D.J., 1997. Genome-wide expression monitoring in Saccharomyces cerevisiae. *Nature biotechnology*, 15(13), pp.1359–1367.

Woelfle, J., Billiard, J. and Rotwein, P., 2003. Acute control of insulin-like growth factor-I gene transcription by growth hormone through Stat5b. *The Journal of biological chemistry*, 278(25), pp.22696–22702.

Woelfle, J., Chia, D.J. and Rotwein, P., 2003. Mechanisms of Growth Hormone (GH) Action. *Journal of Biological Chemistry*, 278(51), pp.51261–51266. https://doi.org/10.1074/jbc.m309486200.

Wood, E.R., Shewchuk, L.M., Ellis, B., Brignola, P., Brashear, R.L., Caferro, T.R., Dickerson, S.H., Dickson, H.D., Donaldson, K.H., Gaul, M., Griffin, R.J., Hassell, A.M., Keith, B., Mullin, R., Petrov, K.G., Reno, M.J., Rusnak, D.W., Tadepalli, S.M., Ulrich, J.C., Wagner, C.D., Vanderwall, D.E., Waterson, A.G., Williams, J.D., White, W.L. and Uehling, D.E., 2008. 6-Ethynylthieno[3,2-d]- and 6-ethynylthieno[2,3-d]pyrimidin-4-anilines as tunable covalent modifiers of ErbB kinases.

Proceedings of the National Academy of Sciences of the United States of America, 105(8), pp.2773–2778.

Woolard, J., Wang, W.-Y., Bevan, H.S., Qiu, Y., Morbidelli, L., Pritchard-Jones, R.O., Cui, T.-G., Sugiono, M., Waine, E., Perrin, R., Foster, R., Digby-Bell, J., Shields, J.D., Whittles, C.E., Mushens, R.E., Gillatt, D.A., Ziche, M., Harper, S.J. and Bates, D.O., 2004. VEGF165b, an Inhibitory Vascular Endothelial Growth Factor Splice Variant. *Cancer Research*, 64(21).

World Health Organization, 2023. *https://www.who.int/*. Cardiovascular diseases (CVDs).

Wu, Q., Wang, T., Chen, S., Zhou, Q., Li, H., Hu, N., Feng, Y., Dong, N., Yao, S. and Xia, Z., 2017. Cardiac protective effects of remote ischaemic preconditioning in children undergoing tetralogy of fallot repair surgery: a randomized controlled trial. *European Heart Journal*, 105, pp.151–154.

Xiao, N., Zhou, A., Kempher, M.L., Zhou, B.Y., Shi, Z.J., Yuan, M., Guo, X., Wu, L., Ning, D., van Nostrand, J., Firestone, M.K. and Zhou, J., 2022. Disentangling direct from indirect relationships in association networks. *Proceedings of the National Academy of Sciences - PNAS*, 119(2), p.1.

Xing, L., Guo, M., Liu, X., Wang, C., Wang, L. and Zhang, Y., 2017. An improved Bayesian network method for reconstructing gene regulatory network based on candidate auto selection. *BMC Genomics*, 18.

Xiong, Z., Yang, F., Li, M., Ma, Y., Zhao, W., Wang, G., Li, Z., Zheng, X., Zou, D., Zong, W., Kang, H., Jia, Y., Li, R., Zhang, Z. and Bao, Y., 2022. EWAS Open Platform: integrated data, knowledge and toolkit for epigenome-wide association study. *Nucleic acids research*, 50(D1), pp.D1004–D1009.

Xu, Y., Yuan, L., Mak, J., Pardanaud, L., Caunt, M., Kasman, I., Larrivée, B., Del Toro, R., Suchting, S., Medvinsky, A., Silva, J., Yang, J., Thomas, J.L., Koch, A.W., Alitalo, K., Eichmann, A. and Bagri, A., 2010. Neuropilin-2 mediates VEGF-C-induced lymphatic sprouting together with VEGFR3. *The Journal of cell biology*, 188(1), pp.115–130.

Yamauchi, T., Ueki, K., Tobe, K., Tamemoto, H., Sekine, N., Wada, M., Honjo, M., Takahashi, M., Takahashi, T., Hirai, H., Tushima, T., Akanuma, Y., Fujita, T., Komuro, I., Yazaki, Y. and Kadowaki, T., 1997. Tyrosine phosphorylation of the EGF receptor by the kinase Jak2 is induced by growth hormone. *Nature 1997 390:6655*, 390(6655), pp.91–96.

Yamazaki, S., Iwamoto, R., Saeki, K., Asakura, M., Takashima, S., Yamazaki, A., Kimura, R., Mizushima, H., Moribe, H., Higashiyama, S., Endoh, M., Kaneda, Y., Takagi, S., Itami, S., Takeda, N., Yamada, G. and Mekada, E., 2003. Mice with defects in HB-EGF ectodomain shedding show severe developmental abnormalities. *The Journal of Cell Biology*, 163(3), p.469.

Yang, E., Wen, Z., Haspel, R.L., Zhang, J.J. and Darnell, J.E., 1999. The Linker Domain of Stat1 Is Required for Gamma Interferon-Driven Transcription. *Molecular and Cellular Biology*, 19(7), pp.5106–5112.

Yang, X., Qiao, D., Meyer, K. and Friedl, A., 2009. STATs MEDIATE FIBROBLAST GROWTH FACTOR INDUCED VASCULAR ENDOTHELIAL MORPHOGENESIS. *Cancer research*, 69(4), p.1668.

Yang, Y., Xu, C., Tang, S. and Xia, Z., 2020. Interleukin-9 Aggravates Isoproterenol-Induced Heart Failure by Activating Signal Transducer and Activator of Transcription 3 Signalling. *Canadian Journal of Cardiology*, 36(11), pp.1770–1781. https://doi.org/10.1016/j.cjca.2020.01.011.

Yang, Y.R., Follo, M.Y., Cocco, L. and Suh, P.G., 2013. The physiological roles of primary phospholipase C. *Advances in Biological Regulation*, 53(3), pp.232–241.

Yarden, Y. and Pines, G., 2012. The ERBB network: at last, cancer therapy meets systems biology. *Nature Reviews Cancer 2012 12:8*, 12(8), pp.553–563.

Yarden, Y. and Sliwkowski, M.X., 2001. *Untangling the ErbB signalling network. Nature Reviews Molecular Cell Biology*, https://doi.org/10.1038/35052073.

Yates, A.D., Achuthan, P., Akanni, W., Allen, J., Allen, J., Alvarez-Jarreta, J., Amode, M.R., Armean, I.M., Azov, A.G., Bennett, R., Bhai, J., Billis, K., Boddu, S., Marugán, J.C., Cummins, C., Davidson, C., Dodiya, K., Fatima, R., Gall, A., Giron, C.G., Gil, L., Grego, T., Haggerty, L., Haskell, E., Hourlier, T., Izuogu, O.G., Janacek, S.H., Juettemann, T., Kay, M., Lavidas, I., Le, T.,

Lemos, D., Martinez, J.G., Maurel, T., McDowall, M., McMahon, A., Mohanan, S., Moore, B., Nuhn, M., Oheh, D.N., Parker, A., Parton, A., Patricio, M., Sakthivel, M.P., Abdul Salam, A.I., Schmitt, B.M., Schuilenburg, H., Sheppard, D., Sycheva, M., Szuba, M., Taylor, K., Thormann, A., Threadgold, G., Vullo, A., Walts, B., Winterbottom, A., Zadissa, A., Chakiachvili, M., Flint, B., Frankish, A., Hunt, S.E., Iisley, G., Kostadima, M., Langridge, N., Loveland, J.E., Martin, F.J., Morales, J., Mudge, J.M., Muffato, M., Perry, E., Ruffier, M., Trevanion, S.J., Cunningham, F., Howe, K.L., Zerbino, D.R. and Flicek, P., 2020. Ensembl 2020. *Nucleic Acids Research*, 48(D1). https://doi.org/10.1093/nar/gkz966.

Yen, H.Y., Liu, Y.C., Chen, N.Y., Tsai, C.F., Wang, Y.T., Chen, Y.J., Hsu, T.L., Yang, P.C. and Wong, C.H., 2015. Effect of sialylation on EGFR phosphorylation and resistance to tyrosine kinase inhibition. *Proceedings of the National Academy of Sciences of the United States of America*, 112(22), pp.6955–6960.

Yip, A.M. and Horvath, S., 2007. Gene network interconnectedness and the generalized topological overlap measure. *BMC Bioinformatics*, 8.

Yip, K.Y., Alexander, R.P., Yan, K.-K. and Gerstein, M., 2010. Improved reconstruction of in silico gene regulatory networks by integrating knockout and perturbation data. *PloS one*, 5(1), pp.e8121–e8121.

You, L., Li, L., Xu, Q., Ren, J. and Zhang, F., 2011. Postconditioning reduces infarct size and cardiac myocyte apoptosis via the opioid receptor and JAK-STAT signaling pathway. *Molecular Biology Reports*, 38(1), pp.437–443.

Yu, C.L., Jin, Y.J. and Burakoff, S.J., 2000. Cytosolic Tyrosine Dephosphorylation of STAT5: POTENTIAL ROLE OF SHP-2 IN STAT5 REGULATION. *Journal of Biological Chemistry*, 275(1), pp.599–604.

Zeng, F., Xu, J. and Harris, R.C., 2009. Nedd4 mediates ErbB4 JM-a/CYT–1 ICD ubiquitination and degradation in MDCK II cells. *The FASEB Journal*, 23(6), pp.1935–1945.

Zeng, F., Zhang, M.Z., Singh, A.B., Zent, R. and Harris, R.C., 2007. ErbB4 Isoforms Selectively Regulate Growth Factor–induced Madin-Darby Canine Kidney Cell Tubulogenesis. *Molecular Biology of the Cell*, 18(11), p.4446.

Zeng, R., Aoki, Y., Yoshida, M., Arai, K. and Watanabe, S., 2002. Stat5B Shuttles Between Cytoplasm and Nucleus in a Cytokine-Dependent and -Independent Manner. *The Journal of Immunology*, 168(9), pp.4567–4575.

Zentilin, L., Puligadda, U., Lionetti, V., Zacchigna, S., Collesi, C., Pattarini, L., Ruozi, G., Camporesi, S., Sinagra, G., Pepe, M., Recchia, F.A. and Giacca, M., 2010. Cardiomyocyte VEGFR-1 activation by VEGF-B induces compensatory hypertrophy and preserves cardiac function after myocardial infarction. *The FASEB journal*, 24(5), pp.1467–1478.

Zhang, D., Sliwkowski, M.X., Mark, M., Frantz, G., Akita, R., Sun, Y., Hillan, K., Crowley, C., Brush, J. and Godowski, P.J., 1997. Neuregulin-3 (NRG3): a novel neural tissue-enriched protein that binds and activates ErbB4. *Proceedings of the National Academy of Sciences of the United States of America*, 94(18), pp.9562–9567.

Zhang, X., Gureasko, J., Shen, K., Cole, P.A. and Kuriyan, J., 2006. An allosteric mechanism for activation of the kinase domain of epidermal growth factor receptor. *Cell*, 125(6), pp.1137–1149.

Zhao, Y., Nakagawa, T., Itoh, S., Inamori, K.-I., Isaji, T., Kariya, Y., Kondo, A., Miyoshi, E., Miyazaki, K., Kawasaki, N., Taniguchi, N., ‡1, ‡ and Gu, J., 2006. N-Acetylglucosaminyltransferase III Antagonizes the Effect of N-Acetylglucosaminyltransferase V on 31 Integrin-mediated Cell Migration *. *THE JOURNAL OF BIOLOGICAL CHEMISTRY*, 281(43), pp.32122–32130.

Zhao, Y.Y., Sawyer, D.R., Baliga, R.R., Opel, D.J., Han, X., Marchionni, M.A. and Kelly, R.A., 1998. Neuregulins promote survival and growth of cardiac myocytes: Persistence of ErbB2 and ErbB4 expression in neonatal and adult ventricular myocytes. *Journal of Biological Chemistry*, 273(17), pp.10261–10269.

Zhen, Y., Caprioli, R.M. and Staros, J. v, 2003. Characterization of Glycosylation Sites of the Epidermal Growth Factor Receptor †. *Biochemistry*, 42(18), pp.5478–5492.

Zhu, M.H., John, S., Berg, M. and Leonard, W.J., 1999. Functional association of Nmi with Stat5 and Stat1 in IL-2- and IFNγ-mediated signaling. *Cell*, 96(1), pp.121–130.

Zhu, S., Wurdak, H., Wang, Y., Galkin, A., Tao, H., Li, J., Lyssiotis, C.A., Yan, F., Tu, B.P., Miraglia, L., Walker, J., Sun, F., Orth, A., Schultz, P.G. and Wu, X., 2009. A genomic screen identifies TYRO3 as a MITF regulator in melanoma. *Proceedings of the National Academy of Sciences*, 106(40), pp.17025–17030.

Zhu, Y., Sullivan, L.L., Nair, S.S., Williams, C.C., Pandey, A.K., Marrero, L., Vadlamudi, R.K. and Jones, F.E., 2006. Coregulation of estrogen receptor by ERBB4/HER4 establishes a growth-promoting autocrine signal in breast tumor cells. *Cancer research*, 66(16), pp.7991–7998.

Zoppi, J., Guillaume, J.F., Neunlist, M. and Chaffron, S., 2021. MiBiOmics: an interactive web application for multi-omics data exploration and integration. *BMC Bioinformatics*, 22(1), pp.1–14.

Zuo, Y., Yu, G., Tadesse, M.G. and Ressom, H.W., 2014. Biological network inference using low order partial correlation. *Methods (San Diego, Calif.)*, 69(3), p.266.

Zurek, M., Johansson, E., Palmer, M., Albery, T., Johansson, K., Rydén-Markinhutha, K. and Wang, Q.D., 2020. Neuregulin-1 Induces Cardiac Hypertrophy and Impairs Cardiac Performance in Post-Myocardial Infarction Rats. *Circulation*, 142, pp.1308–1311.

TURUN
YLIOPISTO
UNIVERSITY
OF TURKU

Painosalama, Turku, Finland 2023

ISBN 978-951-29-9550-9 (PRINT)
ISBN 978-951-29-9551-6 (PDF)
ISSN 0355-9483 (Print)
ISSN 2343-3213 (Online)